JAERI-Tech
98-051

ITER BREEDING BLANKET MODULE DESIGN & ANALYSIS

November 1998

Toshimasa KURODA, Mikio ENOEDA,
Shigeto KIKUCHI, Junji OHMORI,
Shinichi SATO, Toshio OSAKI*,
Kazuyuki FURUYA, Toshihisa HATANO,
Satoshi SATO and Hideyuki TAKATSU

日本原子力研究所
Japan Atomic Energy Research Institute

本レポートは，日本原子力研究所が不定期に公刊している研究報告書です。
入手の問合わせは，日本原子力研究所研究情報部研究情報課（〒319－1195 茨城県那珂郡東海村）あて，お申し越しください。なお，このほかに財団法人原子力弘済会資料センター（〒319－1195 茨城県那珂郡東海村日本原子力研究所内）で複写による実費頒布をおこなっております。

This report is issued irregularly.
Inquiries about availability of the reports should be addressed to Research Information Division, Department of Intellectual Resources, Japan Atomic Energy Research Institute, Tokai-mura, Naka-gun, Ibaraki-ken 〒319－1195, Japan.

編集兼発行　日本原子力研究所

ITER Breeding Blanket Module Design & Analysis

Toshimasa KURODA, Mikio ENOEDA, Shigeto KIKUCHI, Junji OHMORI[+],
Shinichi SATO[+], Toshio OSAKI*, Kazuyuki FURUYA, Toshihisa HATANO,
Satoshi SATO and Hideyuki TAKATSU[++]

Department of Fusion Engineering Research
Naka Fusion Research Establishment
Japan Atomic Energy Research Institute
Naka-machi, Naka-gun, Ibaraki-ken

(Received October 14, 1998)

The ITER breeding blanket employs a ceramic breeder and Be neutron multiplier both in small spherical pebble form. Radial-poloidal cooling panels are arranged in the blanket box to remove the nuclear heating in these materials and to reinforce the blanket structure. At the first wall, Be armor is bonded onto the stainless steel (SS) structure to provide a low Z plasma-compatible surface and to protect the first wall/blanket structure from the direct contact with the plasma during off-normal events. Thermo-mechanical analyses and investigation of fabrication procedure have been performed for this breeding blanket.

To evaluate thermo-mechanical behavior of the pebble beds including the dependency of the effective thermal conductivity on stress, analysis methods have been preliminary established by the use of special calculation option of ABAQUS code, which are briefly summarized in this report. The structural response of the breeding blanket module under internal pressure of 4 MPa (in case of in-blanket LOCA) resulted in rather high stress in the blanket side (toroidal end) wall, thus addition of a stiffening rib or increase of the wall thickness will be needed.

Two-dimensional elasto-plastic analyses have been performed for the Be/SS bonded interface at the first wall taking a fabrication process based on HIP bonding and thermal cycle due to pulsed plasma operation into account. The stress-strain hysteresis during these process and operation was clarified, and a procedure to assess and/or confirm the bonding integrity was also proposed.

Fabrication sequence of the breeding blanket module was preliminarily developed based on the procedure to fabricate part by part and to assemble them one by one.

Keywords: ITER, Breeding Blanket, Pebble Packed Bed, Thermo-mechanical Analysis, Be/SS Bonded Interface, Elasto-plastic Analysis, Fabrication Procedure

---

[+] Department of ITER Project

[++] Office of ITER Project Promotion

* Kawasaki Heavy Industries, Ltd.

ITER増殖ブランケット設計

日本原子力研究所那珂研究所核融合工学部
黒田　敏公・榎枝　幹男・菊池　茂人・大森　順次+・佐藤　真一+
大崎　敏雄*・古谷　一幸・秦野　歳久・佐藤　聡・高津　英幸++

(1998年10月14日受理)

ITER増殖ブランケットでは、トリチウムを生産するためのセラミック増殖材と中性子増倍材としてのベリリウムがいずれも微小球ペブル状で充填される。これらのペブルは、ブランケット容器の補強リブを兼ねた冷却パネルによって冷却され、増殖材からのトリチウム放出及び材料健全性の維持等を考慮した所定の温度範囲に保持される。また、本増殖ブランケットの第一壁には、プラズマ中への不純物低減及び非正常運転時の構造体保護等を目的としたベリリウム・アーマーが構造材としてのステンレス鋼に接合される。ここでは、この増殖ブランケットを対象とし、とくに、ブランケット内のペブル充填層における熱機械特性及びLOCA時等のブランケット内圧上昇に対する容器強度、第一壁のベリリウム/ステンレス鋼接合部における熱機械特性に着目した解析を実施した。また、ブランケット・モジュールの全体製作手順に関する検討を行った。

ペブル充填層の熱機械特性については、汎用熱・構造解析コードABAQUSの特殊計算オプションを適用した解析を試み、定性的な評価が可能であることを明らかにした。尚、本解析の詳細は別途報告する予定であり、ここではその概略を記すことに留める。LOCA時に想定されるブランケット内圧上昇（4 MPa）に対しては、容器側壁の強度が不十分であり、壁厚の増加あるいは補強リブの設置が必要であることを明らかにした。

第一壁のベリリウム/ステンレス鋼接合部について、高温等方加圧（HIP）接合法を想定した製作過程とそれに続くパルス運転時を考慮した弾塑性解析を行い、熱応力履歴を求めると共にこれを反映した接合部強度評価方法について検討した。

ブランケット・モジュールの製作手順としては、第一壁及び冷却パネル、増殖材充填部等の各構成要素を個々に製作し、それらを組み合わせることを基本として各構成要素の製作方法及び組み合わせ手順について検討した。

那珂研究所：〒311-0193　茨城県那珂郡那珂町向山801-1
+　ITER開発室
++　ITER業務推進室
*　川崎重工業（株）

Contents

目　次

This is a blank page.

1. Introduction

The ITER breeding blanket is designed to breed the necessary tritium for ITER operation during the Enhanced Performance Phase by replacing the shielding blanket of the Basic Performance Phase. Similar to the shielding blanket, it has to remove the majority of the fusion power generated by the plasma and to protect the vacuum vessel and the toroidal field coils from excessive nuclear heating and radiation damage. It has to produce a net tritium breeding ratio > 0.8 to satisfy the technical objectives of the Enhanced Performance Phase.

For compatibility with the ITER design and to satisfy the blanket functional requirements, a water-cooled modular solid-breeder blanket with beryllium neutron multiplier has been selected. Lithium zirconate is currently the reference breeder material. Enriched lithium is used to enhance the tritium breeding capability, to reduce the radial blanket thickness, to decrease the breeder material volume, to lower the breeder thermal stresses, and to enhance the shielding capability. Similar to the shielding blanket, the breeding blanket uses Type 316LN-IG austenitic steel structural material.

The design of the ITER breeding blanket has incorporated pebble-beds of breeder and neutron multiplier materials. The internal structure of the breeding blanket exhibits toroidally repeated basic cells, each of which consists of two adjacent poloidal-radial cooling panels, a bundle of breeder rods containing breeder pebbles and placed between the adjacent cooling panels, and beryllium (Be) pebbles filled in the space between the breeder rods and surrounding structures (cooling panels, the first wall and the back shield plate). Beryllium armor tiles are bonded on the stainless steel (SS) first wall structural material for providing low Z plasma-compatible surface and protecting the first wall/blanket structure from the direct contact with the plasma in case of off-normal events.

For examining the performance of this blanket, thermo-mechanical analyses have been performed focusing on thermal and mechanical behavior of the pebble beds. Detailed elasto-plastic thermo-mechanical analyses have also been conducted to evaluate the stress and strain at the Be/SS bonded interface in the first wall. Finally, the fabrication method has been investigated based on the procedure to fabricate part by part and to assemble the fabricated parts one by one.

2. Objectives

The objective of this work is to develop the breeding blanket module design. Specific technical analyses will be performed in support of the design effort to check the capability of the breeding blanket for satisfying the design objectives and the operational requirements.

The following analyses and investigation have been performed here for assessing the performance and developing the design details of the breeding blanket.

Thermo-Mechanical Analyses

Perform thermal and stress analyses for the blanket module number 19 (installed at outboard midplane) to calculate the temperature distribution in the different materials, and the resulting stresses due to the differential thermal expansion of the blanket materials. Check the structural response of the blanket modules under internal coolant pressure of 4 MPa. The main steps are the following:

- Develop two-dimensional geometrical model for the ITER breeding blanket module for thermal and stress analyses.

- Utilize the developed model to calculate the temperature distribution in the different materials. Study the sensitivity of the temperature distribution to the changes in the thermal conductivity and the heat transfer coefficient between the pebbles and the solid surfaces.

- Calculate the stresses due to the differential thermal expansion of the blanket materials. Analyze the corresponding change in the thermal conductivity of the pebble beds and the heat transfer coefficient between the pebbles and the solid surfaces. Update the temperature distribution in the blanket material due to these changes.

- Calculate the structural response of the blanket module under internal pressure of 4 MPa.

Be/SS bonding requirements

Perform detail thermal and stress analyses for the first wall to define the Be/SS bonding requirements. The main steps are the following:

- Develop elastic-plastic model for the first wall for thermal and stress analyses. The model has to have adequate details to address the Be/SS interface issues and good simulation for the boundary conditions.

- Utilize the developed model to calculate the interface stresses and strain histories between the beryllium tiles and the first wall steel structure due to the fabrication procedure, different procedures may be considered, and the typical loading conditions.

- Propose a procedure for assessing the bonding integrity and define the bonding requirements based on the results from the previous step.

Blanket Module Fabrication

Perform fabrication assessment to establish the feasibility to fabricate the blanket module. This work will include the following steps:

- Develop a fabrication procedure for the blanket module including the module filling with the breeder and the multiplier pebbles.

- Develop an inspection procedure for the blanket module to check the compliance with the design specifications.

- Suggest design improvements to reduce the fabrication cost of the blanket module.

3. Thermo-Mechanical Analyses of Breeding Blanket Module

3.1 Breeding Region

The poloidal segmentation of the breeding blanket, which should be the same as the shielding blanket, is shown in Fig. 3.1 [1]. The breeding blanket is also segmented in the toroidal direction. The resulting dimensions of each blanket module by the segmentation are noted in the figure. An exploded view of one blanket module and a detail of a basic cell in the module are illustrated in Figs. 3.2 and 3.3, respectively [1]. As shown in these figures, the design of the ITER breeding blanket has incorporated pebble-beds of breeder and neutron multiplier materials and poloidal-radial cooling panels. The internal structure of the breeding blanket exhibits toroidally repeated basic cells, each of which consists of two adjacent cooling panels, a bundle of breeder rods placed between the adjacent cooling panels and Be pebbles filled in the space between the breeder rods and surrounding structures (cooling panels, the first wall and the back shield plate). Beryllium armor tiles are bonded on the SS first wall structural material. Detail dimensions of a basic cell are indicated in Fig. 3.4.

Thermo-mechanical analysis of the unit cell in #19 ITER breeding blanket module has been conducted taking into account the spatially varying effective thermal conductivity and heat transfer coefficient at the contacting wall of Be pebble bed depending on stresses due to the differential thermal expansion of the blanket. The #19 module is installed at outboard midplane where the neutron wall loading, thus the heat loads due to the nuclear heating, becomes maximal. Since the detail procedure and results of this analysis will be presented in another report [2], they are briefly summarized here.

Special calculation option "modified Drucker-Prager/Cap plasticity model" of ABAQUS code is used so as to deal with mechanical features of pebble bed such as shear failure flow and hydrostatic plastic compression. The coupled temperature-displacement procedure of ABAQUS code is also utilized so that the thermal conductivity of the pebble beds is automatically calculated according to the stress.

Though mechanical properties data of the pebble bed necessary for conducting above analysis are very limited or unavailable at present, some of them are estimated by theoretical correlation [3] and from experimental results [4] while others are audaciously assumed. The correlation between the thermal properties (effective thermal conductivity and heat transfer coefficient at wall) and stress is also estimated based on the experimental results [5] and additional thermo-mechanical analyses.

Prior to the analysis of the breeding blanket, pre-analyses are performed to examine the applicability of above method. For the uniaxial compressive experiment of the pebble bed [4] shown in Fig. 3.5, the analysis results represent well the following mechanical behavior of the pebble bed as shown in Fig. 3.6.

(1) Elastic compression (first loading)
(2) Hydrostatic plastic compression (first loading)
(3) Elastic expansion (first unloading)
(4) Shear failure (first unloading)

(5) Elastic compression (second loading)
(6) Hydrostatic plastic compression (second loading)

Another pre-analysis was conducted to apply this method to a heat transfer experiment [5]. Temperature distribution across the pebble bed measured in the experiment and analysis result are shown in Fig. 3.7 and Fig. 3.8, respectively. The analysis results also represent the slight convex curvature of the temperature distribution observed in the experimental results. The convex curvature is due to higher thermal conductivity in higher temperature, thus higher compressive stress, region in the tested pebble bed.

After above qualitative validation of the analysis method by comparing the experimental results, thermo-mechanical analyses of the basic cell of the ITER breeding blanket have been performed. The analysis model is a half of horizontal cross-section of the basic cell as shown in Fig. 3.9 taking thermally and mechanically symmetrical conditions into account. Analyses results of temperature and stresses distributions are shown in Figs. 3.10-3.12. Consequently, the breeder temperature ranges from 317 °C to 554 °C which satisfy the specified design temperature range, 300-800 °C, while the maximum temperature of Be multiplier, 554 °C, slightly exceeds the design temperature limit of 500 °C.

Through this analysis study, the method and procedure to calculate the thermo-mechanical behavior of the pebble bed are preliminary established. However, quantitative improvement is needed, especially by experimental measurement and accumulation of mechanical properties data of pebble beds including Young's modulus, Poisson's ratio and the data with regard to shear failure.

3.2 Structural Response under Internal Pressure

The breeding blanket module consists of basic cells separated by SS cooling panels. When the coolant in the cooling panel is discharged into the blanket in case of an accidental case such as in-blanket LOCA, the cooling panel and the blanket box walls are loaded with internal pressure, possibly of the same level as the coolant pressure, 4 MPa. The pressure load subjecting to the cooling panel can be supported by the pressure load on the other side of the cooling panel and the packed pebbles in the adjacent basic cell. Therefore, the mechanical integrity of the toroidal end wall of the blanket box is examined against the internal pressure load of 4 MPa here.

3.2.1 Calculation model

Figure 3.13 shows the toroidal end wall to be analyzed. For the calculation model, a rectangular plate fixed at all edges is assumed as shown in Fig. 3.14. The maximum deflection (w_{max}) and bending stress (σ_{max}) of the plate are obtained by the following equations:

$$w_{max} = \alpha P a^4/(E h^3)$$
$$\sigma_{max} = \beta P a^2/h^2$$

where P, a, E and h are pressure, short edge length, Young's modulus and plate thickness, respectively. Coefficients, α and β, are to be decided depending on the ratio of long/short edge lengths.

3.2.2 Calculation results

Figure 3.15 shows the maximum deflection of the toroidal end plate. With the short edge length of 247 mm for the #19 blanket module, the maximum deflection is 0.45 mm at the center of the plate. The maximum bending stress is 390 MPa in the middle of the long edge as shown in Fig. 3.16 for the present short edge length and the wall thickness of 247 mm and 18 mm, respectively. However, this maximum stress exceeds the limit of 1.5 Sm for the primary bending stress of SS316L(N)-IG structural material, i.e., 206 MPa at 200 °C [6]. The dependence of the maximum bending stress on the plate thickness is shown in Fig. 3.17. In order to reduce the maximum bending stress within the limit, the thickness of the toroidal end wall needs to be increased to 26 mm, or stiffening rib structure should be added inside the toroidal end wall.

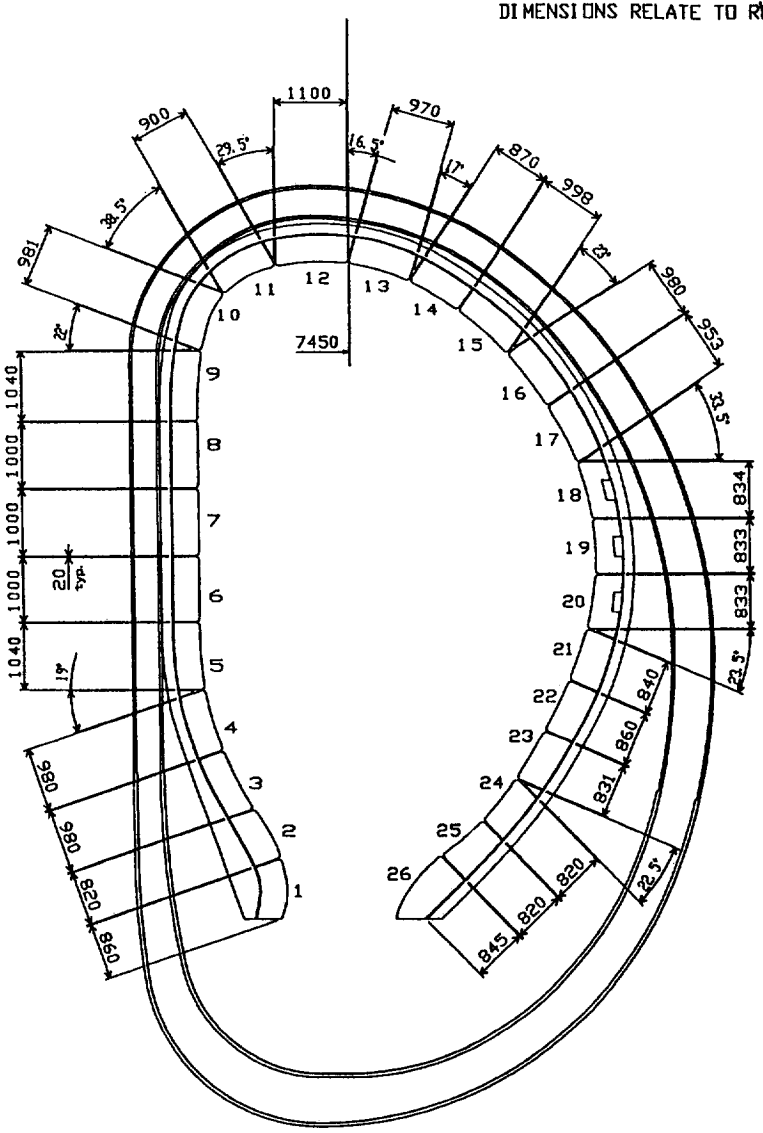

Module No.	Volume (litter)	Weight (ton)	Toroidal length (mm)	Poloidal width (mm)	Thickness (mm)
1	656	4.20	1968	860	401
2	658	4.21	1938	820	442
3	666	4.26	1811	980	395
4	615	3.94	1672	980	395
5	630	4.03	1592	1040	395
6	602	3.85	1573	1000	395
7	602	3.85	1573	1000	395
8	602	3.85	1573	1000	395
9	630	4.03	1592	1040	395
10	623	3.99	1695	981	395
11	658	4.21	1938	900	397
12	652	4.17	1523	1100	418
13	665	4.25	1744	970	418
14	660	4.22	1922	870	415
15	626	4.01	1559	998	418
16	662	4.24	1673	980	420
17	664	4.25	1745	953	403
18	575	3.68	2001	834	398
19	587	3.76	2020	833	400
20	638	4.08	2020	833	420
21	672	4.30	1777	840	458
22	667	4.27	1732	860	459
23	601	3.84	1668	831	455
24	530	3.39	1580	820	420
25	538	3.44	1496	820	430
26	670	4.29	1403	845	430

2-3-4 configuration
4.30 tonne limit
20 mm poloidal gap
20 mm toroidal gap
outboard modules do not have parallel sides
Total no. of modules = 730

Fig. 3.1 Breeding blanket segmentation [1]

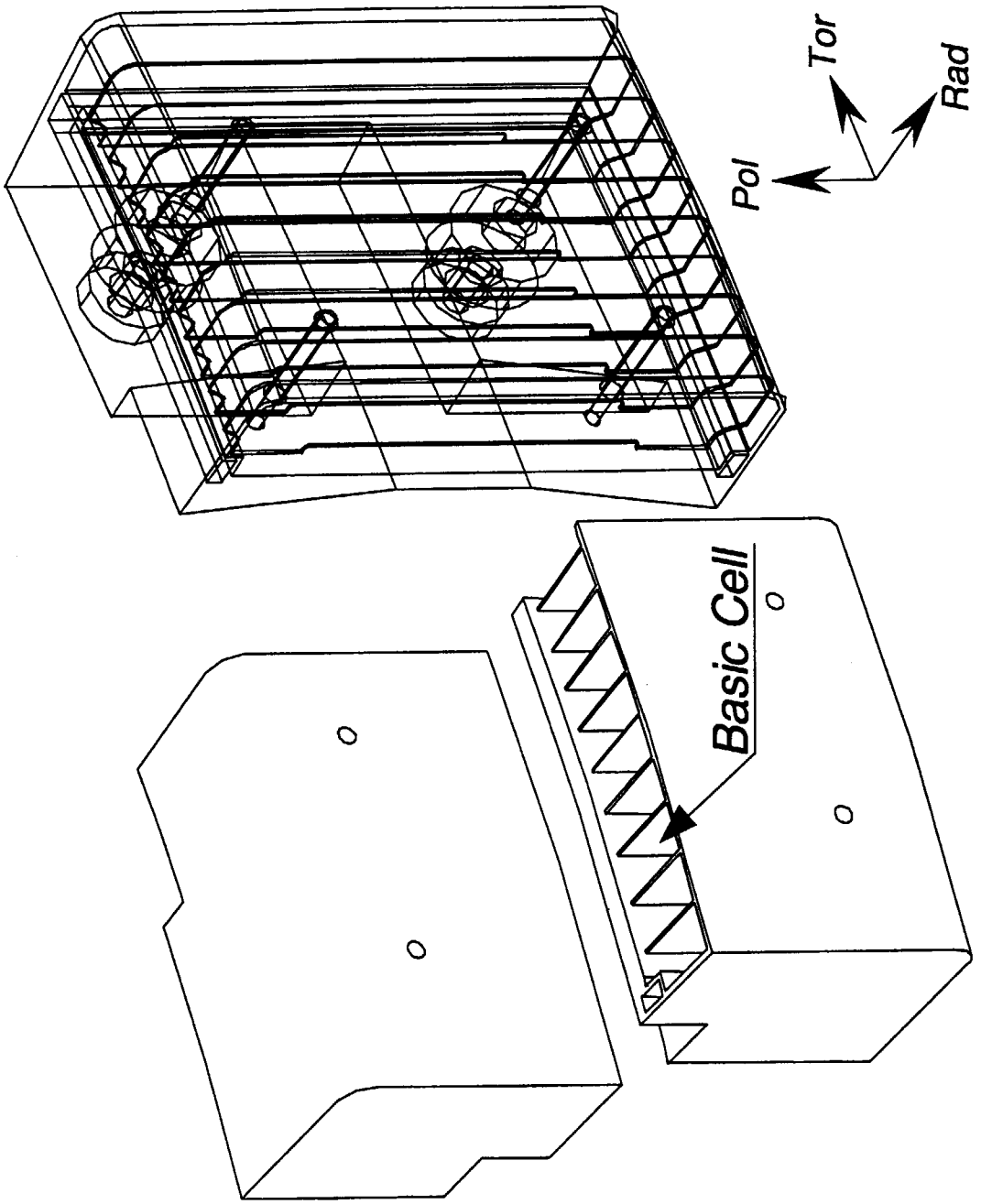

Fig. 3.2 Exploded view of a box module [1]

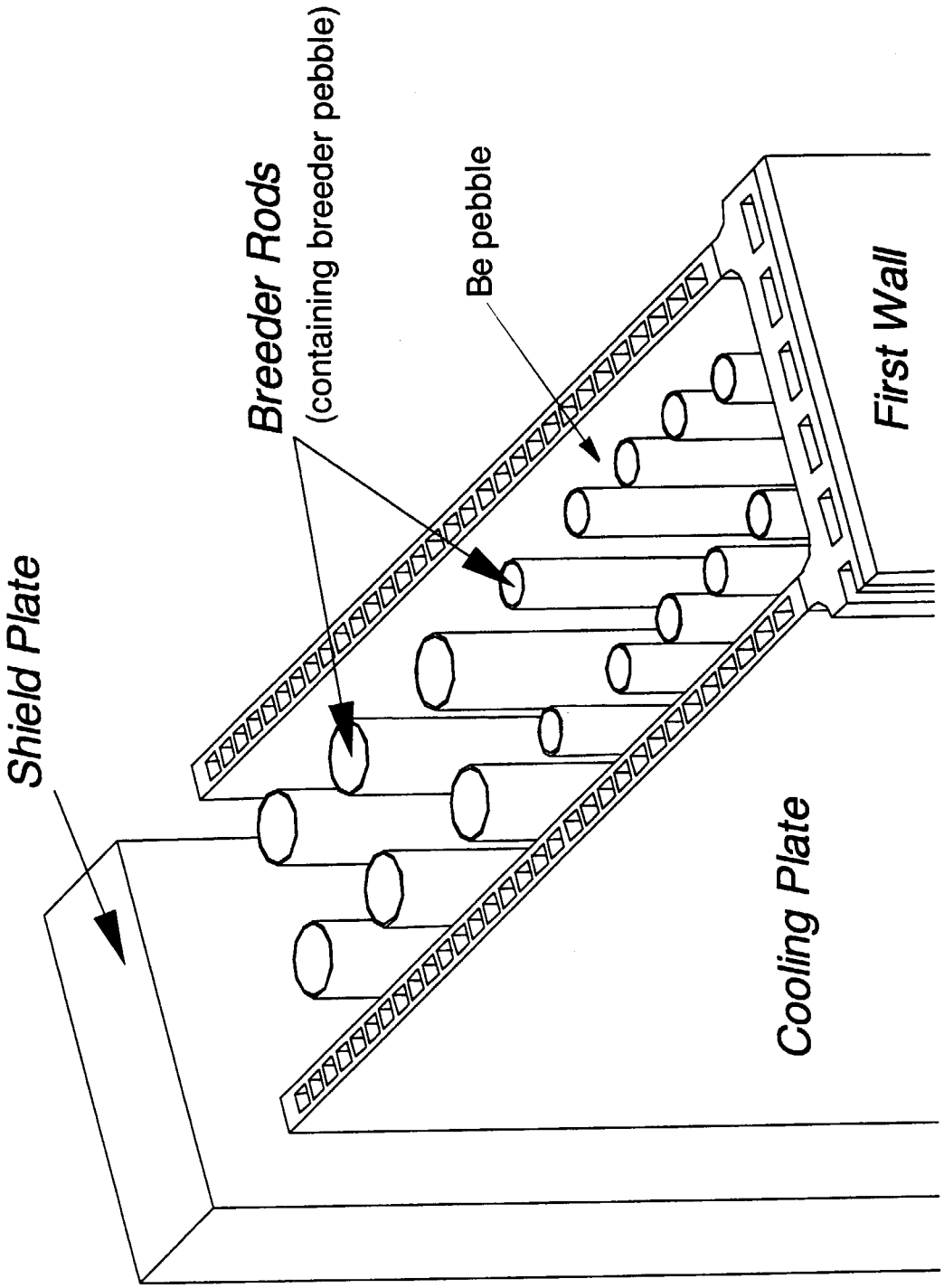

Fig. 3.3 Detail of a basic cell [1]

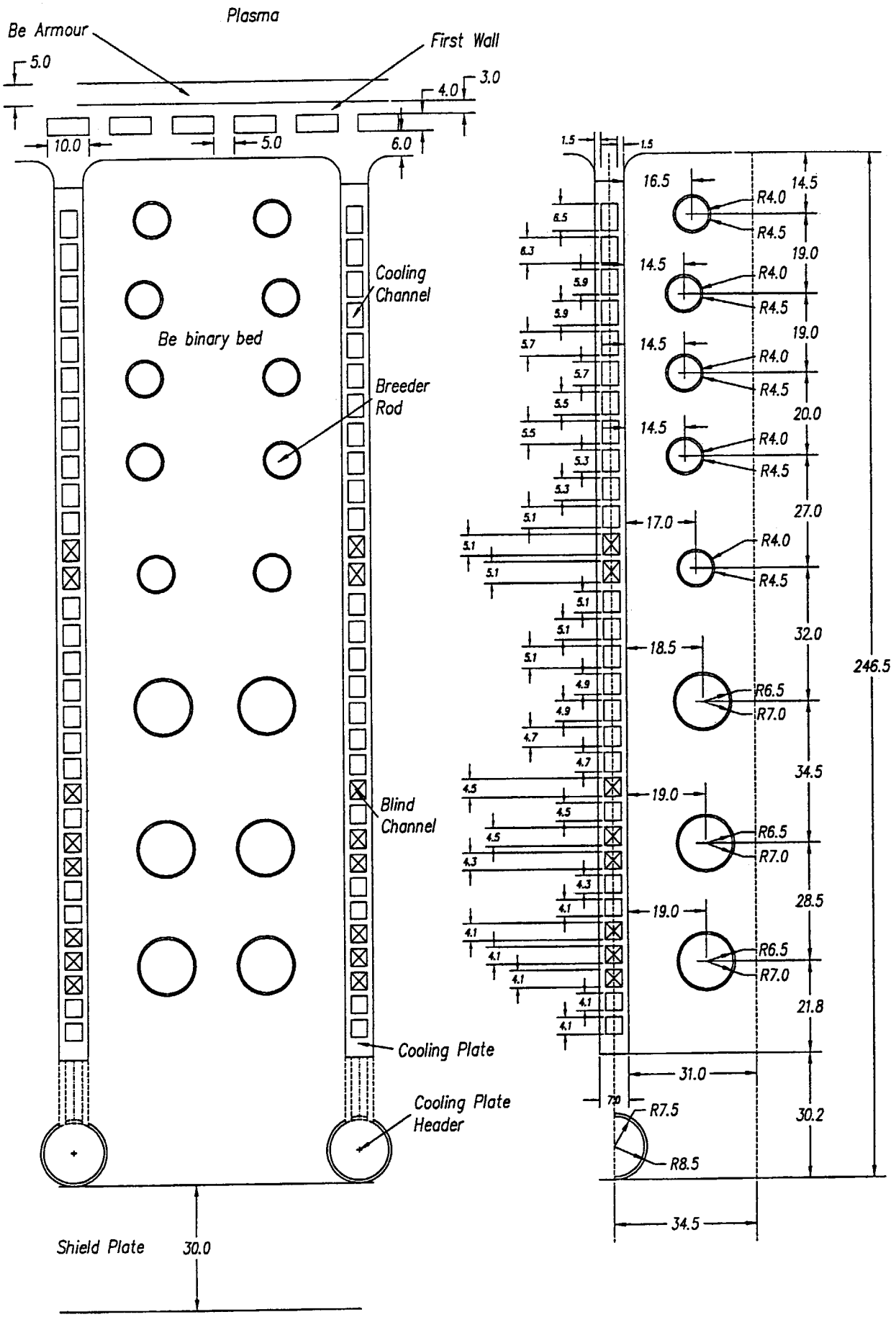

Fig. 3.4 Basic cell of module #19 (outboard region) [1]

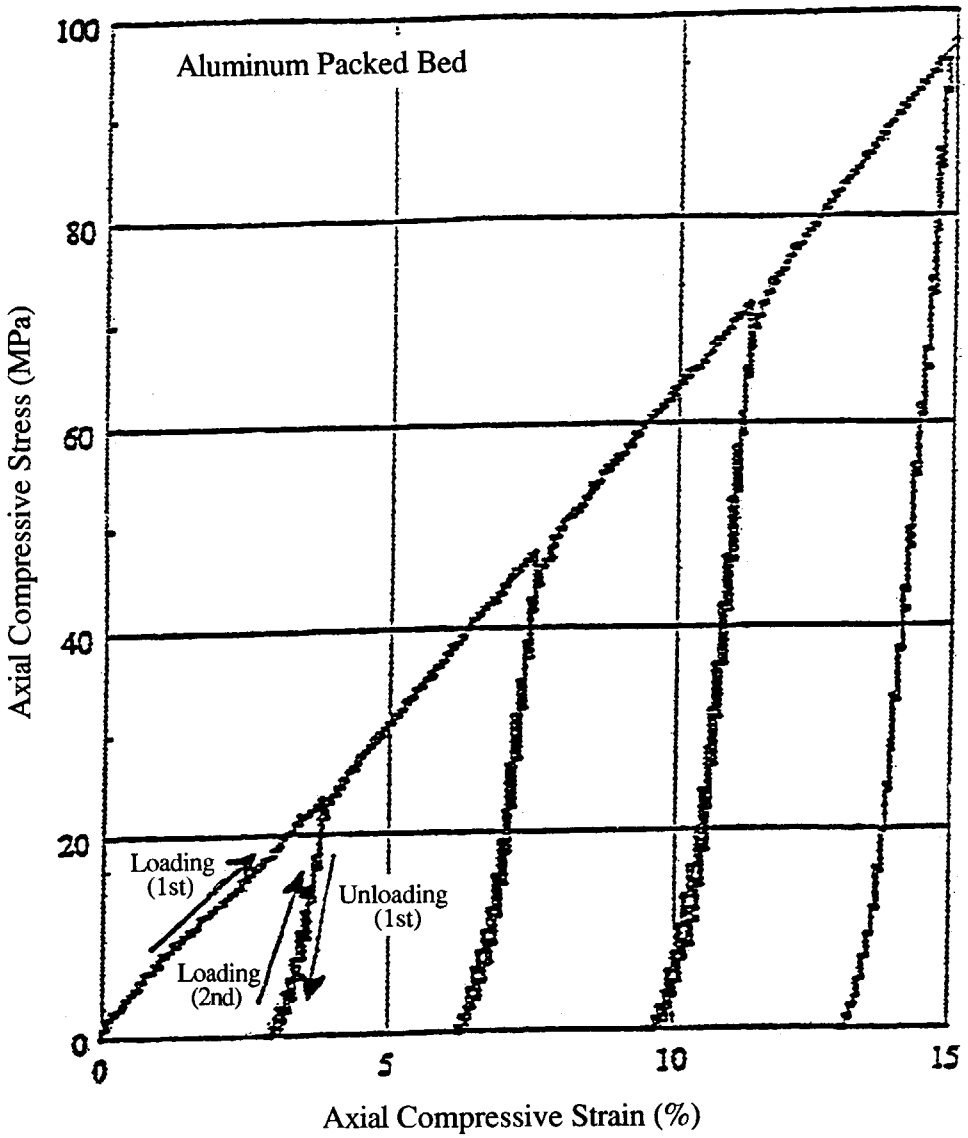

Fig. 3.5 Stress vs. strain during cyclic loading and unloading tests of aluminum pebble packed bed [4]

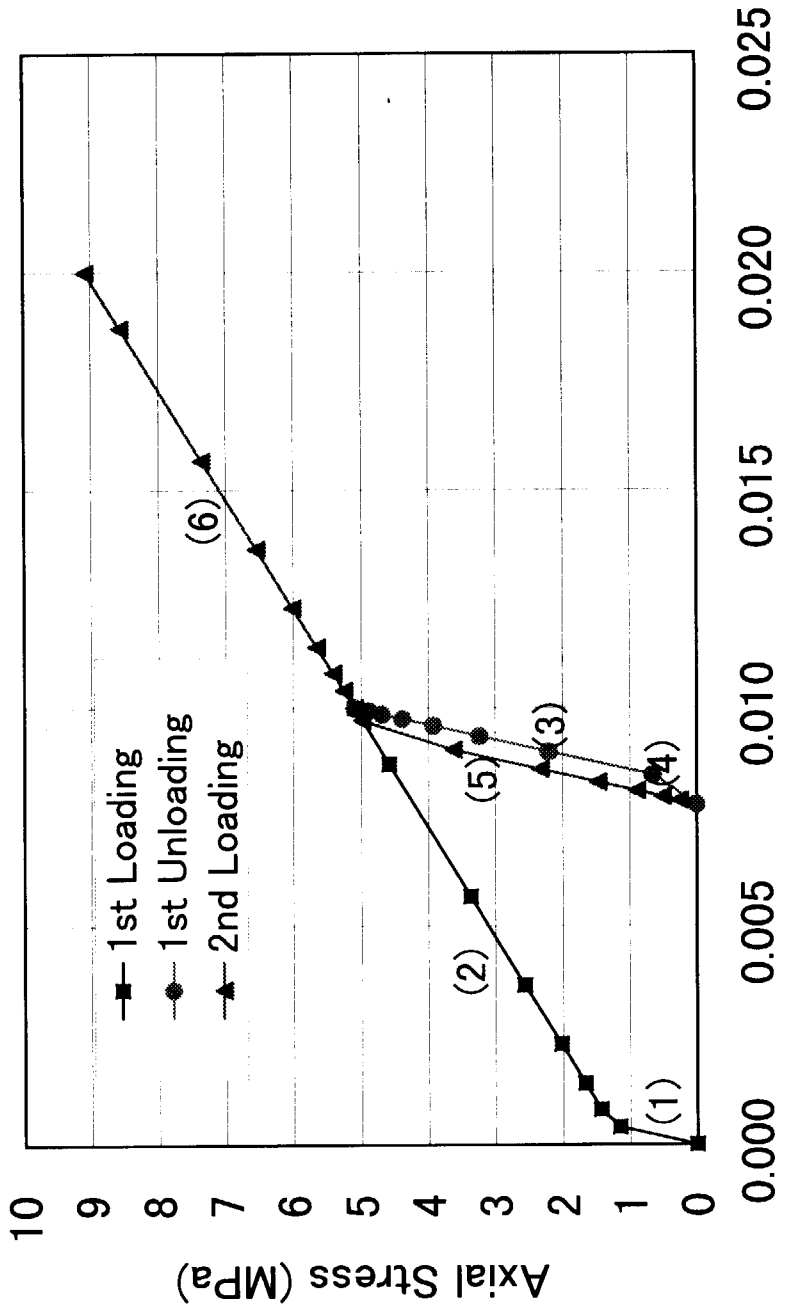

Fig. 3.6 Analyzed results of uni-axial compressive experiment [2]
(Axial stress vs. axial strain)

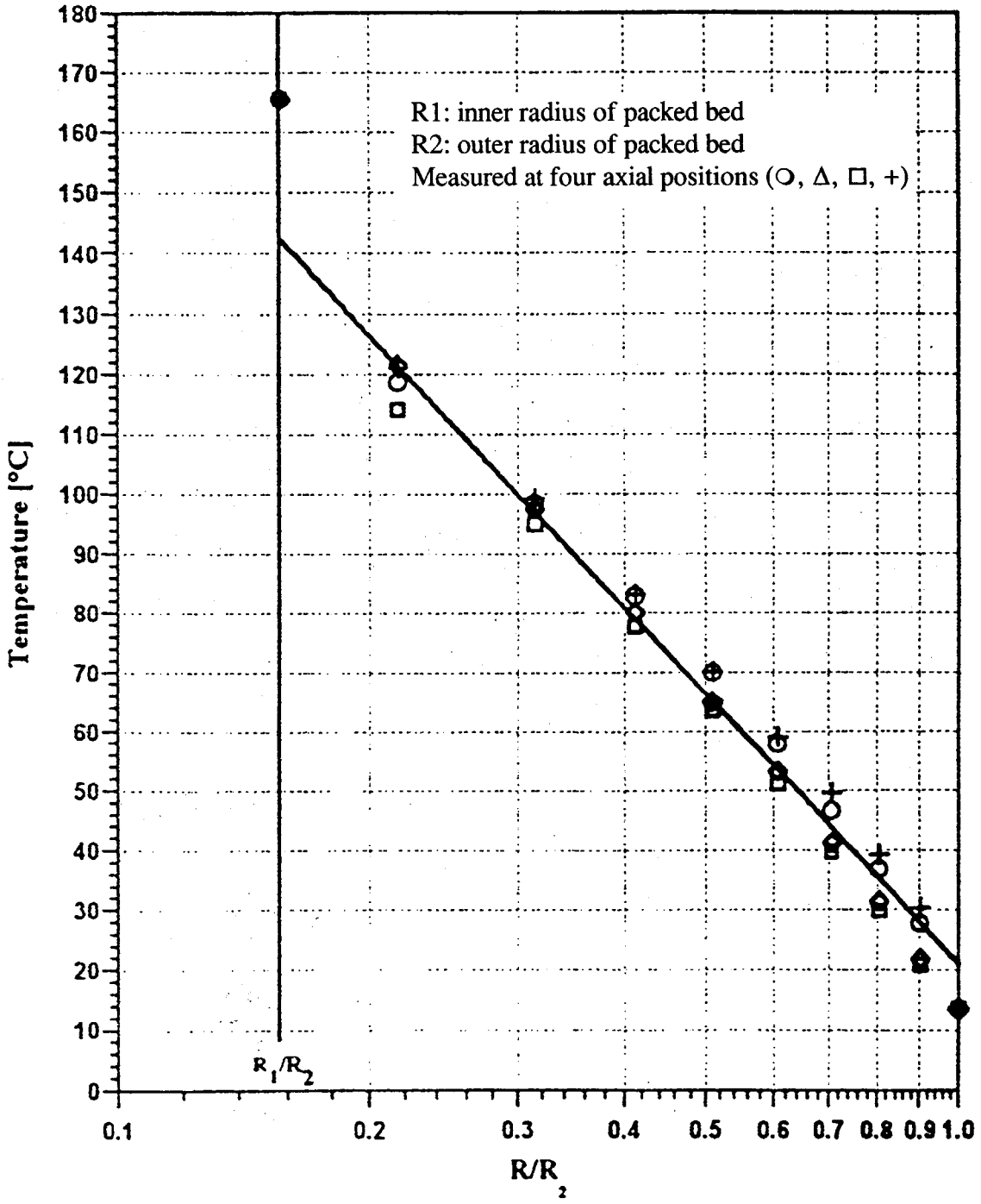

Fig. 3.7 Radial temperature distribution across pebble packed bed in heat transfer experiment [4]

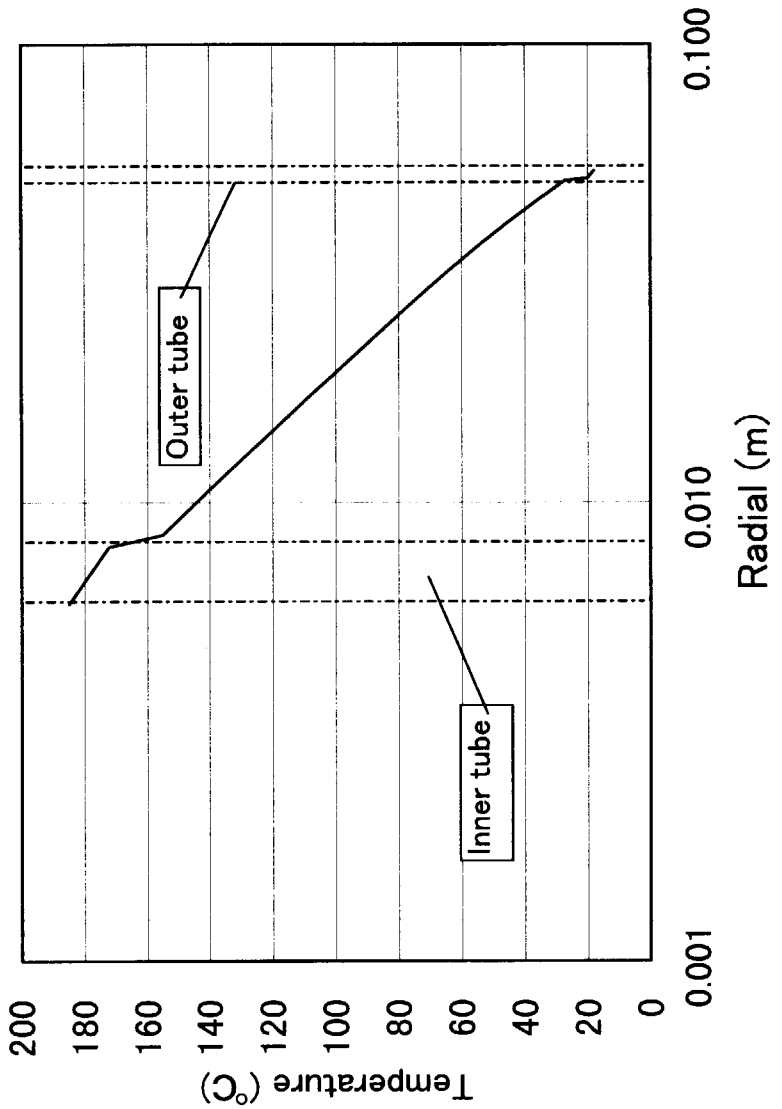

Fig. 3.8 Analyzed temperature distribution of heat transfer experiment [2]

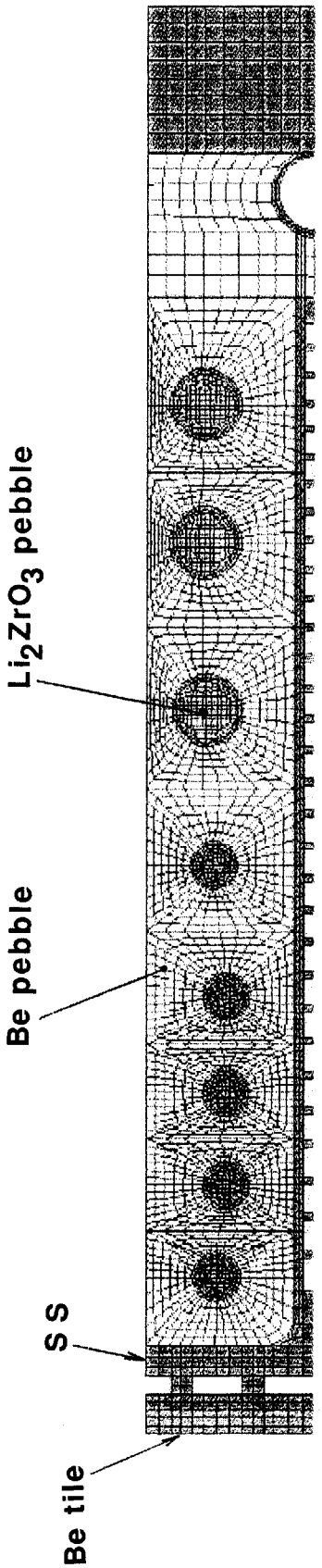

Fig. 3.9 Analysis model of ITER #19 breeding blanket basic cell [2]

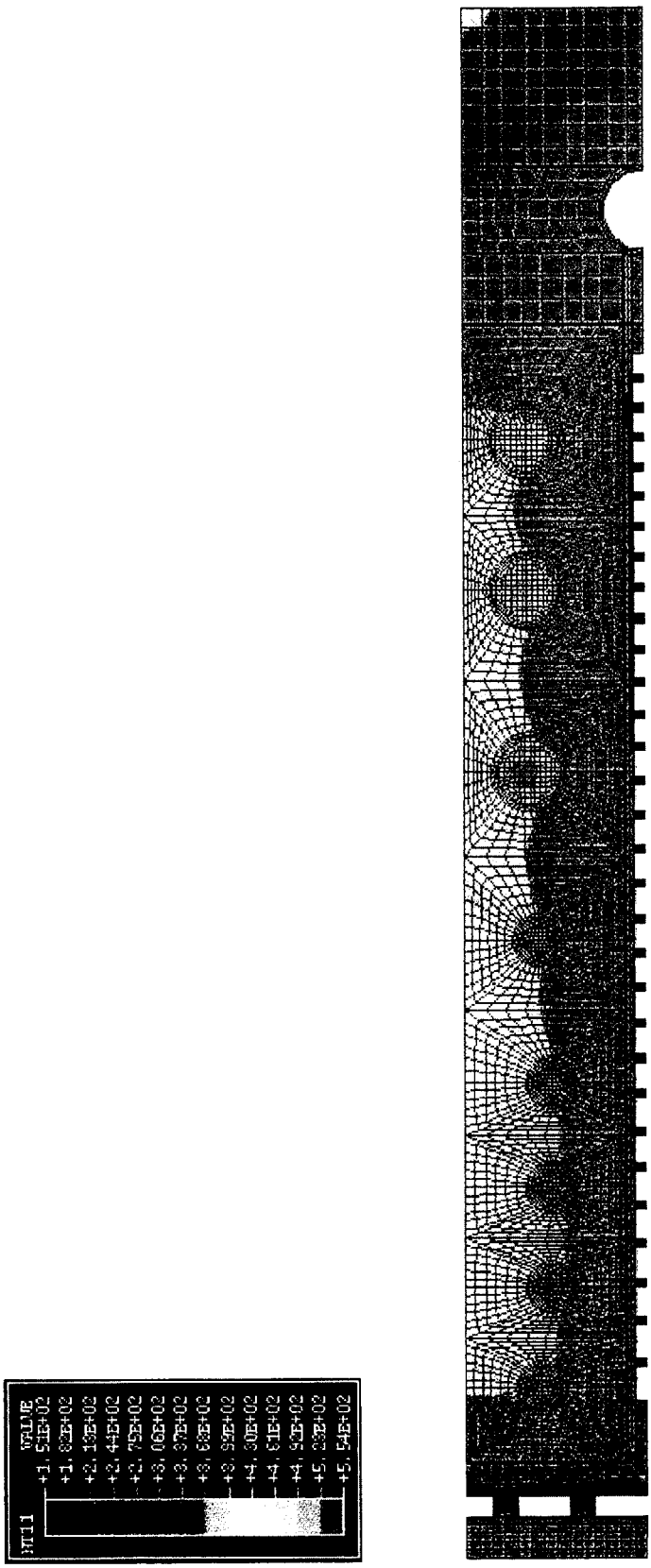

Fig. 3.10 Temperature distribution in basic cell [2]

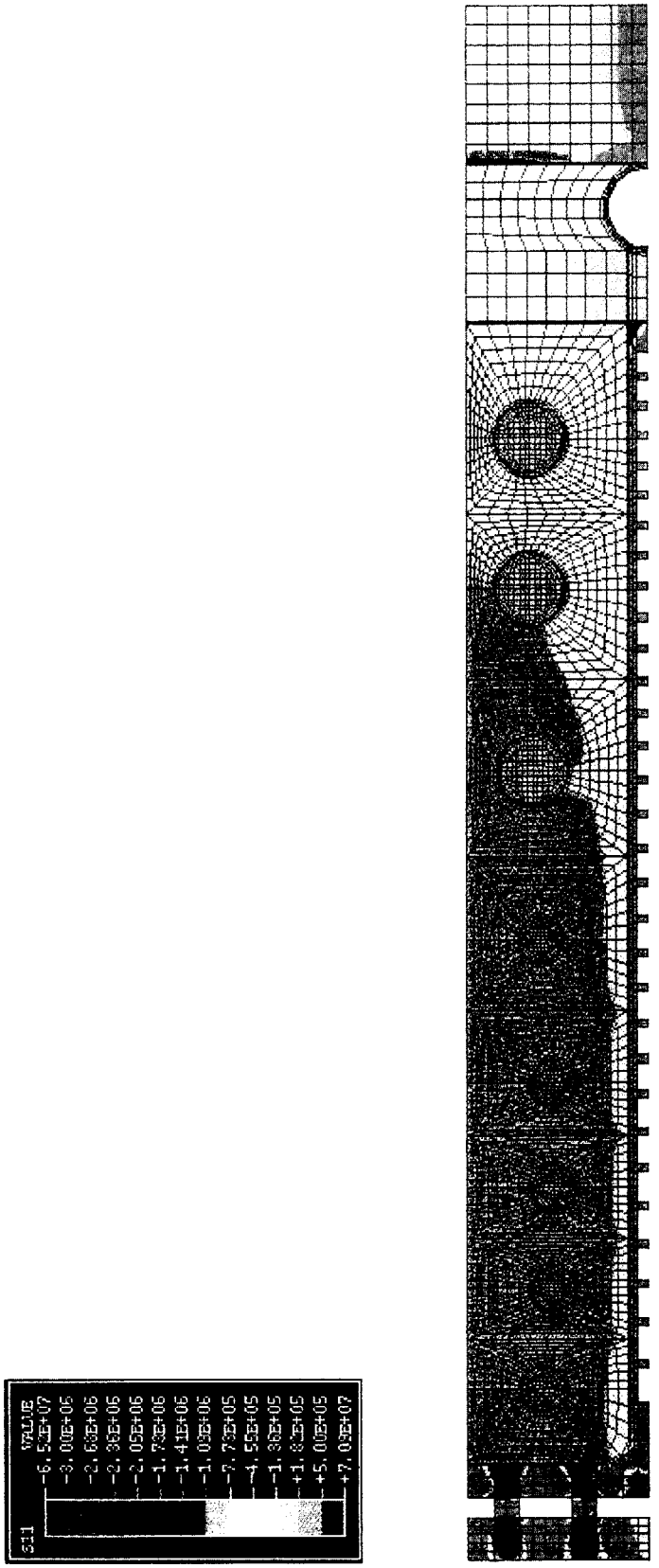

Fig. 3.11 Stress (σ_x) distribution in basic cell [2]

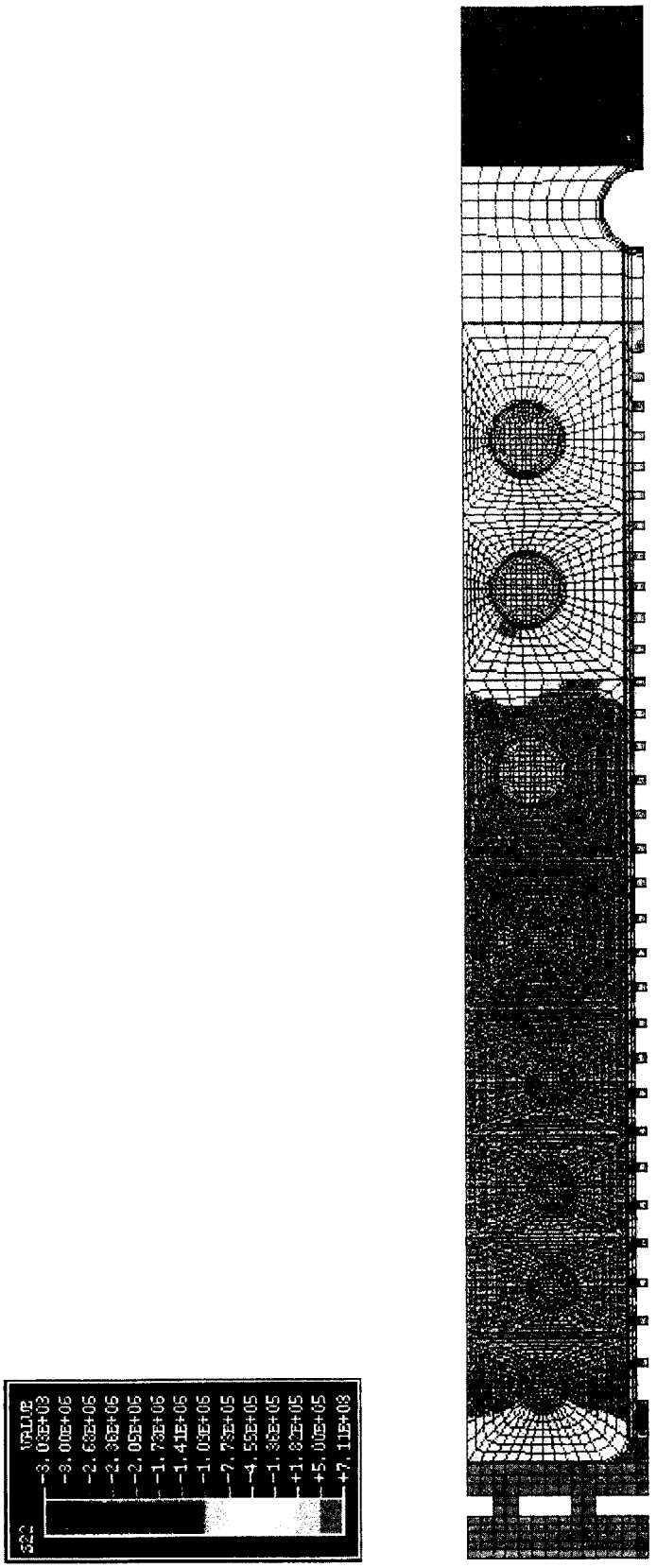

Fig. 3.12 Stress (σ_y) distribution in basic cell [2]

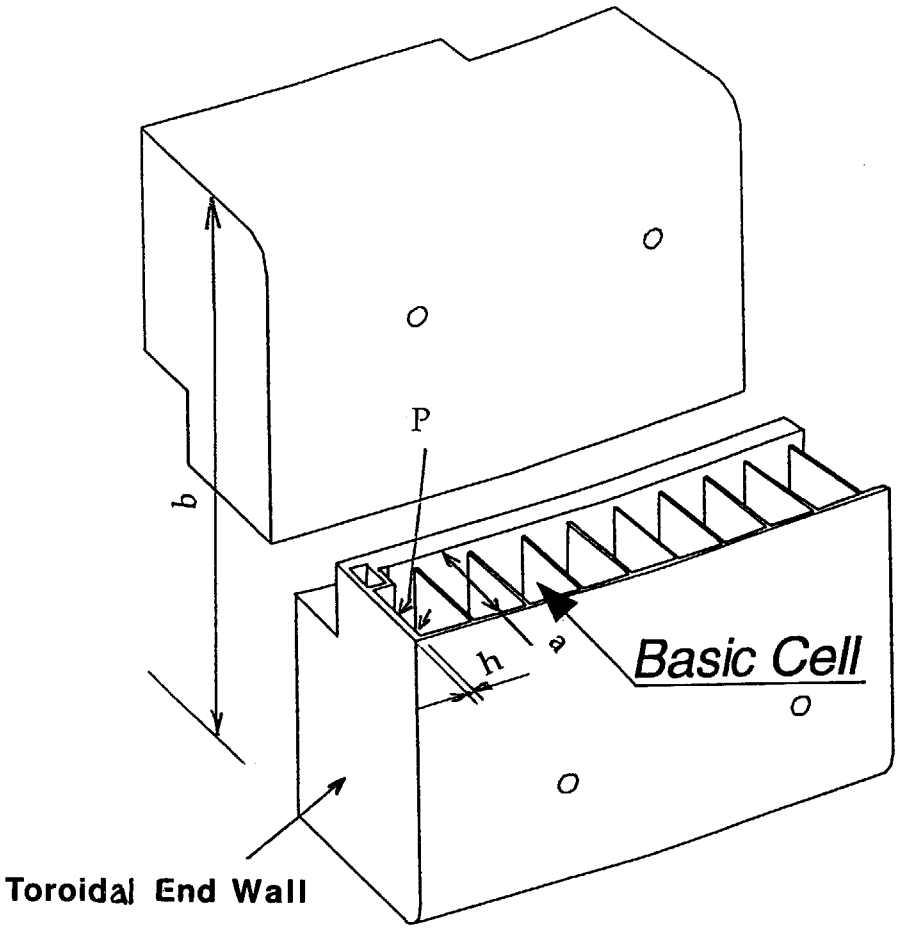

Fig. 3.13 Toroidal end wall of blanket module [1]

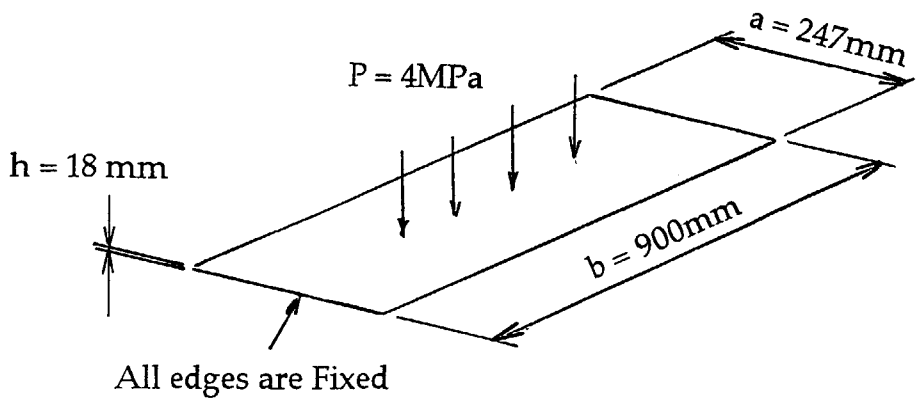

Fig. 3.14 Calculation model

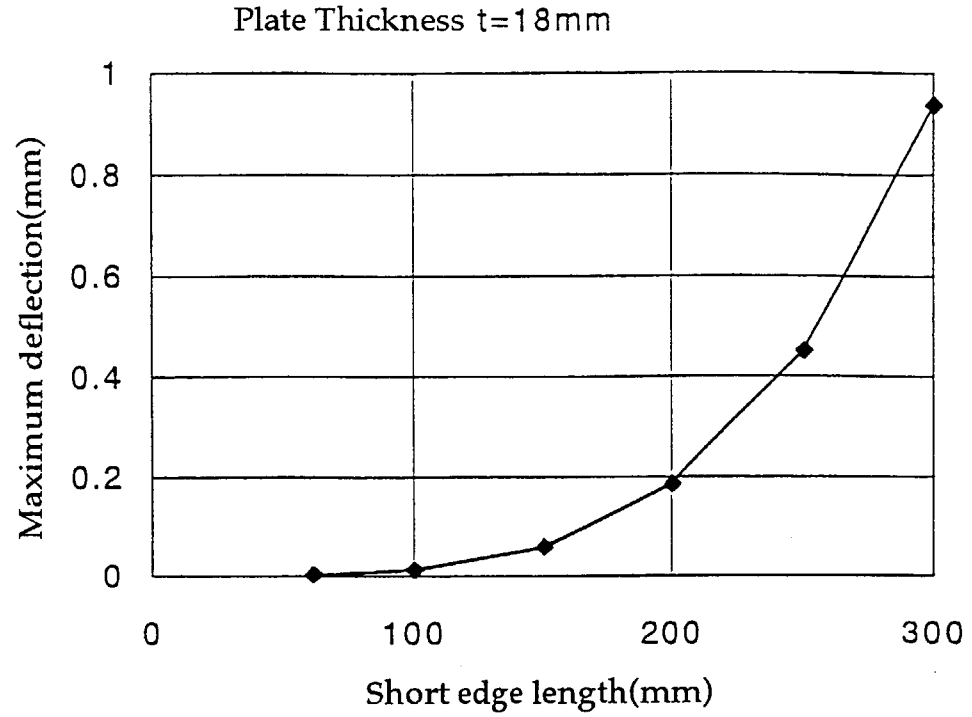

Fig. 3.15 Maximum deflection of toroidal end wall under internal pressure of 4 MPa

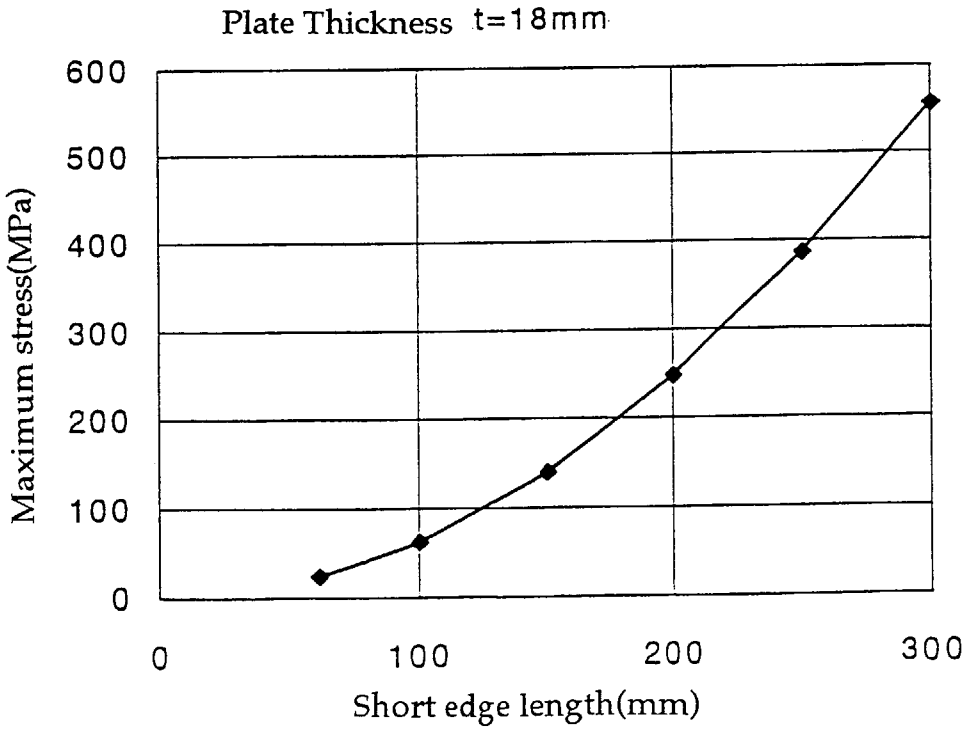

Fig. 3.16 Maximum stress in toroidal end wall under internal pressure of 4 MPa

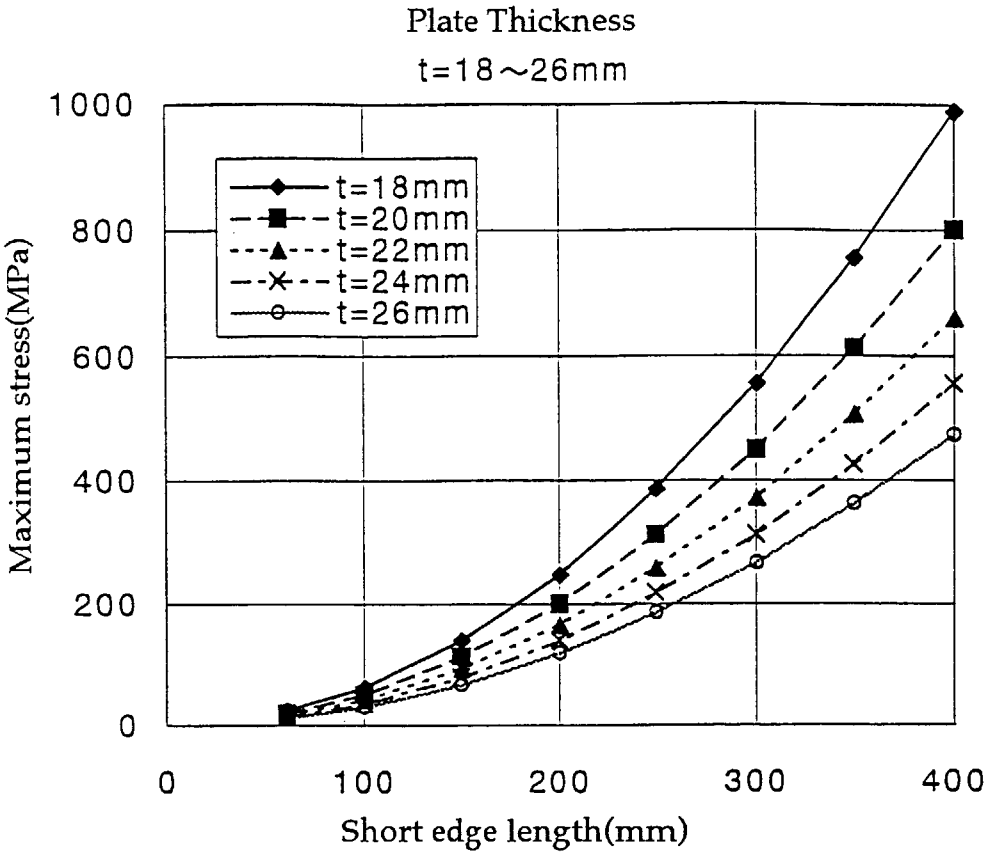

Fig. 3.17 Dependence of maximum stress on plate thickness under internal pressure of 4 MPa

4. Thermo-mechanical Behavior of Be/SS Bonded Interface

In ITER breeding blanket design, beryllium (Be) armor is bonded on stainless steel (SS) structure because of its plasma compatible low atomic number and in order to protect the blanket structure from the off-normal thermal loads. The evaluation of the bonding integrity is important to define the lifetime of the first wall. In this section, Be/SS bonding requirements are discussed in terms of the stresses generated at the bonded interface. Though the bonding techniques for Be/SS are being developed [7], HIP is temporarily assumed for the bonding method of Be/SS with the assumption of HIP temperature at 760 °C in order to evaluate the effect of residual stress during the fabrication.

4.1 2-Dimensional Thermal and Stress Analyses

In order to estimate stress and strain ranges at Be/SS bonded interface during the fabrication process and thermal cycles due to the pulsed plasma operation, 2-dimensional thermal and stress analyses have been carried out. The stress analyses were focused on the stress distribution around the bonded interface, especially at the interface edge. As residual stress remains in the bonded surface after fabrication, elasto-plastic analyses have been applied to consider the plastic behavior of the materials both in fabrication and thermal cycling processes.

4.1.1 Analysis Models

The structure of the breeding blanket first wall (FW) is shown in Fig. 4.1 [1]. The thickness of Be tile is 5 mm and that of SS wall is 13 mm including the coolant channel. The analysis model consists of a half of Be tile and corresponding FW cooling channel as shown in Fig. 4.2. The mesh pattern of the model is shown in Fig. 4.3. Fine meshes are applied to the edge of the bonded interface to calculate detail stress and strain distributions around the edge area.

Figure 4.4 shows the boundary conditions for the thermal and stress analyses. The surface heat flux is 0.5 MW/m^2 and the volumetric heating is 6.5 MW/m^3 for Be tile and 9.1-8.8 MW/m^3 for SS. The heat transfer coefficient is 27400 W/m^2K and the coolant temperature is 145 °C. The boundary conditions for the stress analysis are that the rear surface of SS wall is fixed in the Y-direction as shown in Fig. 4.4 (b). One of the side surfaces of the model has a coupled constraint in the X-direction and the condition of the other side surface is free. The FW at the blanket edge can be modeled by this boundary condition. The elements used in the analysis are generalized plane strain elements.

Temperature response during the thermal cyclic operation is shown in Fig. 4.5. The surface temperature of FW is 295 °C, and the interface temperature is 278 °C after reaching thermal steady state. Figure 4.6 shows the deformation after cooling to room temperature from 760 °C which is the stress free temperature at which Be and SS are assumed to be bonded by HIP. Be tile is compressed by the shrinkage of SS after being cooled to room temperature.

Material properties used in the analyses are shown in Figs. 4.7-4.10. Figures 4.7 and

4.8 are stress-strain curves for Be and SS, respectively. The temperature dependence of Young's modulus is shown in Fig. 4.9 and that of thermal expansion coefficient in Fig. 4.10. Three steps are considered for the stress analysis.
(1) Residual stress after cooling to room temperature from 760 °C
(2) Stress due to plasma operation (burning)
(3) Stress after cooling to room temperature again from plasma operation condition

4.1.2 Analyses Result

Figure 4.11 shows the stress distribution in the Be along the bonded interface after cooling to room temperature from 760 °C. Figure 4.12 shows the stress distribution in the Be along the first wall edge perpendicular to the bonded interface. The dominant stresses to cause crack around the bonded interface are stress perpendicular to the interface (σ_y), especially in tensile mode, and shearing stress (τ_{xy}) along the interface. The σ_y in the Be near the interface is tensile, especially the maximum tensile stress of 300 MPa appears at a little upper position from the bonded interface as shown in Fig. 4.12. Shearing stress, τ_{xy}, in the Be is low compared with the stress in the Y-direction.

Figure 4.13 shows the stress distribution in the Be along the bonded interface under the surface heat flux of 0.5 MW/m^2. Tensile stress in the Y-direction (σ_y) along the bonded interface is less than 50 MPa. Figure 4.14 shows the stress distribution of Be along the first wall edge, and the stress in the Y-direction (σ_y) is compressive. This means that the stresses under the surface heat flux of 0.5 MW/m^2 are insignificant for the failure (exfoliation) of the bonded interface.

Figure 4.15 shows the stress distribution in the Be along the bonded interface after cooling to room temperature following the first plasma operation. Figure 4.16 shows the stress distribution in the Be along the first wall edge. Stress distributions of σ_y and τ_{xy} are very similar to those after HIP treatment (Figs. 4.11 and 4.12). This means that the influence of the residual stress on the bonding integrity is significant. Therefore, the stress in the Y-direction, σ_y, at a little upper position from the bonded interface is, again, dominant for the bonding integrity.

Figure 4.17 shows the stress-strain hysteresis of Be at the bonded interface edge. In the beginning, stress is free at the HIP temperature of 760 °C. During the cooling process after HIP bonding, the strain perpendicular to the bonded interface, ε_y, is compressive while the corresponding stress, σ_y, is slightly compressive first then changes to tensile. (See curve "S22" in Fig. 4.17.) At the end of cooling, the tensile stress σ_y reaches 180 MPa. Then the thermal cycle due to plasma operation causes a hysteresis of the stress σ_y (S22). Another stress, τ_{xy} ("S12" in Fig. 4.17), that would contribute to the exfoliation of the bonded interface, also shows a hysteresis but results in smaller stress and strain ranges than those of σ_y. Figure 4.18 shows the hysteresis for 2 plasma operation cycles. The hysteresis for the second cycle is almost coincident with that for the first cycle.

Figure 4.19 is the stress-strain hysteresis of SS at the bonded interface edge for 2

operation cycles. The hysteresis of σ_y (S22) and τ_{xy} (S12) are in smaller stress and strain ranges than those of Be.

4.1.3 Effect of Castellation

Castellation of the FW surface, i.e., Be armor and even up to some-mm-depth into the SS wall, would be required to reduce the thermal stress. The castellated FW is analyzed with the model shown in Fig. 4.20. The pitch of the castellation is assumed to be 29 mm. The depth of the castellation into SS is assumed to be 2 mm from the Be/SS interface in this model. The boundary conditions are also shown in Fig. 4.20, namely, one side of the SS wall is constrained in the X-direction because of its continuation in this direction.

The deformation after cooling to room temperature following the HIP process is shown in Fig. 4.21. Figures 4.22 and 4.23 show the stress-strain hysteresis of Be and SS at the bonded interface edge, respectively. The hysteresis is very similar to that of the results for the non-castellated first wall. This means that the castellation through the Be armor and up to the depth of 2 mm in SS wall does not have significant influence on the stress-strain distribution in the first wall, especially around the bonded interface edge, or the castellation pitch would need to be much smaller than 29 mm to reduce the stress.

4.2 Assessment Method for Be/SS Joint

There are some parameters proposed to assess the bonding integrity. One of the widely used parameters is a set of the heat flux and the number of cycles in the thermal fatigue tests. These parameters would be used for the confirmation of the bonding integrity. But the most serious problem to use them is that the number of tests and test pieces are limited.

Another parameters are mechanical properties generally used for evaluating fatigue lifetime. Plastic strain range $\Delta\varepsilon_p$ or total strain range $\Delta\varepsilon_{total}$ represents the material characteristic for the fatigue lifetime. But there is a difficulty to define the $\Delta\varepsilon_p$ or $\Delta\varepsilon_{total}$ of a bonded specimen in basic material tests such as using simple tensile specimen. The strain measured in a tensile test of a bonded specimen is not the strain of the thin bonded layer but the added strains of bonded materials.

The stress range $\Delta\sigma$, especially of the stress perpendicular to the interface, $\Delta\sigma_y$, or the shearing stress, $\Delta\tau_{xy}$, also seems to be one of the parameters to assess the bonding integrity. Because these stresses are dominant to initiate a crack at the bonded interface. It is easy to define these stresses in basic material tests.

Figure 4.24 shows the stress and strain ranges for the Be/SS FW under the fabrication process and following pulsed plasma operation. From the stress-strain hystereses, it could be assessed that the stress and strain ranges of Be at the bonded interface edge are $\Delta\sigma_y$ = 241 MPa and $\Delta\varepsilon_y$ = 0.00171, respectively. Those ranges of SS are $\Delta\sigma_y$ = 87 MPa and $\Delta\varepsilon_y$ = 0.00391, respectively, as shown in Fig. 4.19. The Be and

SS themselves should be required to withstand against the stress or strain range.

These assessment parameters should be used properly by the position of failure. If failure starts at the bonded interface, stress range would be a preferable assessment parameter because of no definition of strain range available at the bonded interface. On the other hand, if failure starts in the bonded material, strain range would be preferable. Strain range is the commonly used parameter for assessment of the fatigue lifetime of metal.

One of possible assessment steps can be considered as follows:

(1) Screening of the bonding procedure
Bonding procedure is screened with tensile tests and/or shearing tests at room and elevated temperatures.

(2) Evaluation of the bonding integrity
Bonding lifetime is evaluated by fatigue tests and/or thermal fatigue tests. As the practicable numbers of thermal cycles and specimens are limited, the relation between stresses or stress ranges and the allowable number of cycles (fatigue lifetime at elevated temperatures and/or thermal fatigue lifetime) should be established. Then the bonding integrity at the first wall could be evaluated by analyzing the structural responses of the first wall under the operation conditions and comparing them with the established relation.

(3) Confirmation of the bonding procedure
Candidate bonding procedure should be confirmed by cyclic heat load test. The change of material characteristic due to irradiation, heat treatment and softening/hardening should be also included by using such affected specimens.

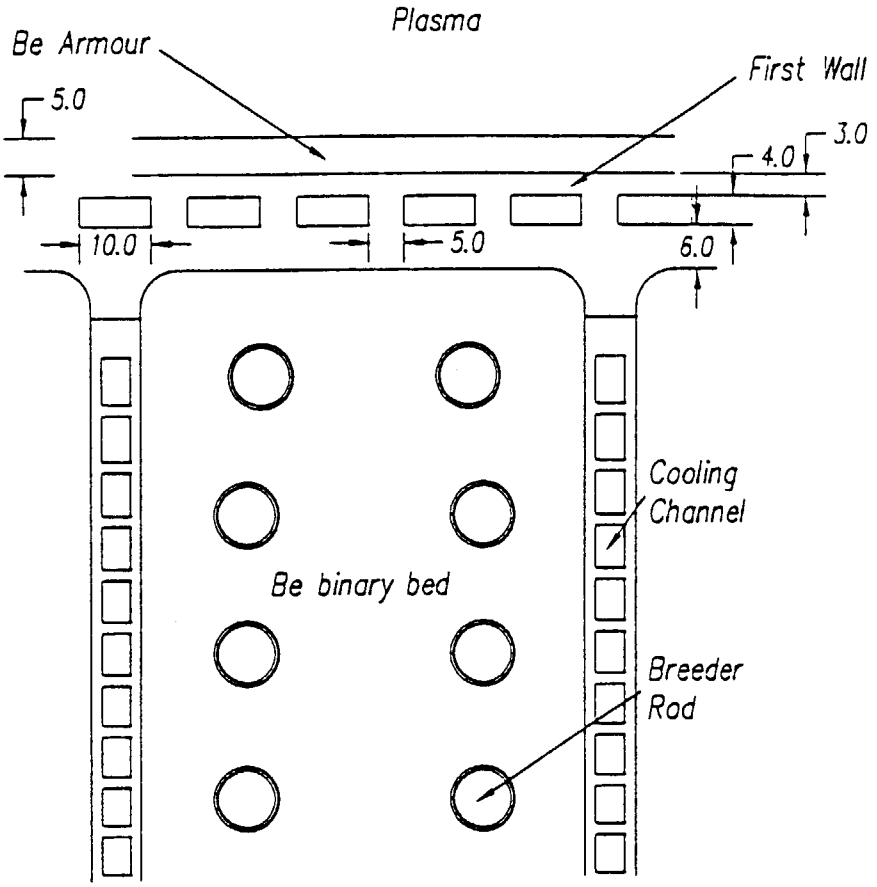

Fig.4.1 Basic cell of Breeding Blanket Module [1]

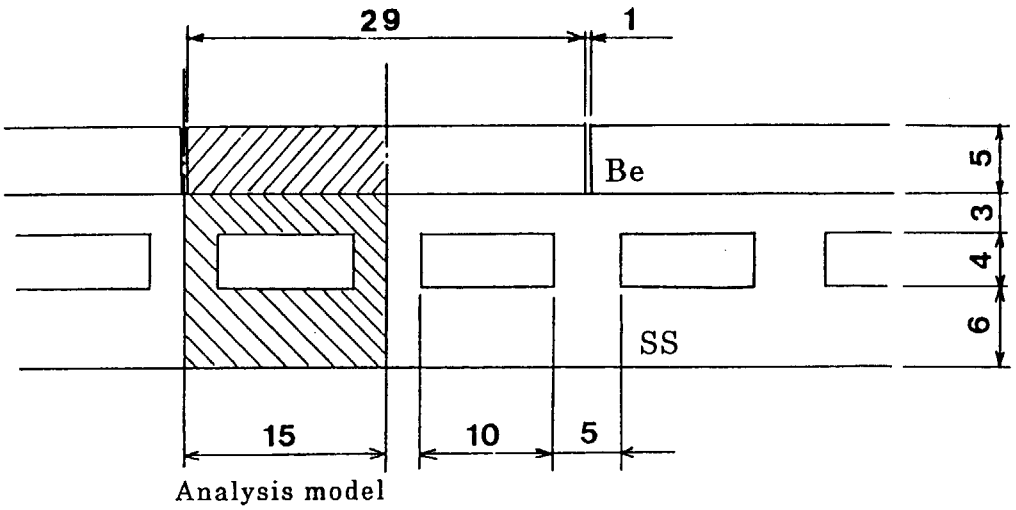

Fig. 4.2 Breeding Blanket First Wall

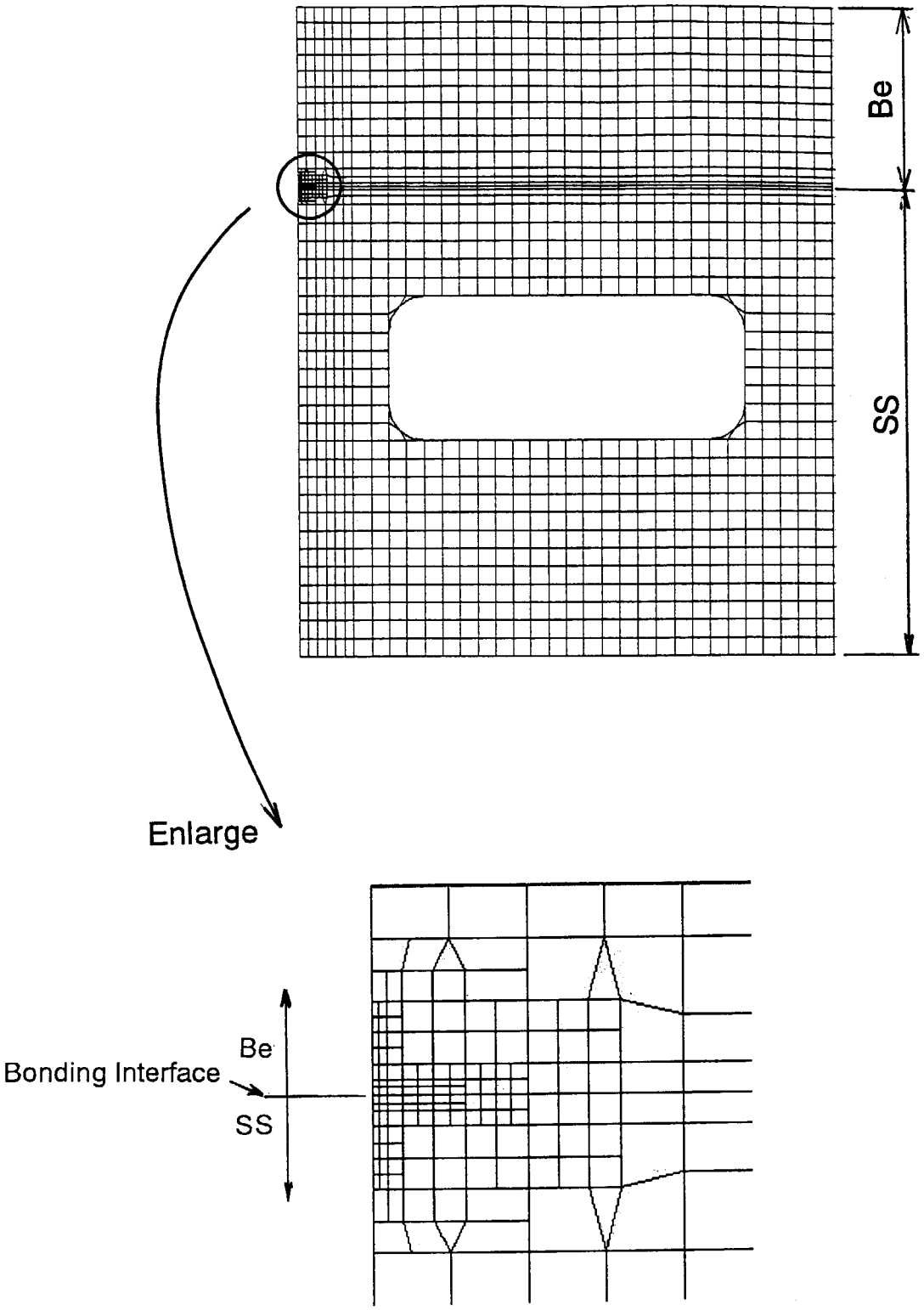

Fig. 4.3 Mesh Pattern for First Wall

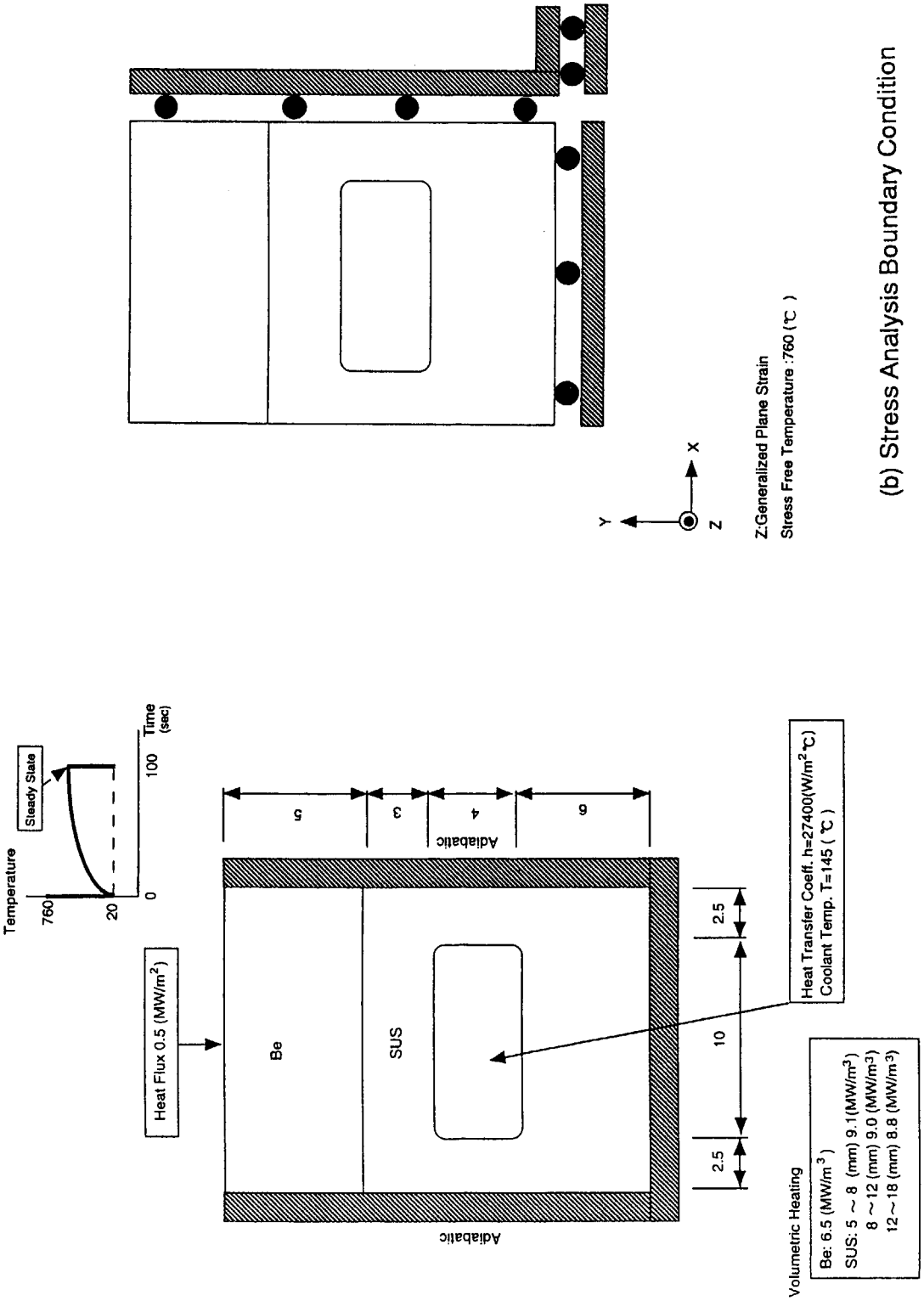

(a) Thermal Analysis Boundary Condition

(b) Stress Analysis Boundary Condition

Fig. 4.4 Boundary Conditions

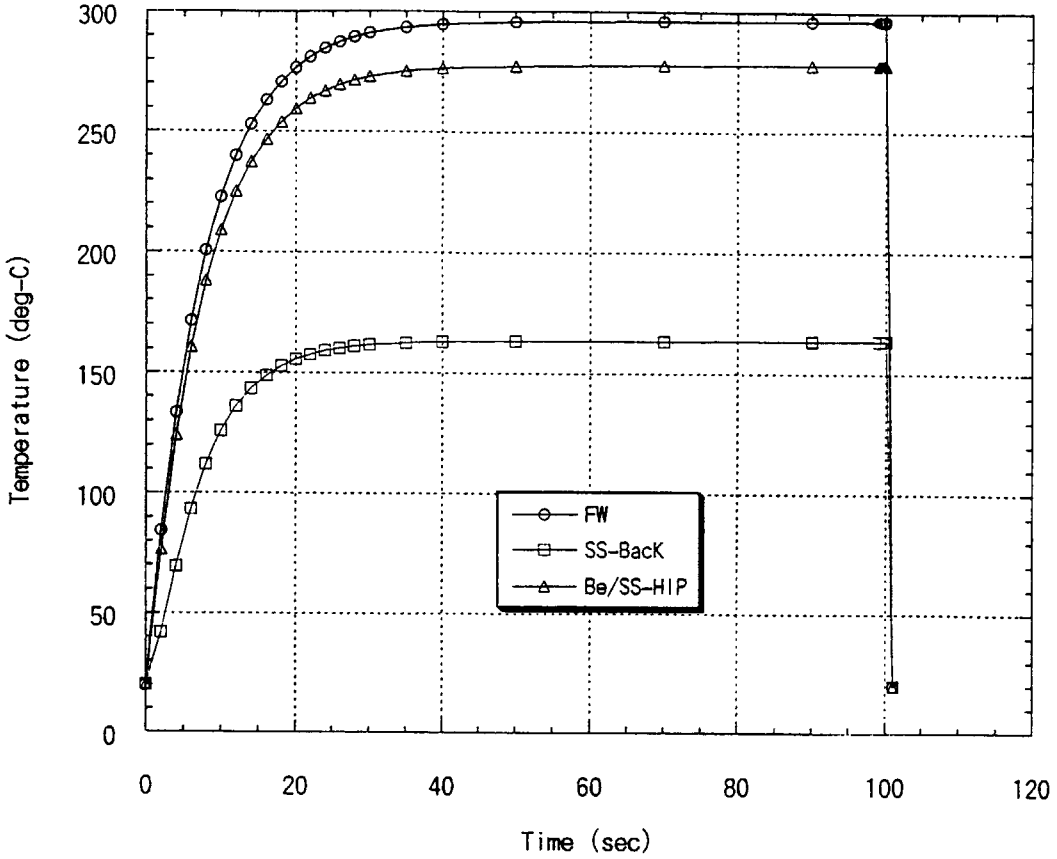

Fig.4.5 Temperature Response under 0.5 MW/m^2

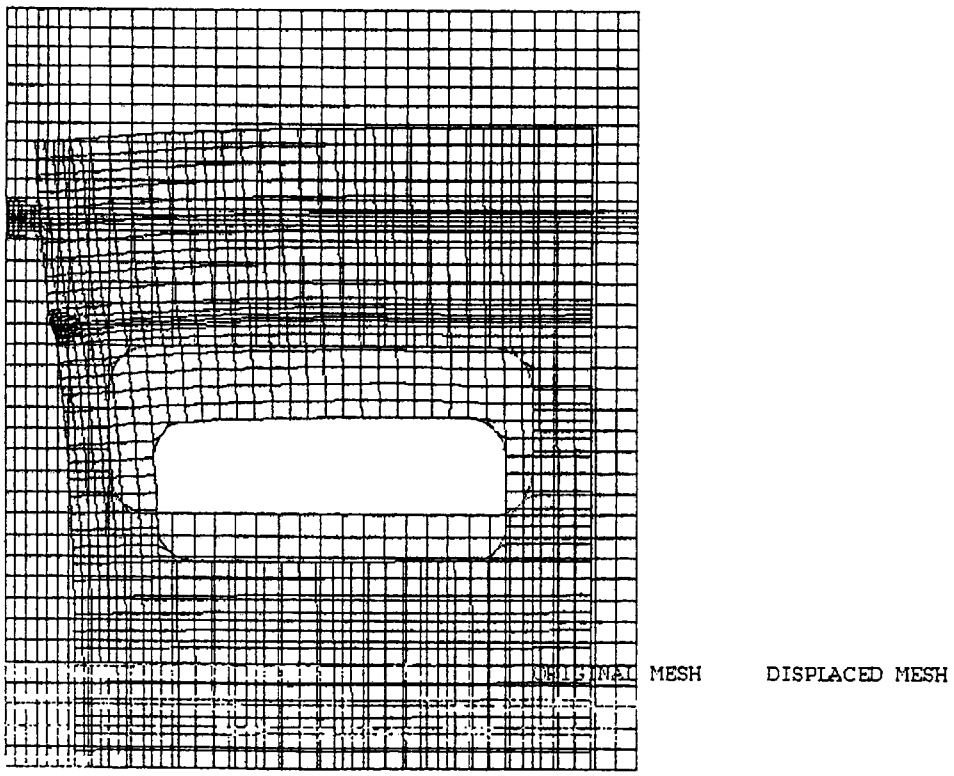

Fig.4.6 Deformation after Cooling to Room Temperature from 760℃

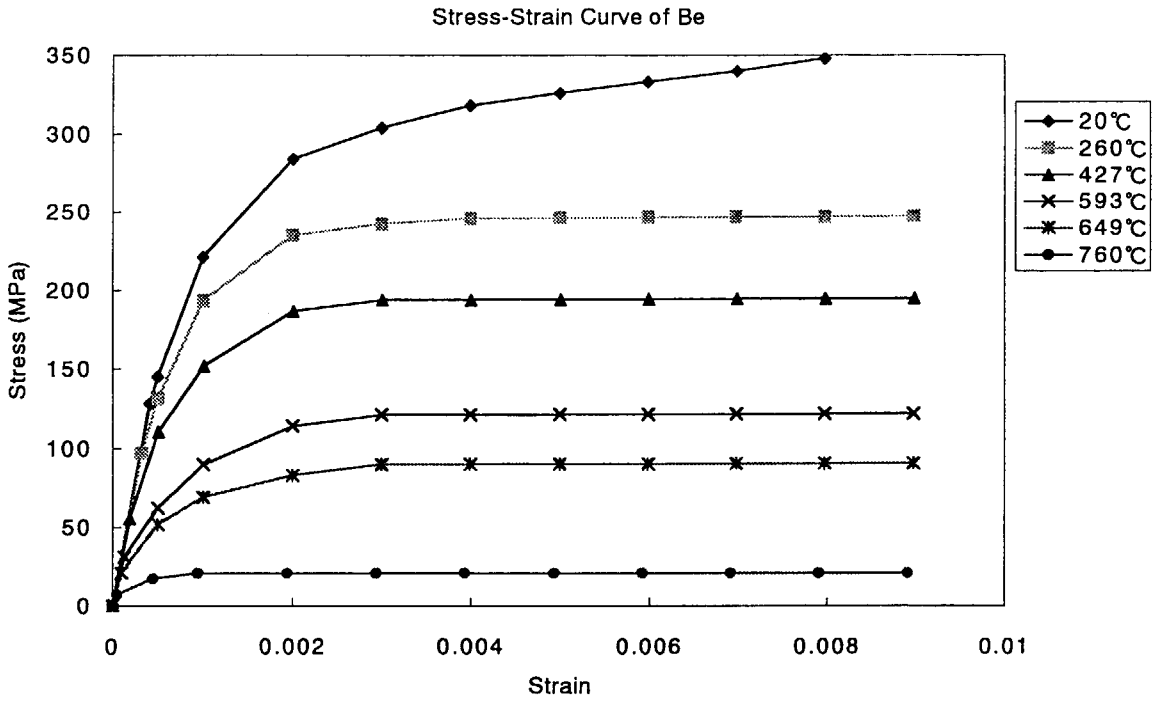

Fig. 4.7 Stress-Strain Curve of Be

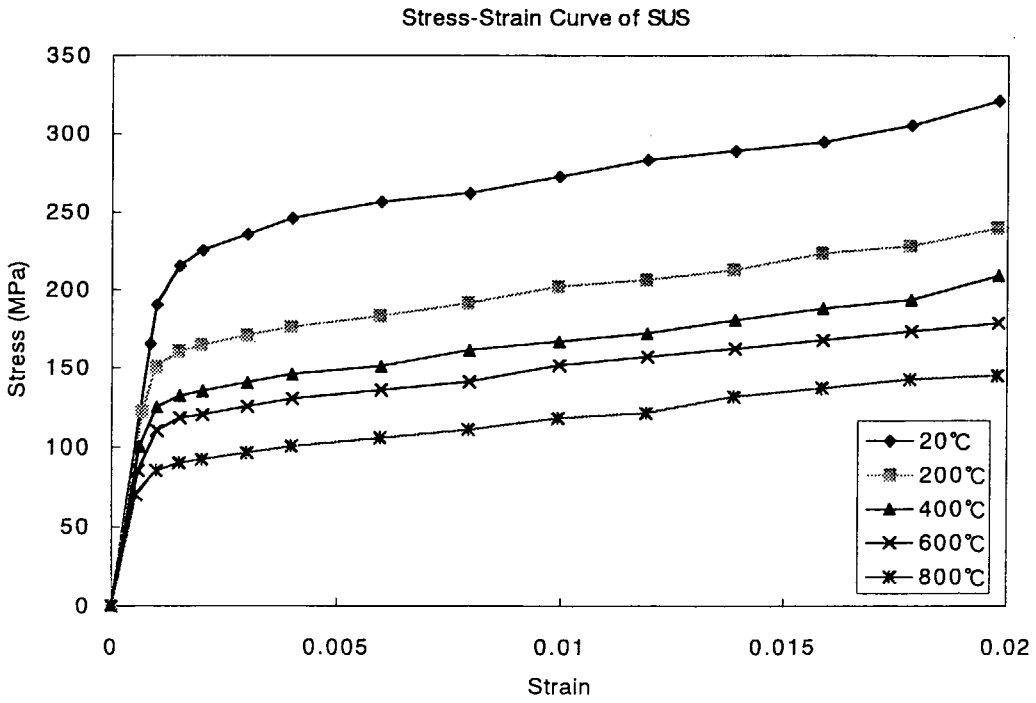

Fig. 4.8 Stress-Strain Curve of Stainless Steel

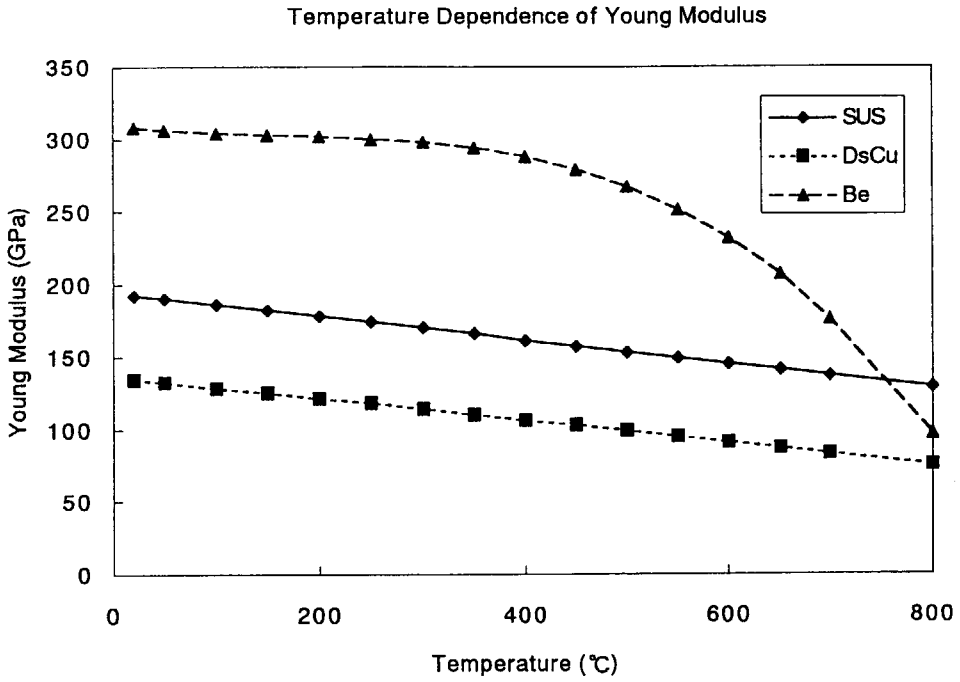

Fig. 4.9 Temperature Dependence of Young Modulus

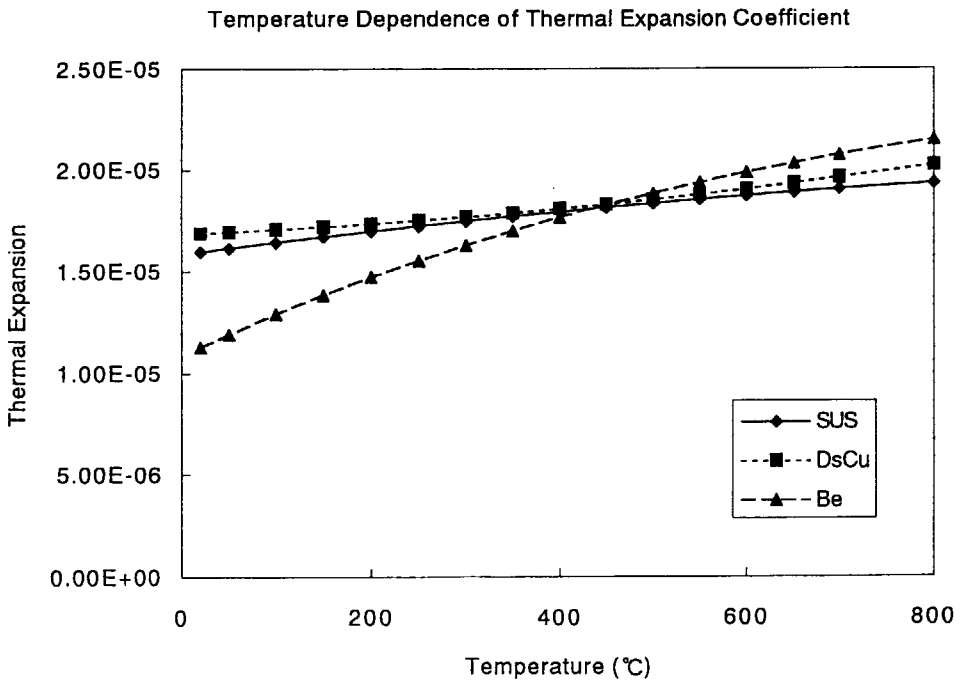

Fig. 4.10 Temperature Dependence of Thermal Expansion Coefficient

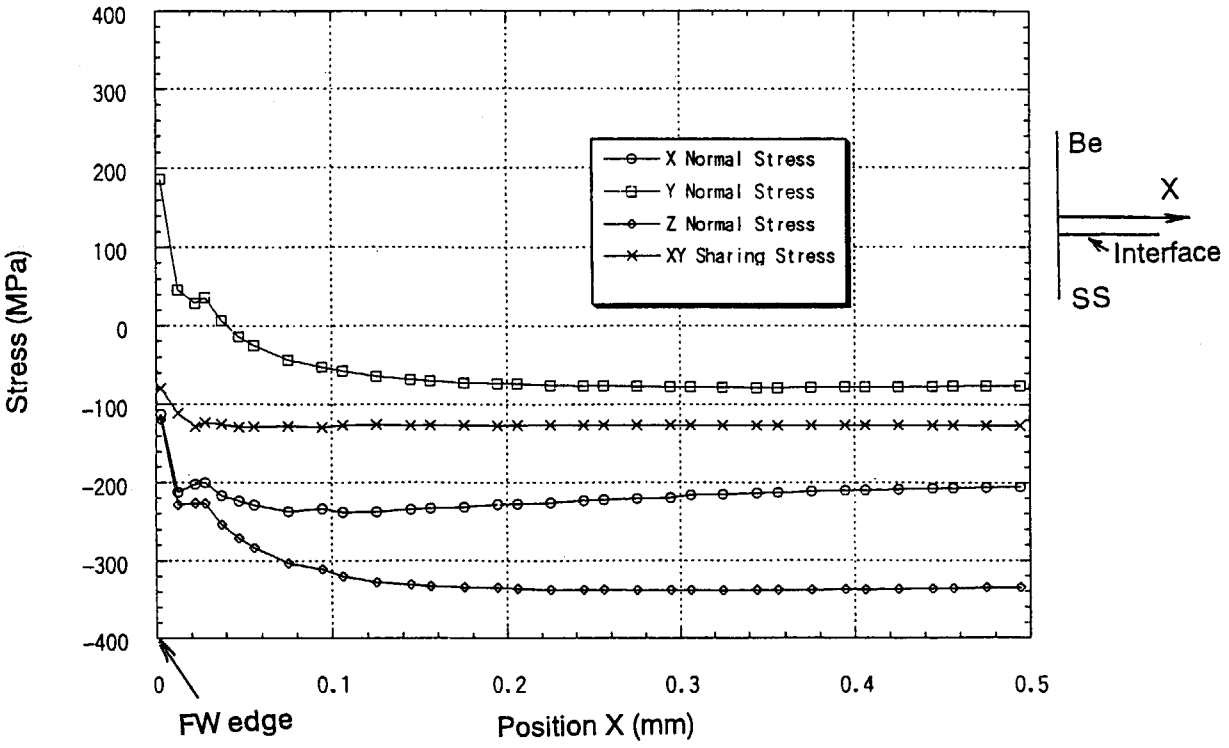

Fig. 4.11 Stress Distribution of Be along the Bonding Interface after Cooling to Room Temperature from 760℃

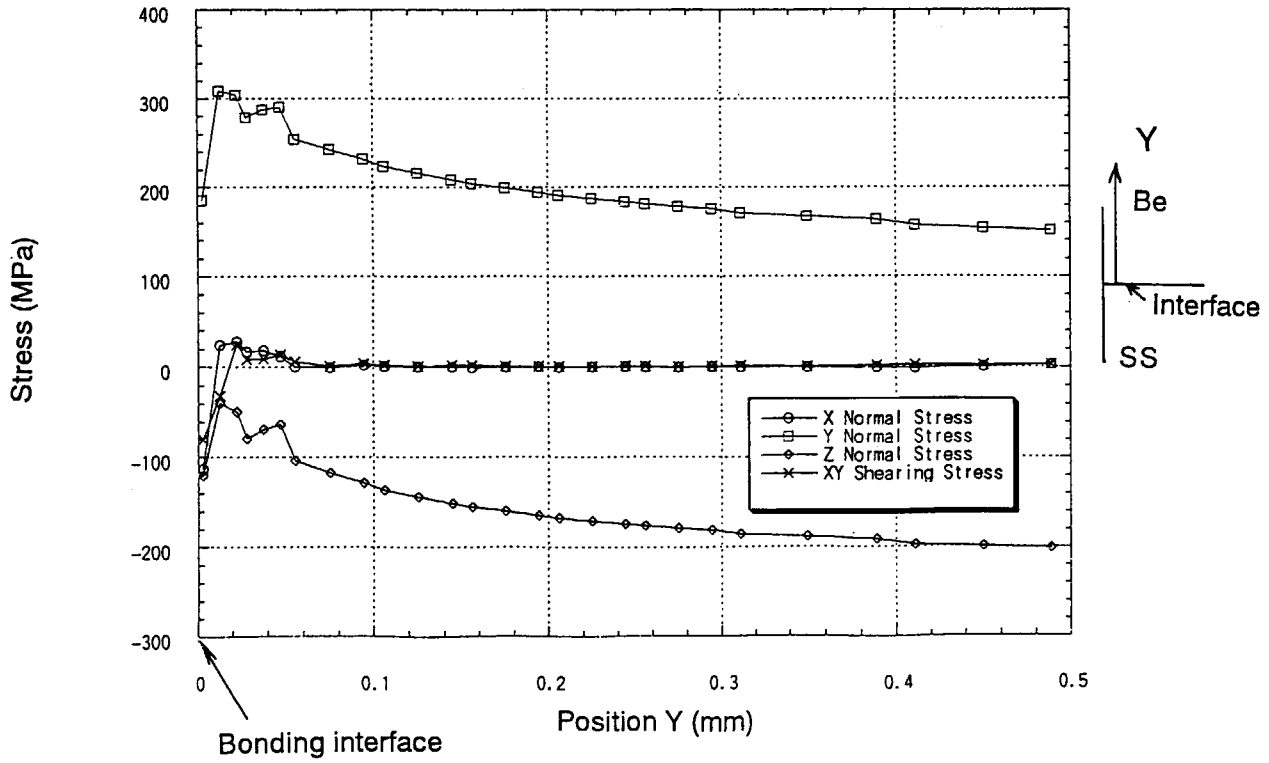

Fig. 4.12 Stress Distribution of Be along the First Wall Edge after Cooling to Room Temperature from 760℃

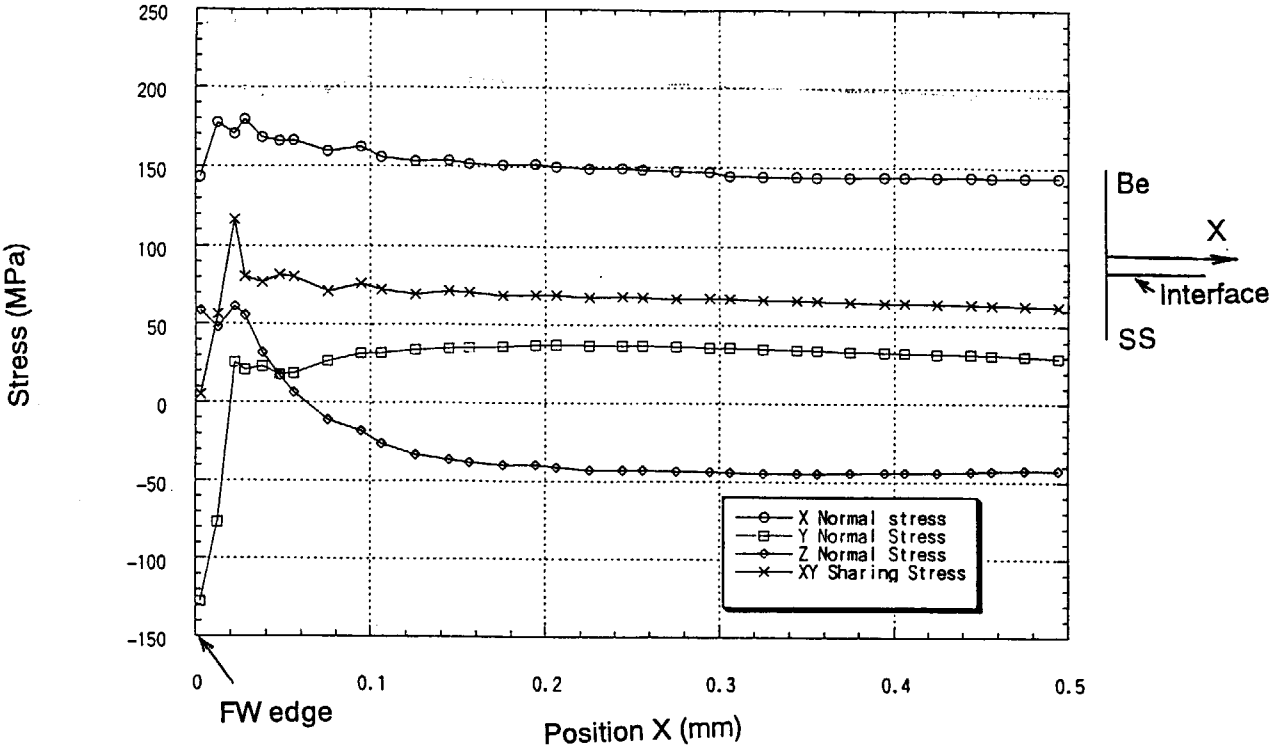

Fig. 4.13 Stress Distribution of Be along the Bonding Interface under the Heat Load of 0.5 MW/m^2

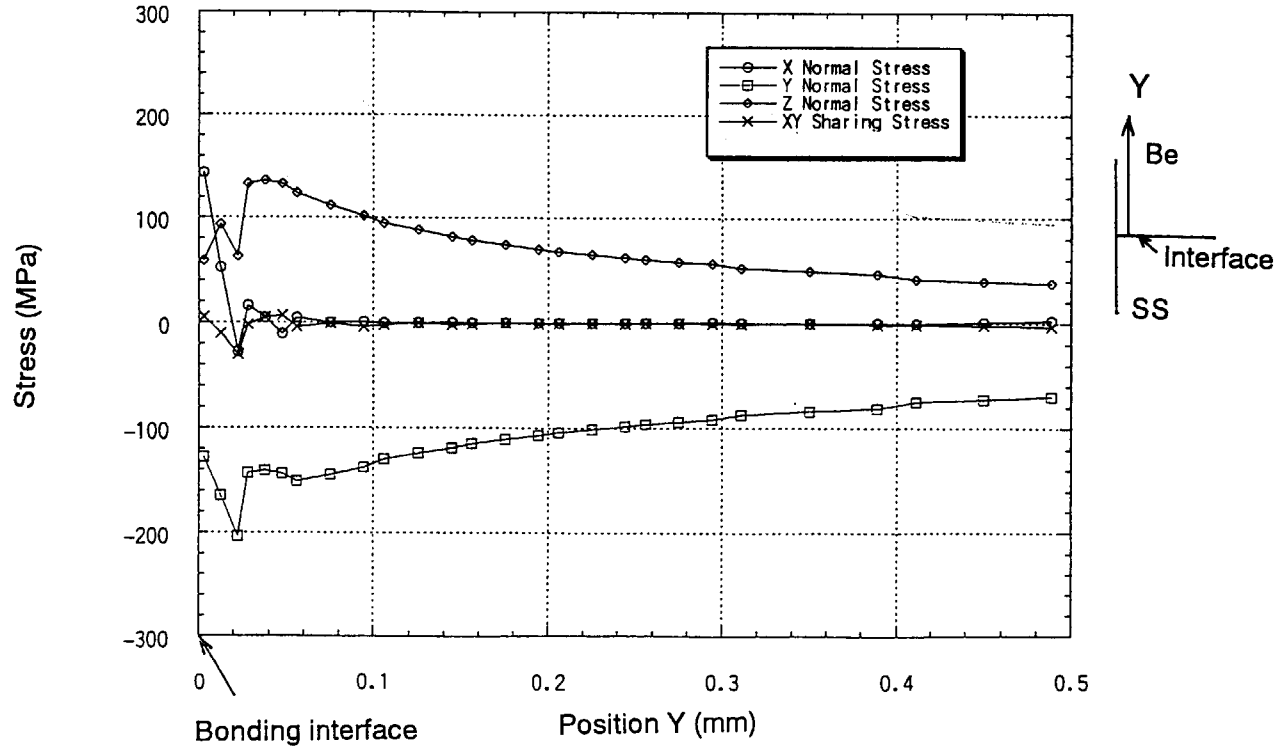

Fig. 4.14 Stress Distribution of Be along the First Wall Edge under the Heat Load of 0.5 MW/m^2

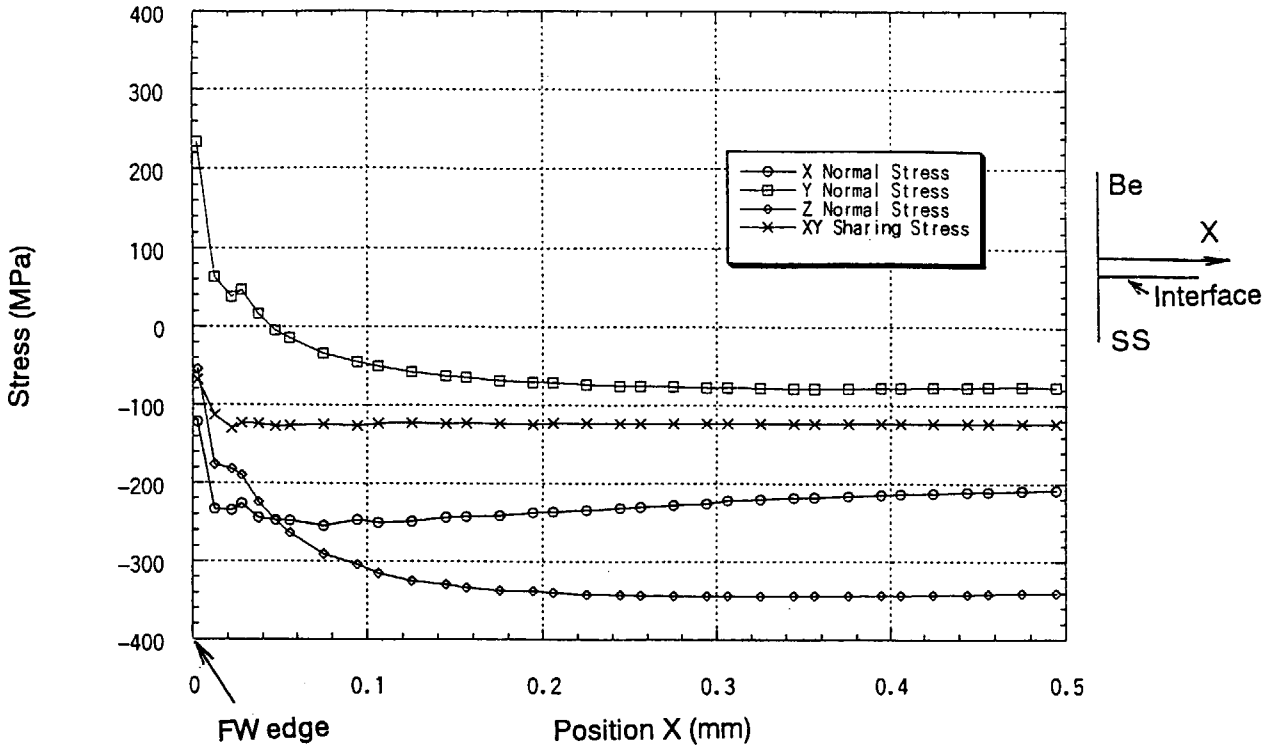

Fig. 4.15 Stress Distribution of Be along the Bonding Interface after Cooling to Room Temperature in the First Operation Heat Cycle

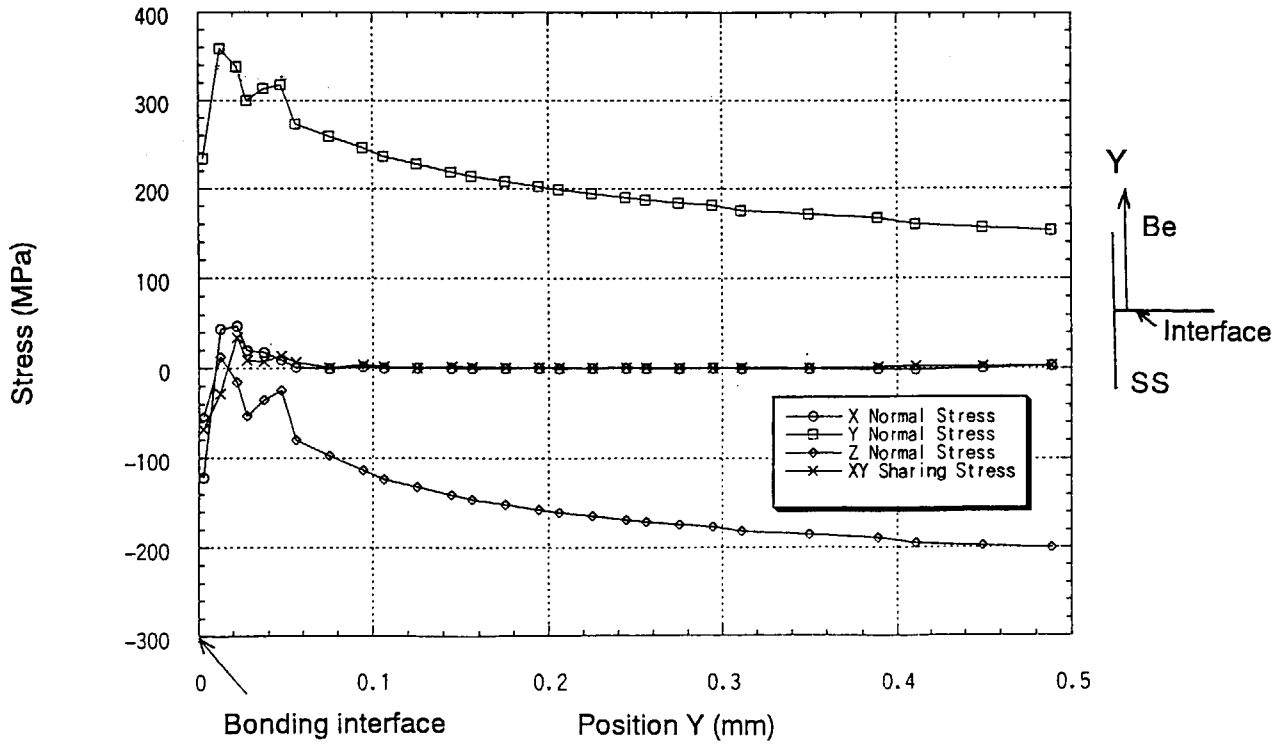

Fig. 4.16 Stress Distribution of Be along the First Wall Edge after Cooling to Room Temperature in the First Operation Heat Cycle

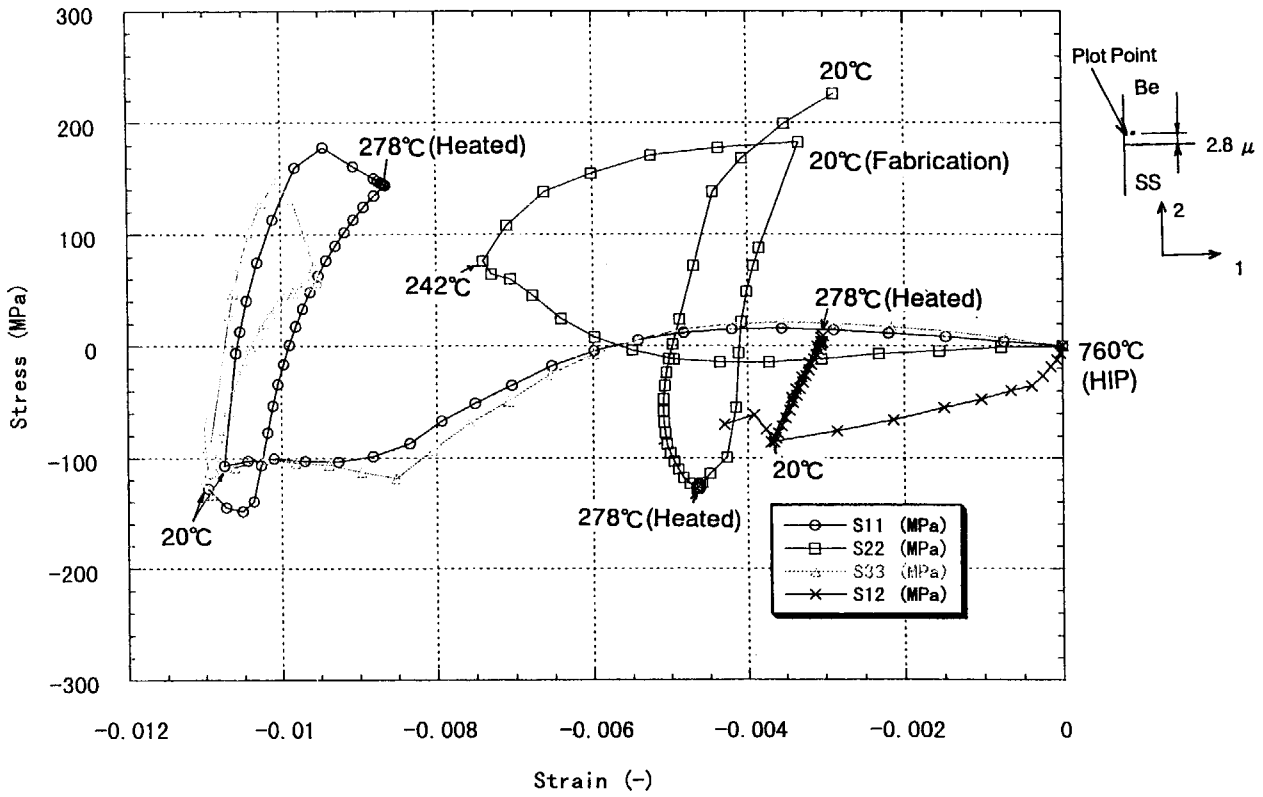

Fig. 4.17 Stress - Strain Hysteresis of Be at the Be/SS Bonding Interface Edge

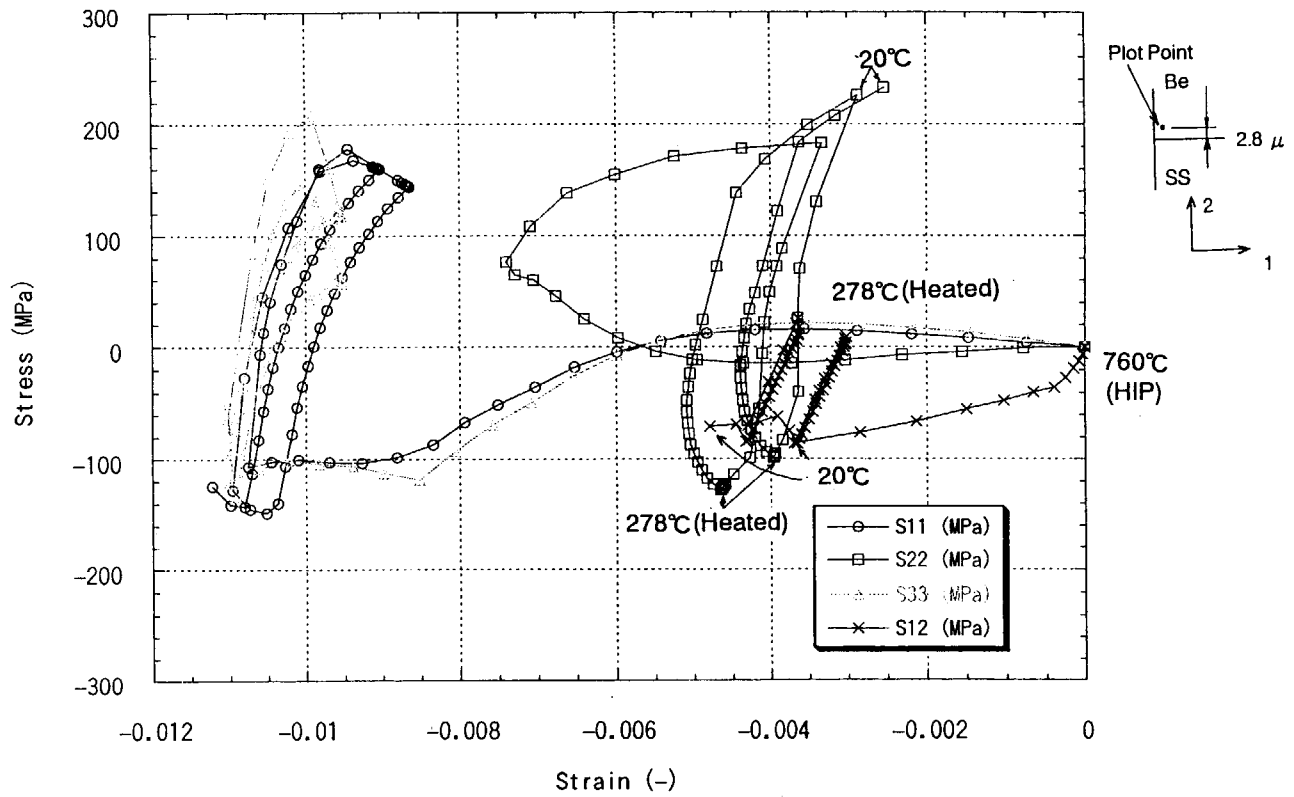

Fig. 4.18 Stress - Strain Hysteresis of Be at the Be/SS Bonding Interface Edge for 2 cycles

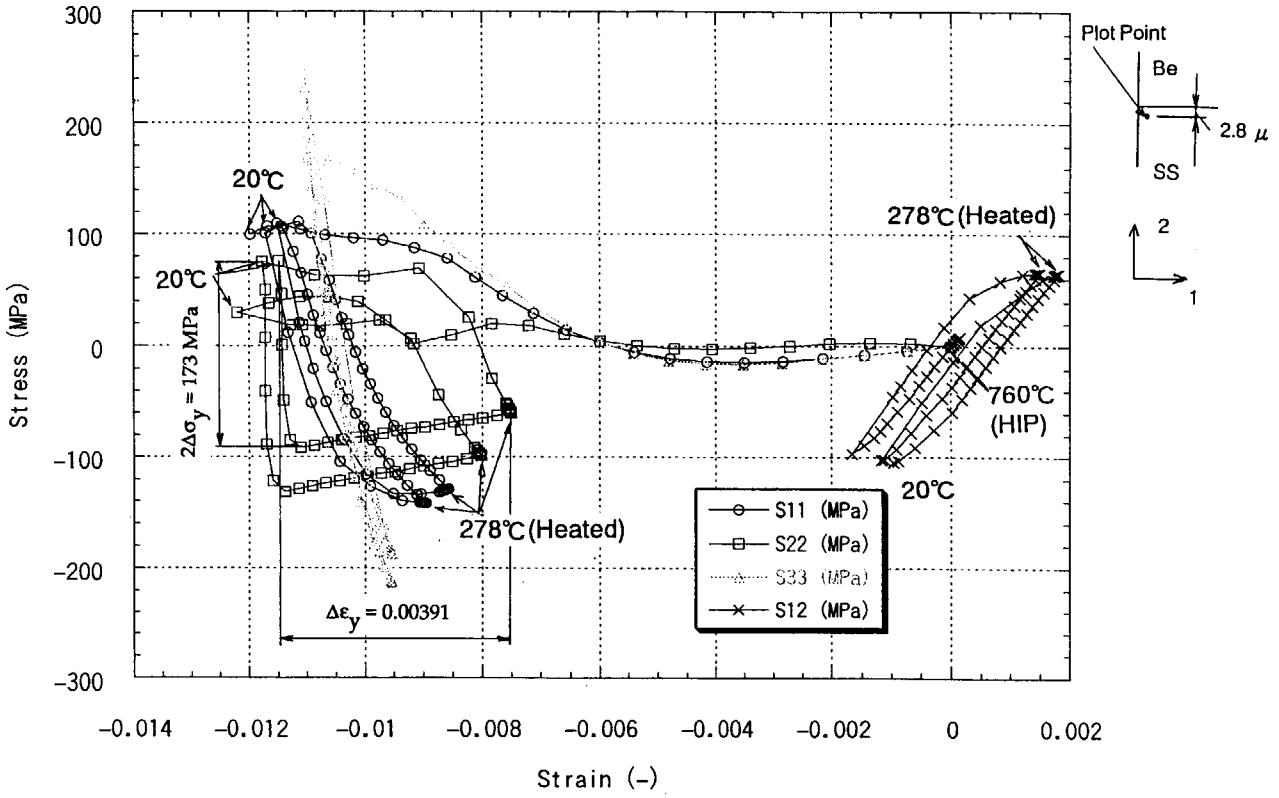

Fig. 4.19 Stress - Strain Hysteresis of SS at the Be/SS Bonding Interface Edge for 2 cycles

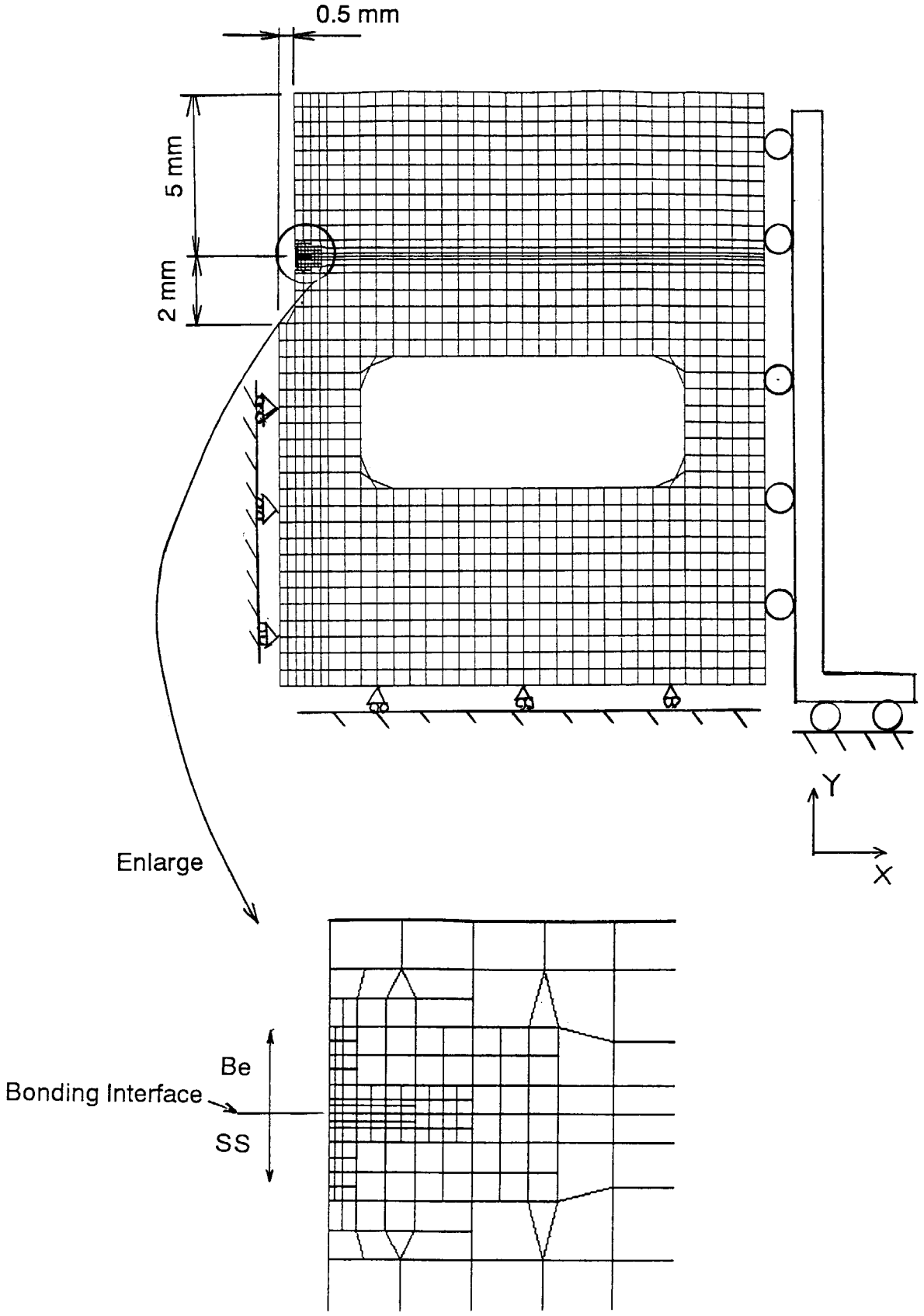

Fig. 4.20 Mesh Pattern for Castelated First Wall

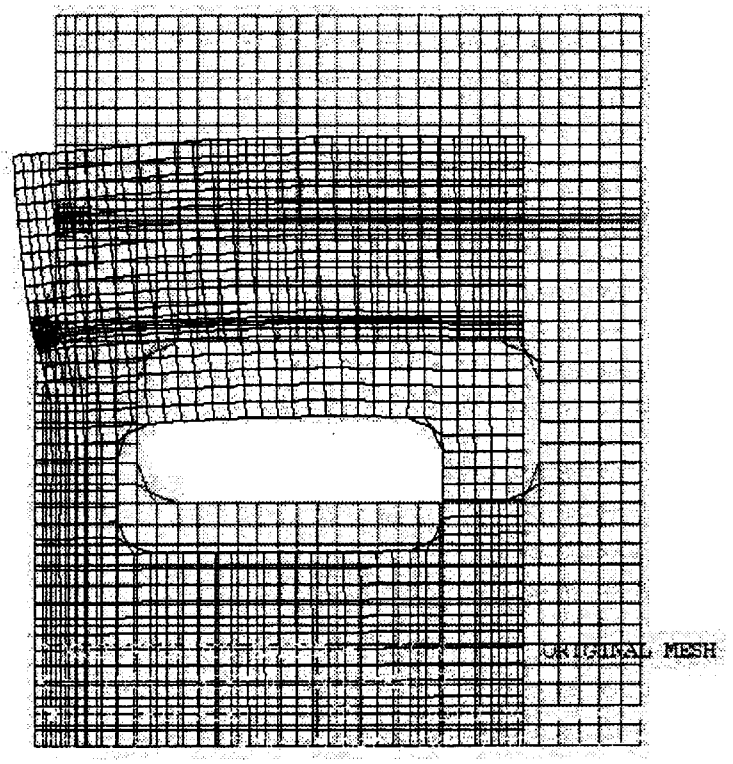

Fig. 4.21 Deformation after Cooling to Room Temperature from 760℃ for Castelated First Wall

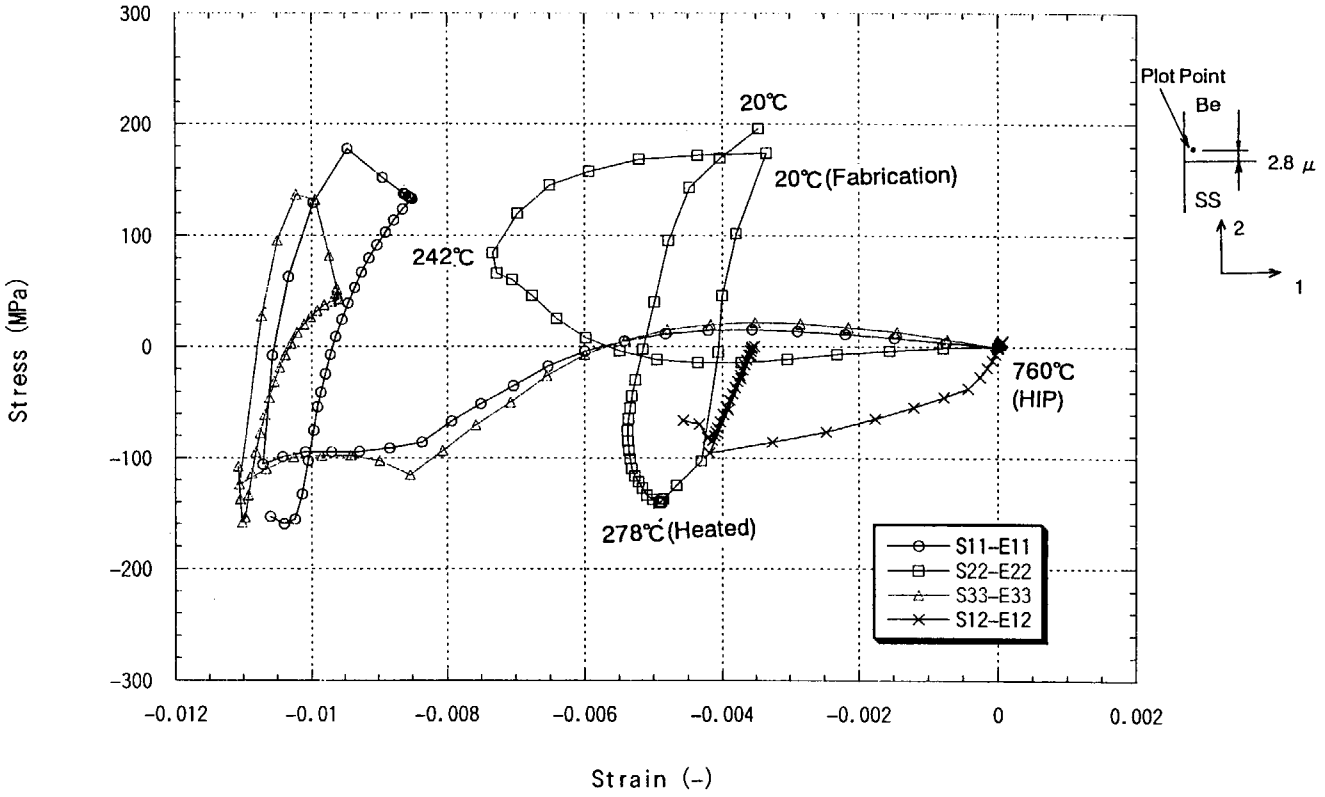

Fig. 4.22 Stress - Strain Hysteresis of Be at the Be/SS Bonding Interface Edge for Castelated First Wall

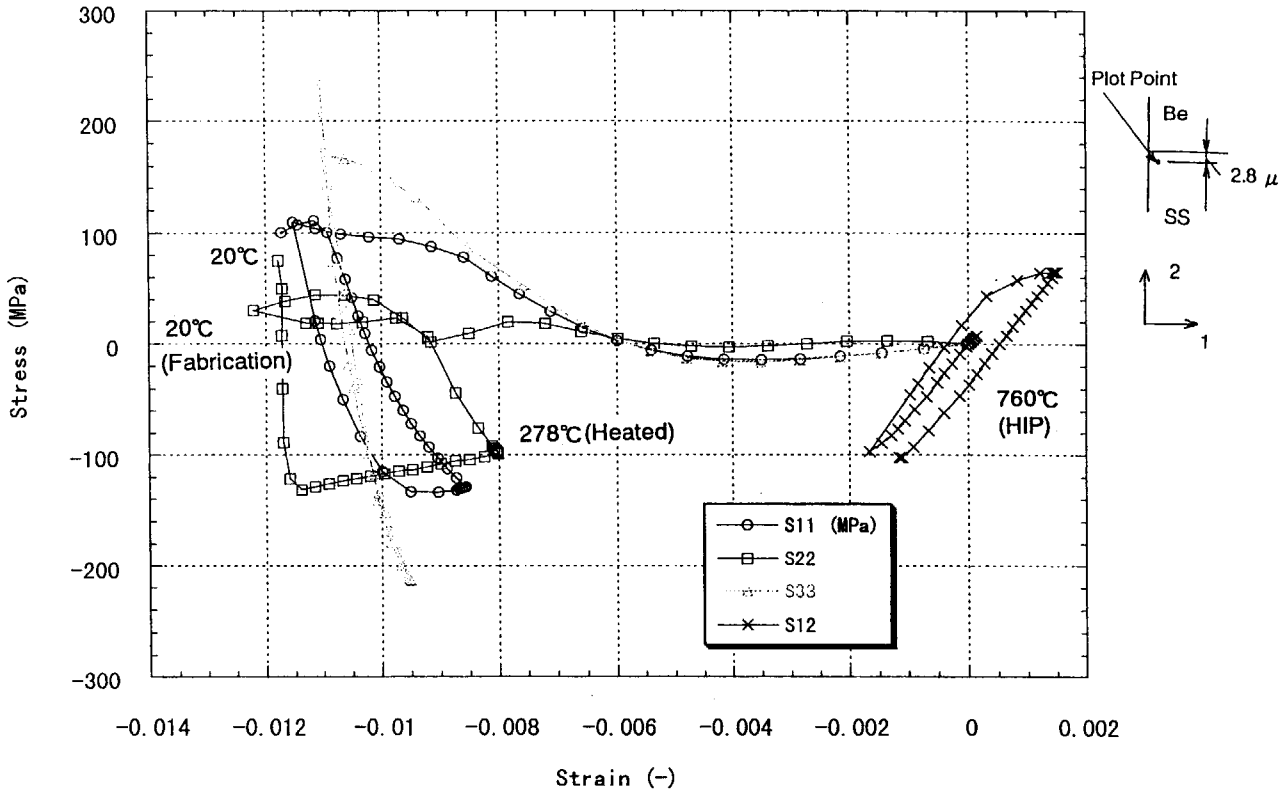

Fig. 4.23 Stress - Strain Hysteresis of SS at the Be/SS Bonding Interface Edge for Castelated First Wall

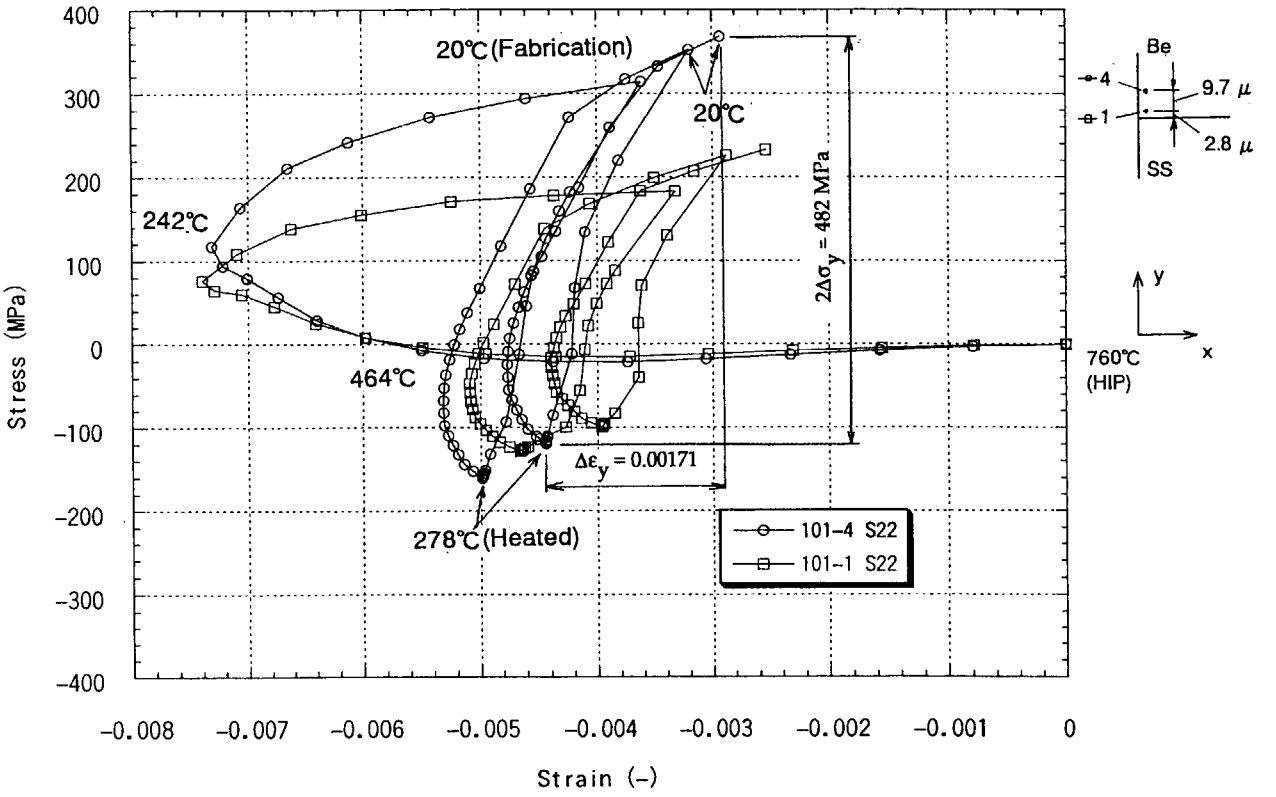

Fig. 4.24 Stress - Strain Hysteresis of Be at the Be/SS Bonding Interface Edge

5. Blanket Module Fabrication

The ITER breeding blanket module exhibits a toroidal repetition in which the space between two adjacent cooling panels represents a basic cell as shown in Figs. 5.1 and 5.2 [1, 7]. As shown in these figures and Fig. 5.3, a small bundle of poloidal breeder rods is located in the basic cell. Each breeder rod is composed of a steel tube with the breeder material in the form of a pebble bed inside. All the space between the breeder rods and the surrounding structures (the first wall, cooling panels and the shield plate) is filled with the neutron multiplier material also in the form of a pebble bed. In this section, a fabrication procedure of the breeding blanket is investigated.

5.1 Overall Fabrication Procedure

In the fabrication procedure, the parts of the breeding blanket such as the first wall, the structure for the front access hole, the cooling panel, the breeder rod bundle, the toroidal end wall and the shield plate are separately fabricated and assembled one by one. The bonding of Be armor on the fist wall will follow this fabrication of the blanket box structure with the internals except for Be neutron multiplier pebbles. The insertion of the Be pebbles will be the final step of the fabrication. The overall fabrication procedure is summarized in Fig. 5.4.

5.2 Fabrication of First Wall

For the fabrication of the first wall, a SS inner plate, a SS outer plate and SS rectangular tubes shown in Fig. 5.5 are assembled and joined by Hot Isostatic Pressing (HIP). The inner plate is prepared for sandwiching the rectangular tubes together with the outer plate and also for preventing a excessive deformation during the HIP process while maintaining the specified curvature of the first wall surface. Especially for the latter purpose, a thick plate, e.g., 30-50 mm or even up to 100 mm, is used for the inner plate. The thick plate is bent to have approximate toroidal curvature first and then machined for the specified curvature on the first wall surface.

The outer plate is thinner, e.g., 3-5 mm, leaving a thickness for final machining. The outer plate is divided in the toroidal direction to accommodate the toroidal curvature of the blanket module. The number of the toroidal pieces would be 15 or more to minimize the assembling gap between adjacent pieces as shown in Fig. 5.6. Because the gaps in the assembly are likely to cause deformation during the HIP process, thus to be minimized.

The rectangular tubes and the outer plate are bent to have the specified poloidal curvature including the top and bottom corner regions and assembled to the inner plate as shown in Fig. 5.7. The outer surface of the assembly is, then, sealed by tungsten inert gas (TIG) welding and joined by HIP with the conditions of temperature at 1050 °C, pressure of 150 MPa and holding time of 2 hours.

For the part where the front access hole is provided, an extruded boss structure as shown in Fig. 5.8 needs to be prepared on the inner surface of the first wall structure. This boss structure is used for the coolant connection to the structure of the front access hole as shown in Fig. 5.8. (See section 5.7 for the connection method

of the first wall and the front access hole structure.) Figures 5.9 and 5.10 show a fabrication method of the boss structure. Namely, rectangular tubes are assembled through the inner plate in the assembly to be HIP bonded. After the HIP bonding, the hatched region in Fig. 5.10 is machined out.

5.3 Fabrication of Front Access Hole Structure

The front access hole structure is a thick circular tube with drilled coolant channels as shown in Fig. 5.8. Both longitudinal ends are machined to provide coolant collectors for connecting with the first wall and making the return flow of the coolant. (See Fig. 5.17.)

5.4 Fabrication of Cooling Panel

The HIP bonding is also applied to fabricate the cooling panel in similar manner to the first wall. However, thin plates are used to sandwich the rectangular plate for the cooling panel instead of the thick inner plate for the first wall. The concept of the cooling panel is shown in Fig. 5.11. Here, TIG or electron beam (EB) welding of the rectangular tube at top and bottom corners before assembling for HIP is considered. Because a bending radius larger than about 50 mm would be required for the rectangular tube to avoid its excessive deformation during the bending. This required radius would make the tube arrangement too sparse for efficient heat removal. If the above-mentioned bending radius is allowed, the bending, not the welding, of the tube will be adopted. If the tubes are not necessary to be placed side by side, two thin plates sandwiching the tubes are machined to have grooves on one surface each to mate the rectangular tubes.

5.5 Fabrication of Breeder Rod Bundle

A fabrication procedure of the breeder rod is shown in Fig. 5.12. A part of a circular tube near the lower end is expanded to mate the tube support provided in the lower rod end structure. This expanded part is provided for allowing the differential movements and rotation between the tube and the support due to thermal expansion of the tube. The expansion of the tube will be performed by an internal high pressure process as shown in Fig. 5.13. The external surface of the expanded part is coated to avoid the seizing of the tube with the support, e.g., by TiN or Ti_2N. After the bending of the partly expanded tube, a SS porous plug is attached inside the lower end of the tube. This porous plug allows the flow of the helium purge gas while it prevents the breeder pebbles from spilling out of the tube. Then the breeder pebbles are filled in the tube with vibration, and the upper porous plug is attached. Finally, an outer ring made of SS is welded to the upper end of the breeder tube (rod) to mate the tube support provided in the upper rod end structure.

A fabrication procedure of the rod end structure is illustrated in Fig. 5.14. For both of the upper and lower rod end structures, the same structure is used. It is fabricated simply by machining and drilling of a SS block or thick plate and TIG welding of the purge gas manifold.

The fabricated breeder rods and the rod end structures are assembled to form a breeder rod bundle as shown in Fig. 5.15.

5.6 Fabrication of Toroidal End Wall

The fabrication method and procedure for the toroidal end wall shown in Fig. 5.16 are basically the same as those for the cooling panel. Attention should also be paid on the required coolant tube arrangement and applicable bending radius of the tube.

5.7 Assembly of Fabricated Parts

The above-fabricated parts are assembled, basically from the front to the back with the following procedure:

(1) The front access structures are connected to the bosses from the first wall by TIG welding at the coolant collector. (Fig. 5.17)
(2) The cooling panels are welded to the first wall by narrow gap TIG (NGTIG) or laser welding. A cooling panel at one toroidal end is welded first and then one after another to the other end (Fig. 5.18), or a cooling panel in the middle first and one after another to the both ends.
(3) The breeder rod bundles are inserted into the first wall structure (with top/bottom walls) by sliding along a key provided on the inner surface of the top/bottom walls. (Fig. 5.19)
(4) The manifolds for the cooling panel coolant are welded by TIG welding. Purge gas manifolds are also welded to the rod end structures by TIG welding. (Fig. 5.20) Concepts for the coolant manifold placement are illustrated in Figs. 5.21 and 5.22, either of which will be selected after detail examination of the space available in the blanket. A fabricating process of the manifold is shown in Fig. 5.23.
(5) The toroidal end walls are welded to the first wall and top/bottom walls by TIG or NGTIG welding. Then the shield plate is welded to top/bottom walls and the toroidal end walls by TIG or NGTIG welding. A part of the cooling panel extruded from its back through a slot in the shield plate is also welded to the shield plate by TIG welding. (Fig. 5.24) In the shield plate, some holes are left open for filling Be neutron multiplier pebbles into the blanket.
(6) The Be armor is bonded on the first wall, possibly by HIP [8], and the slots of the Be armor is machined. It should be noted that the HIP bonding of the Be armor might affect the materials filled in the blanket, especially the breeder and the multiplier pebbles. One of other possible steps of the Be armor bonding is just after the fabrication of the first wall. However in this case, the bonded Be armor would be affected by the welding of the toroidal end walls and even by the welding of the cooling plates and the shielding plate. Careful attention should also be paid not to damage the bonded Be armor tiles during the other fabrication steps. The appropriate step of the Be armor bonding should be investigated in more detail.
(7) Beryllium pebbles are filled, possibly with vibration, through the holes of the shield plate.
(8) Finally, closure plugs of the holes are welded by TIG welding.

5.8 Inspection Procedure

For the inspection, the checking of the integrity of the pressure boundary is the most important. For this purpose, all welds at pressure boundary are examined by

penetrant and radiographic testings after each or a series of welding is performed. As there would be some difficulties foreseen for the latter testing, e.g., at a closing weld of the coolant manifolds, more detail investigation would be required. In addition, pressure and helium leak tests are also performed to confirm the soundness of the pressure boundary.

The HIP bonded interface is also examined by ultrasonic testing to confirm no harmful defects at the bonded interface. A small ultrasonic testing probe to be inserted into the first wall coolant tube can be developed. However, it should be noted that extensive investigation will be needed to define the size of the harmful defects at the HIP bonded interface.

For the pebble packing behavior, a computer tomography (CT) scanning technique can be applied, especially for a detail examination of uniform packing and packing fraction of the breeder pebbles in the breeder rod [9].

5.9 Design Improvements to Reduce Fabrication Cost

For reducing the fabrication cost of the breeding blanket, the design simplification is essential. In this sense, the following items need to be investigated:

(1) Curvature of the blanket module
The 3-D (toroidal and poloidal) curvature, especially of the first wall, is extremely difficult to fabricate and thus costly. The 3-D curvature requires special bending or pressing jigs and numerical control (NC) machines for final machining, and more partitioning of the parts to be fabricated or bonded, e.g., division between the first wall and top/bottom walls. A 2-D (either toroidal or poloidal) curvature makes the fabrication easier. A flat surface of the first wall is the most desirable in terms of fabrication.

The internals of the breeding blanket, especially the breeder rods, could accommodate the 3-D curvature since they consist of bent tubes and breeder pebbles filled in the tubes. However, the poloidally oriented breeder rods would have some difficulty to accommodate the poloidal curvature with precise placement of the rods. Therefore, a poloidally flat shape for the module would contribute to reduce the fabrication cost.

For HIP bonding of the first wall structure, the 3-D curved module requires larger HIP facility than a flat-shaped module with the same first wall area. With the increase of the dimension of the module shape, i.e., 1-D (flat), 2-D and 3-D, the total depth of the module increases. Thus the module shape with higher dimension requires a HIP facility with larger radius which is critical for the cost of HIP facility. Therefore, a flat-shaped module is, again, the most desirable in terms of fabrication.

(2) Slotting of Be armor
Since the Be armor bonded on the first wall surface is a brittle material, careful attention should be paid to prevent the armor and the joint with the SS structure from being damaged by the slotting. From this viewpoint, the number of the slots should be minimized. For the slotting of the Be armor, a mechanical cutting with a disc saw, disc grinder or wire cutter, or an electro discharge machining could be used. The electro discharge machining is extremely costly, especially for the 3-D

curved surface, though the slotting accuracy would be excellent. The wire cutter would not be used for the 3-D curved surface, either. Therefore, the use of the disc saw or disc grinder can be considered. For longer lifetime of the cutting disc thus to reduce the fabrication cost, a little wider slot width, e.g., 1.5-2.0 mm, than that of the present design, 1 mm, would be desirable. Here again, a flat-shaped first wall is desirable to reduce the slotting cost because it requires the simplest movement of the cutting tool without a complicated numerical control.

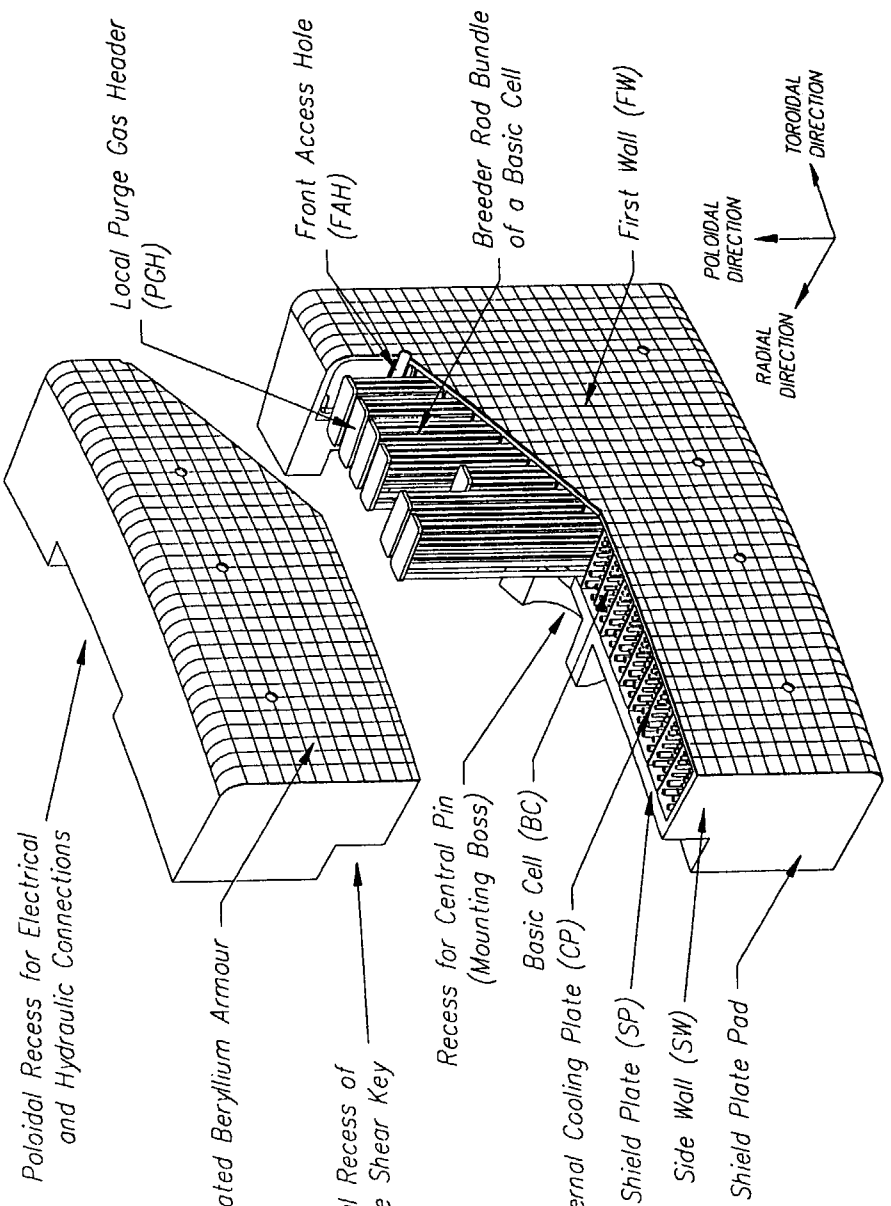

Fig. 5.1 Isometric sketch view of breeding blanket module [7]

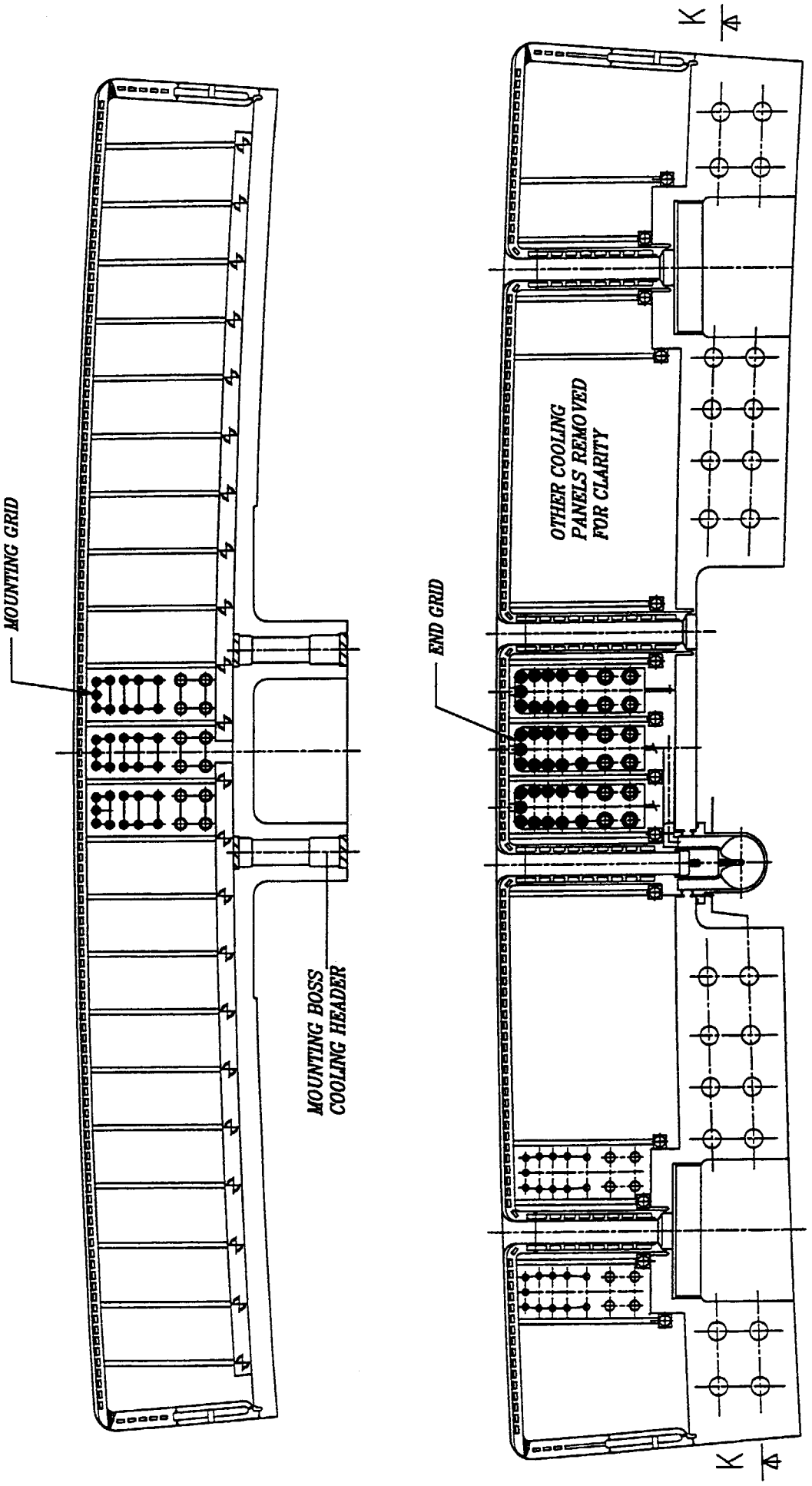

Fig. 5.2 Breeding blanket concept - inboard No. 11 module [1]

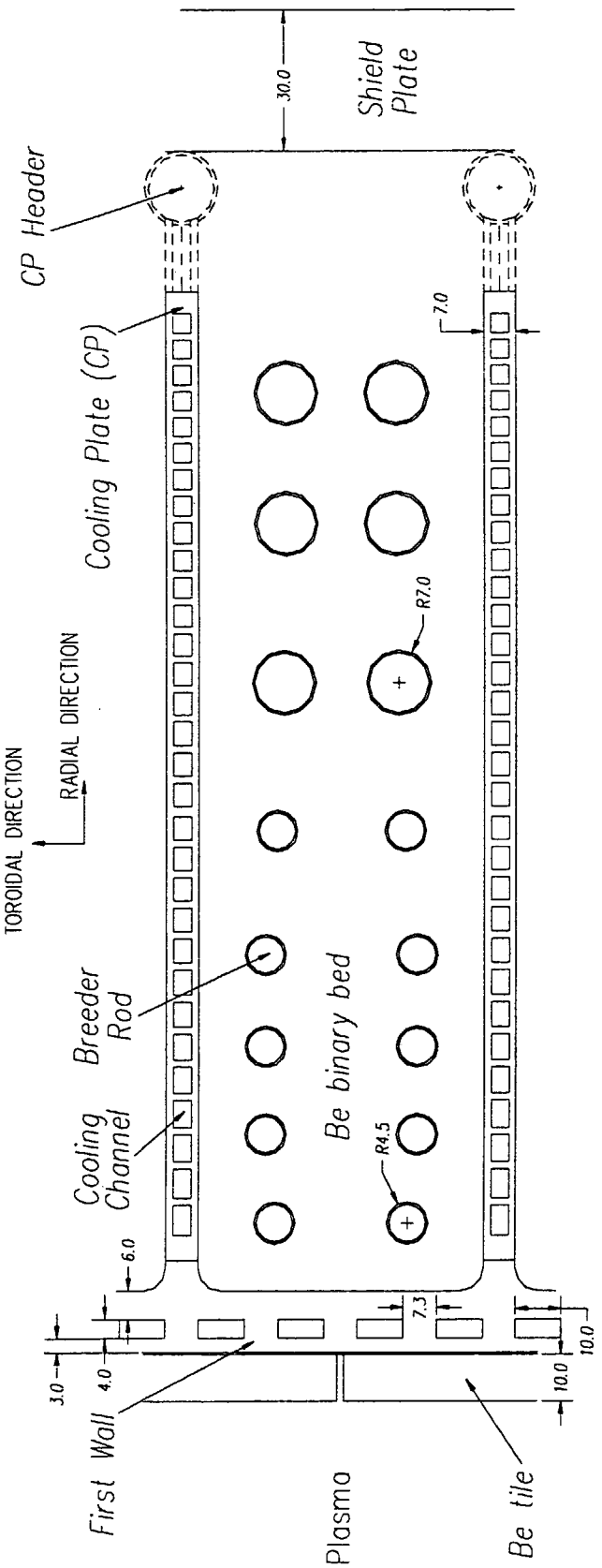

Fig. 5.3 Illustrative sketch of breeding blanket unit cell [7]

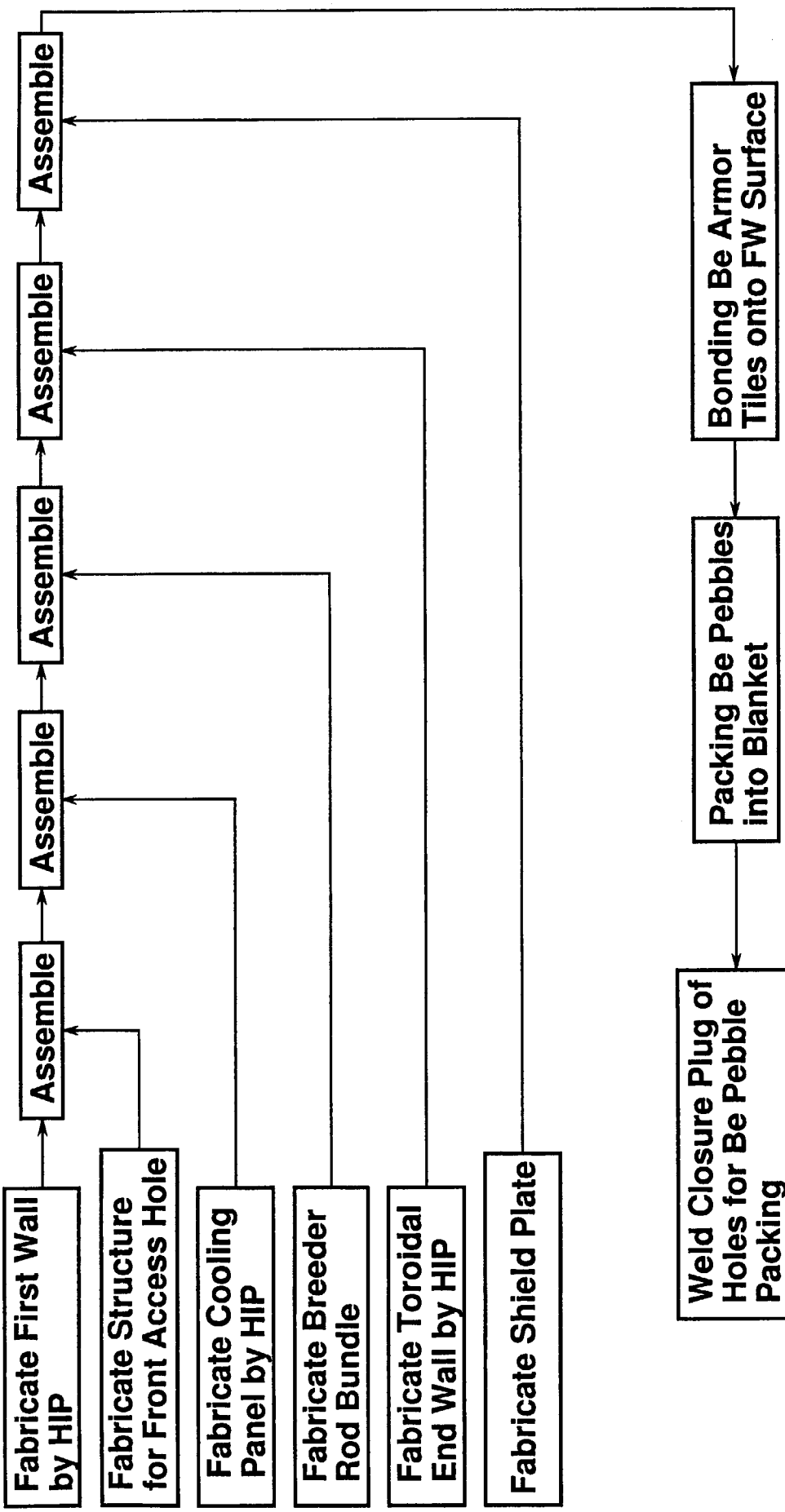

Fig. 5.4 Overall fabrication procedure of breeding blanket

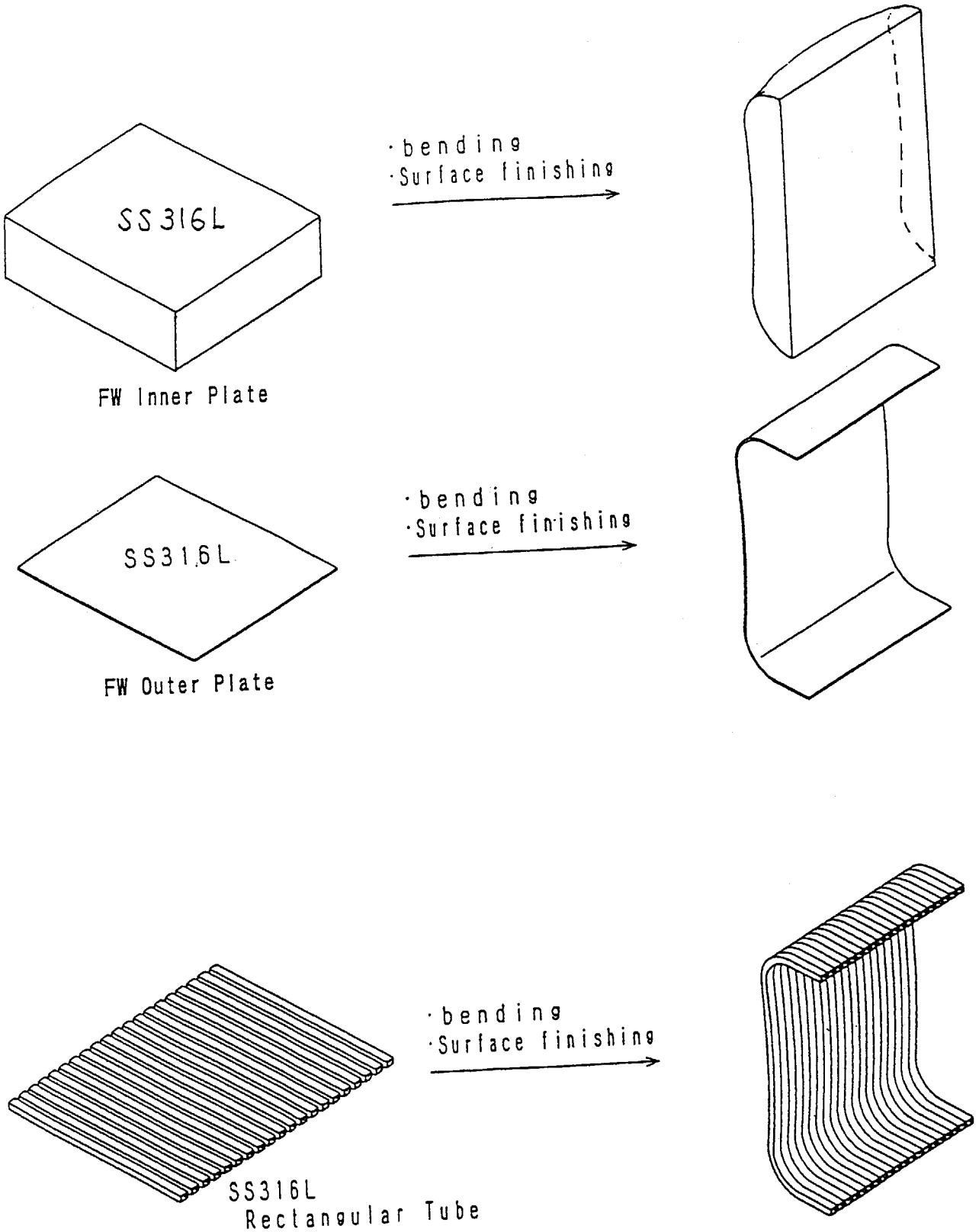

Fig. 5.5 Fabrication of first wall parts

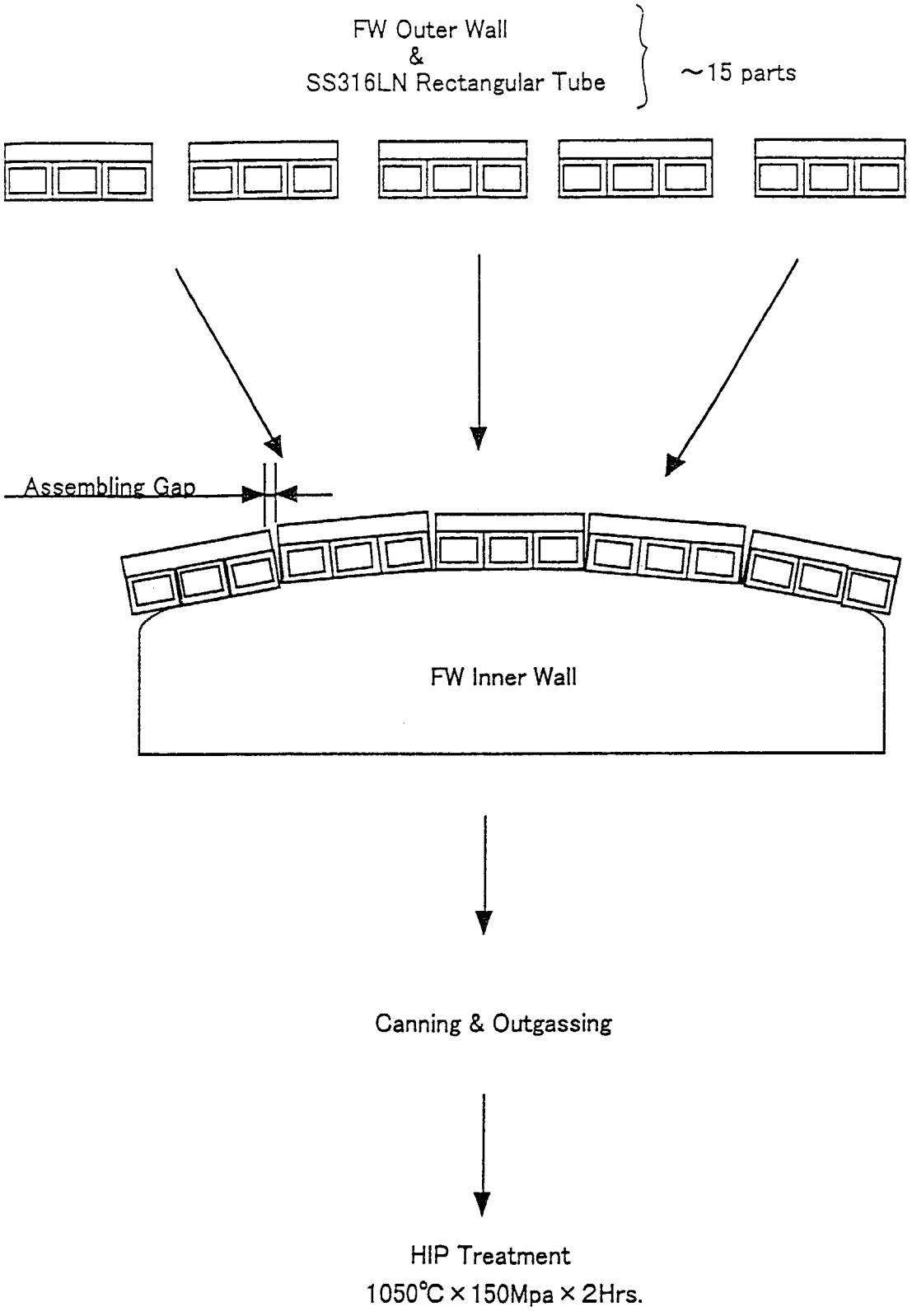

Fig. 5.6 Division of outer plate

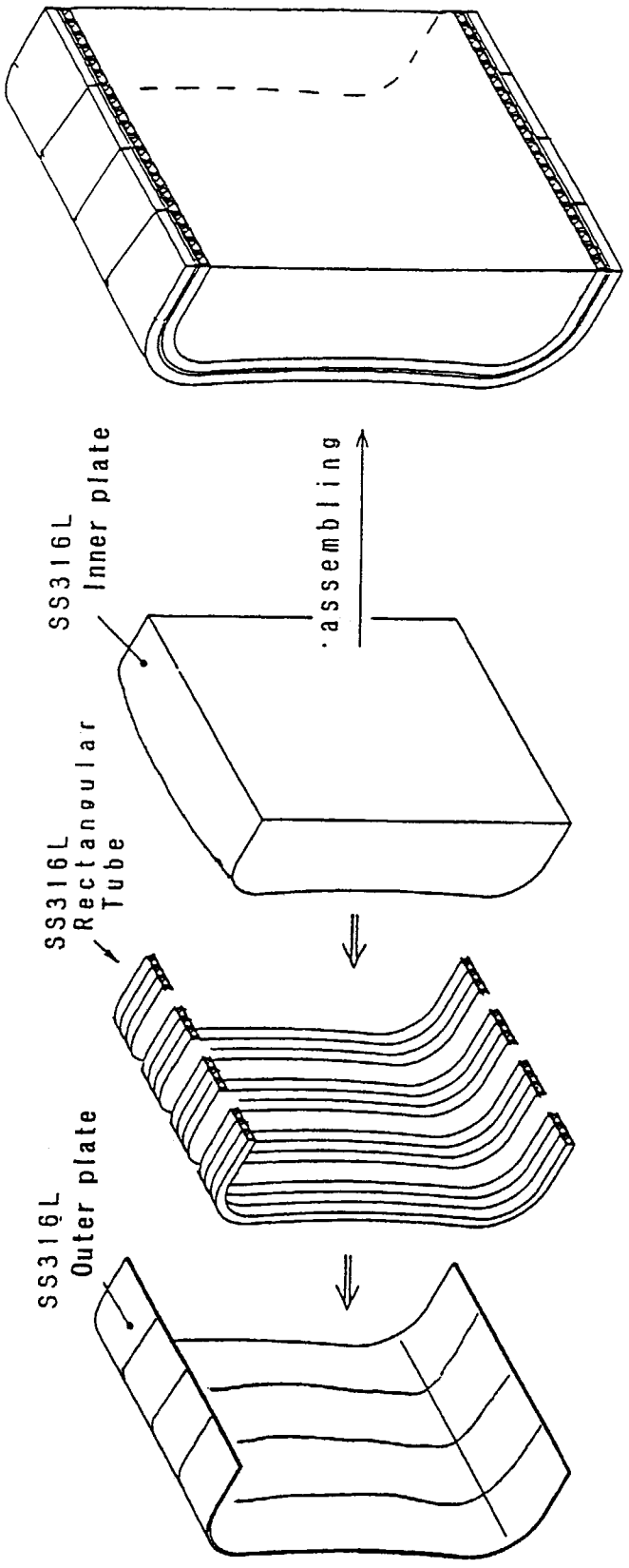

Fig. 5.7 Assembly of first wall parts

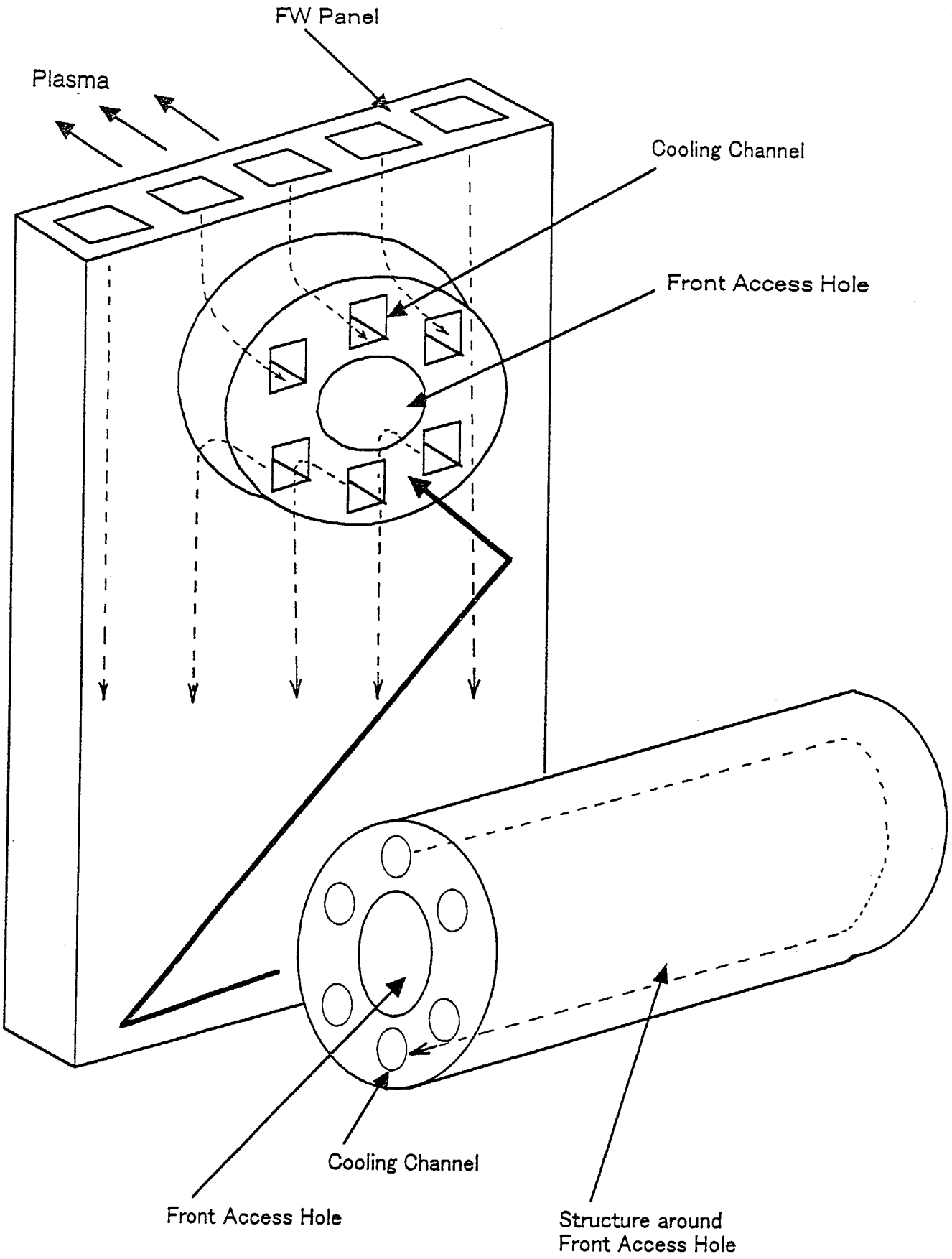

Fig. 5.8 Structure for front access hole

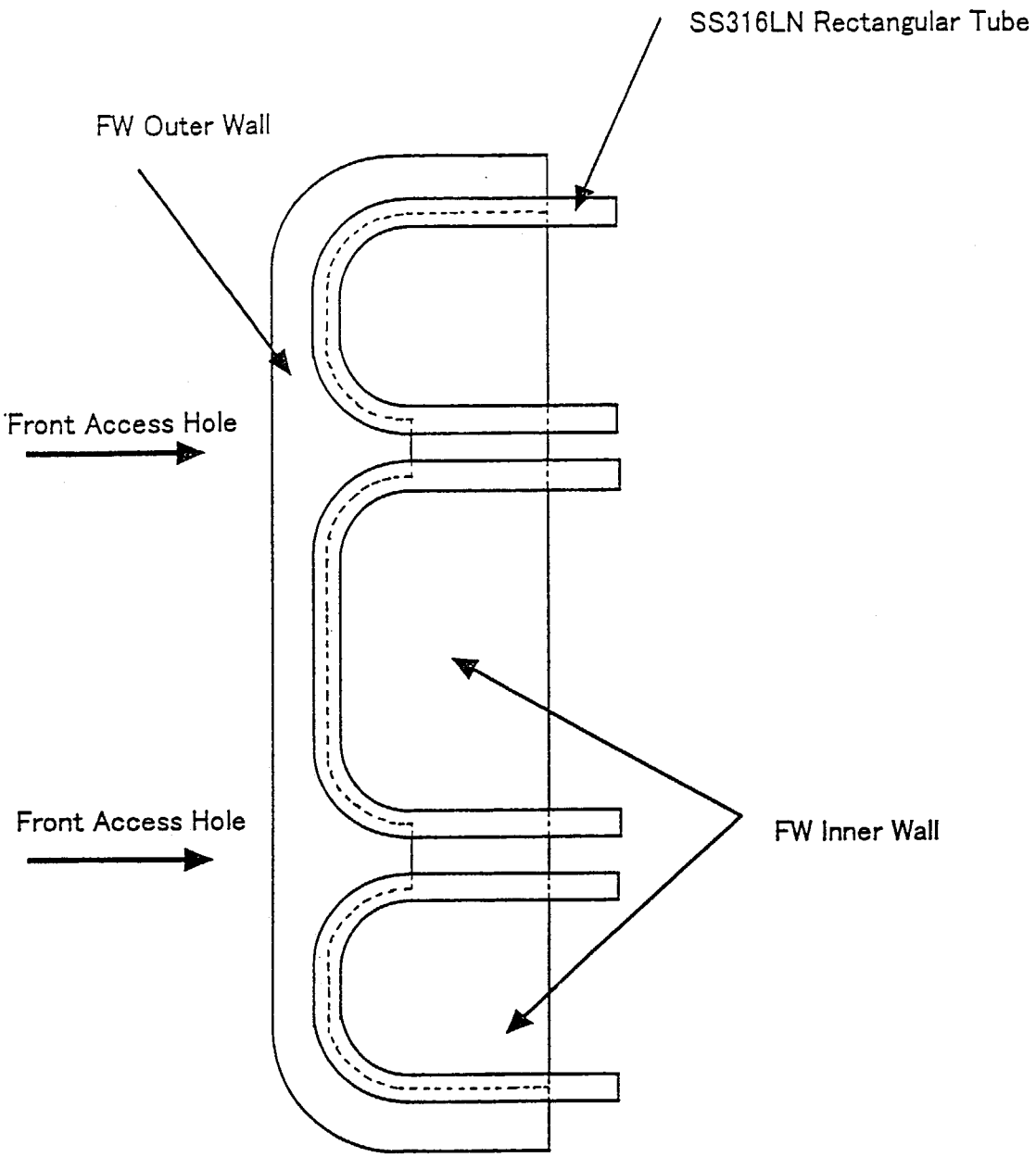

Fig. 5.9 First wall assembly for front access hole structure before HIP

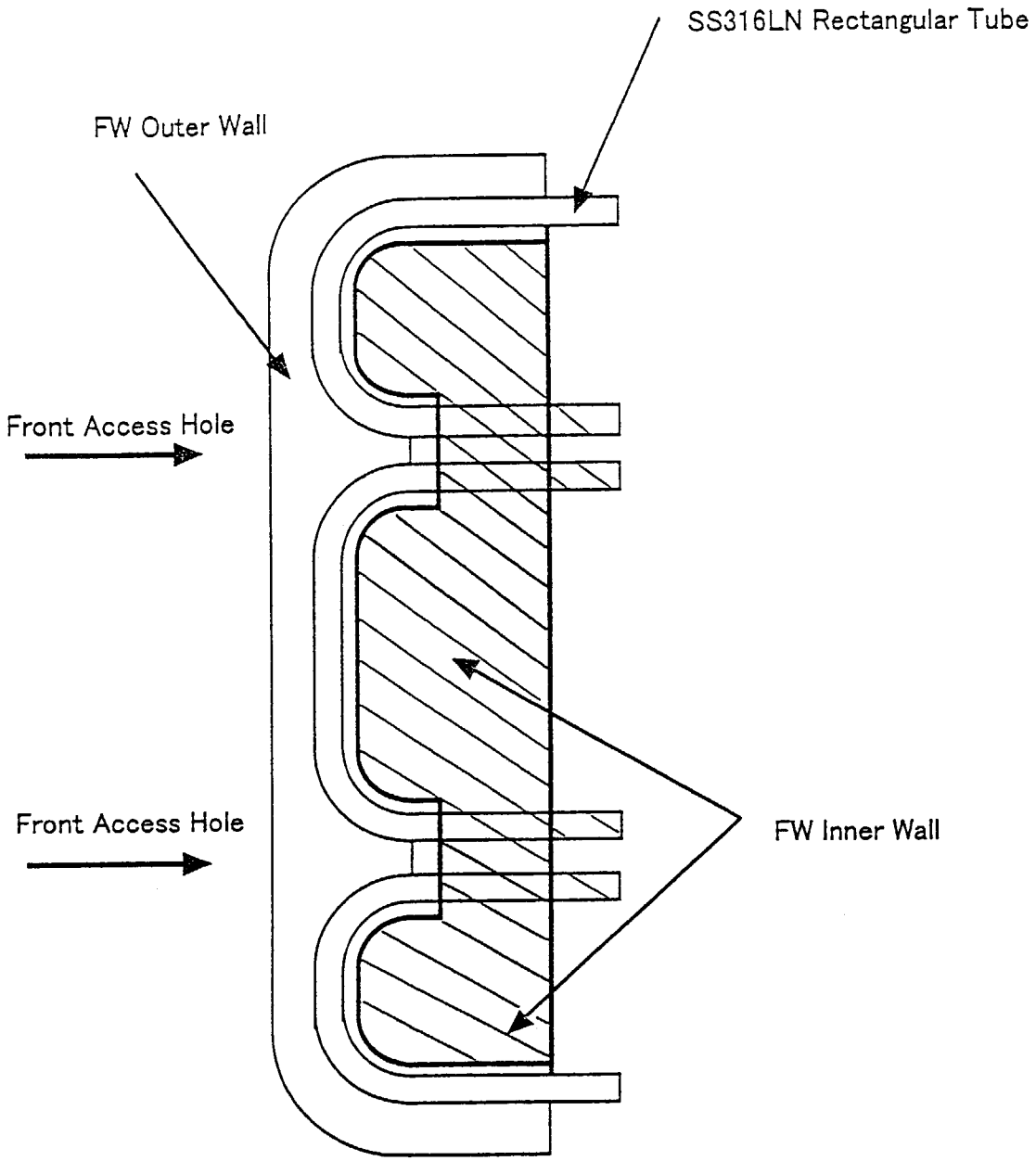

Fig. 5.10 Machining of first wall inner plate after HIP

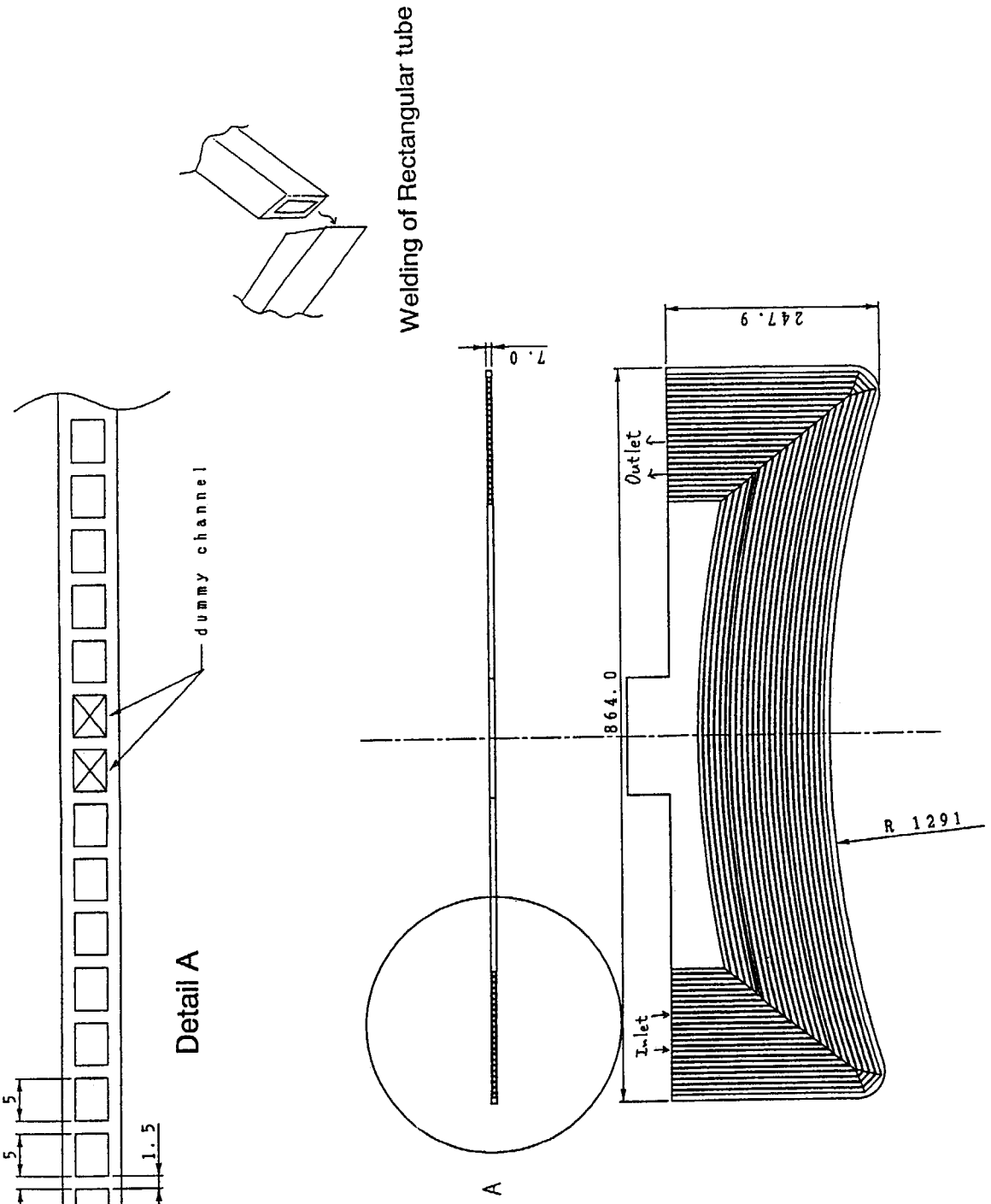

Fig. 5.11 Cooling panel

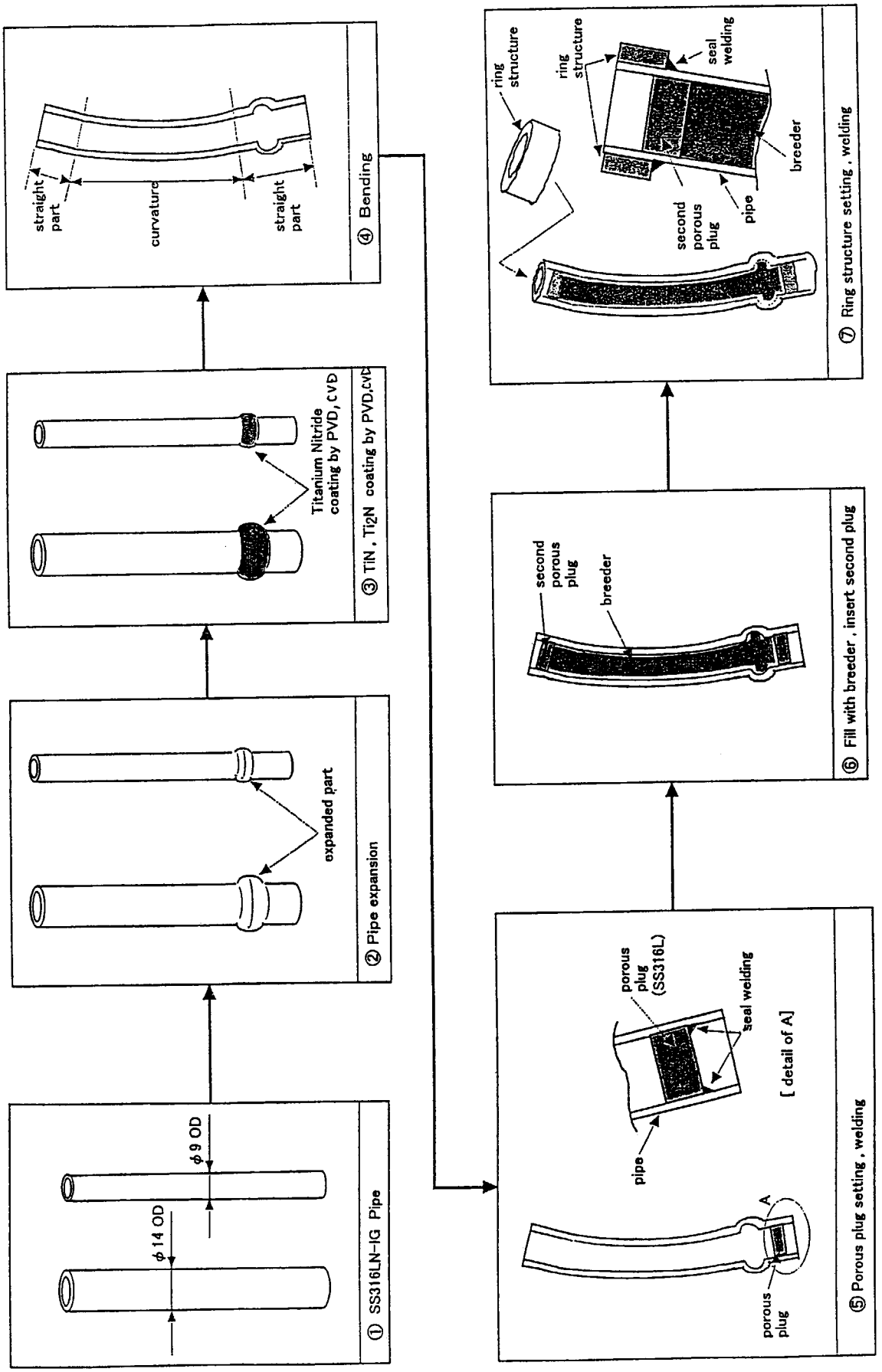

Fig. 5.12 Fabrication procedure of breeder rod

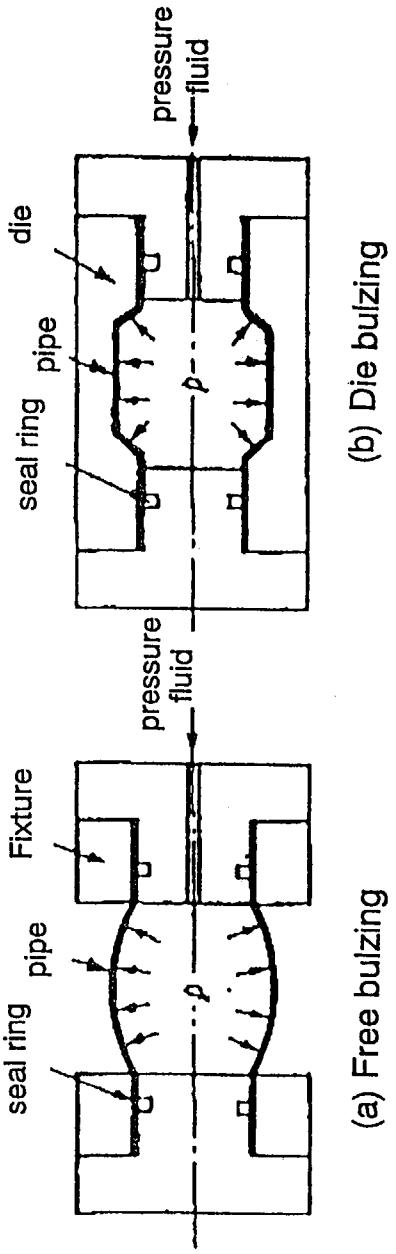

Fig. 5.13 Internal high pressure process of pipe

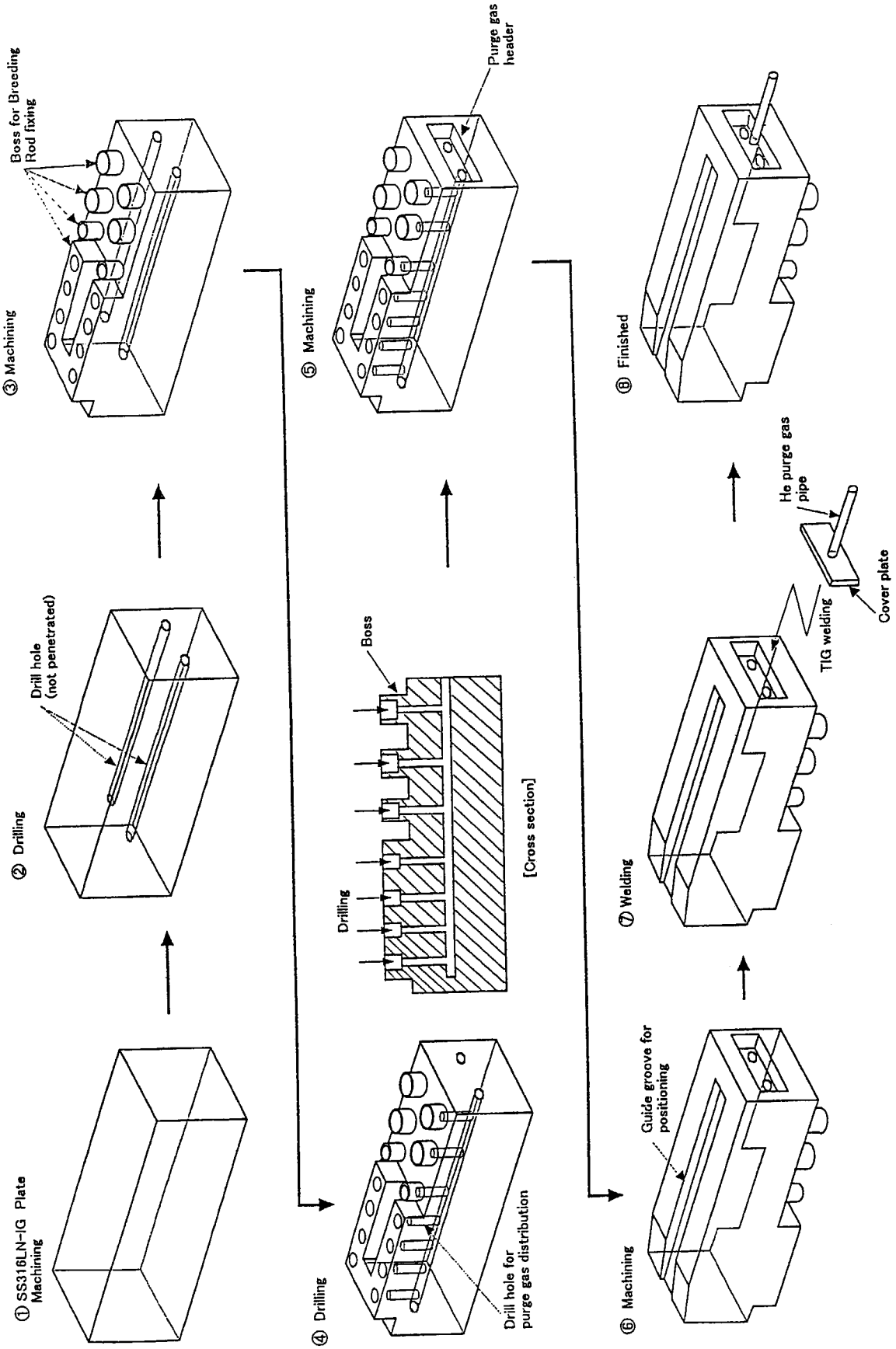

Fig. 5.14 Fabrication procedure of rod end structure

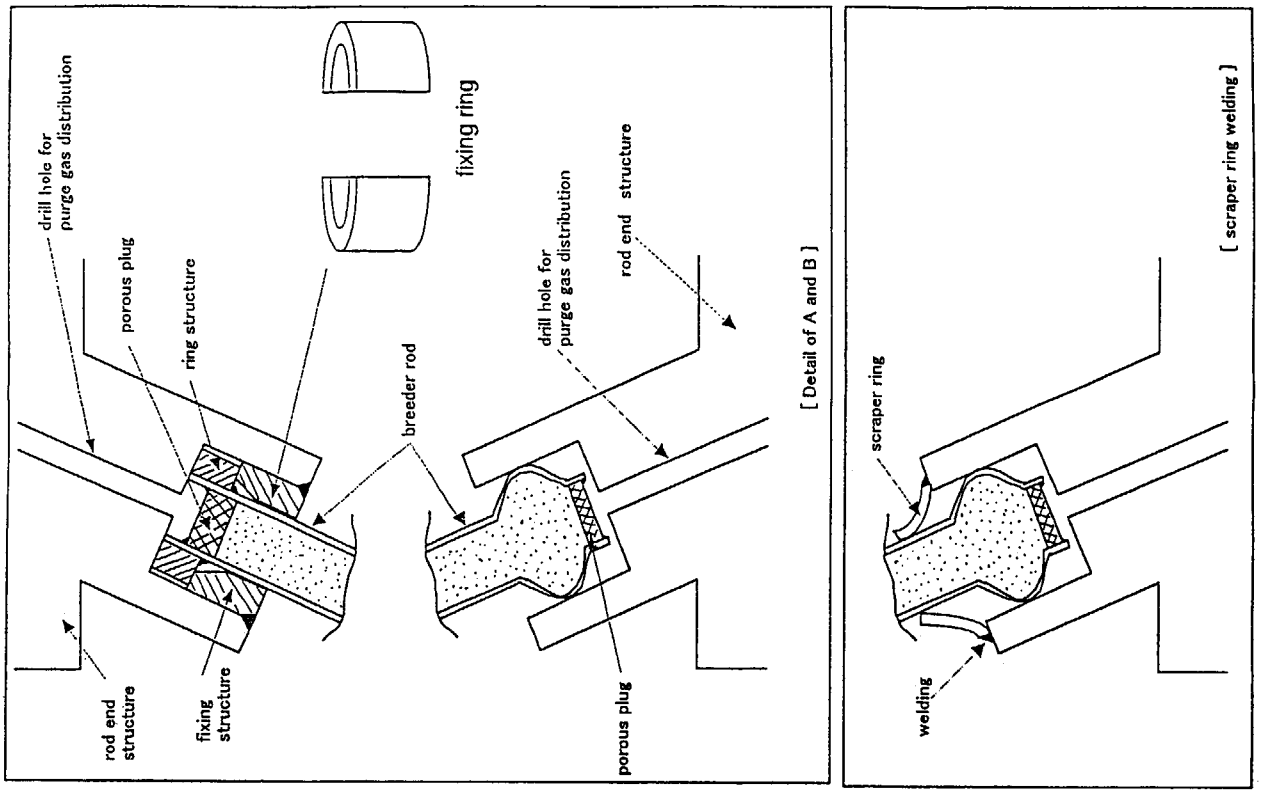

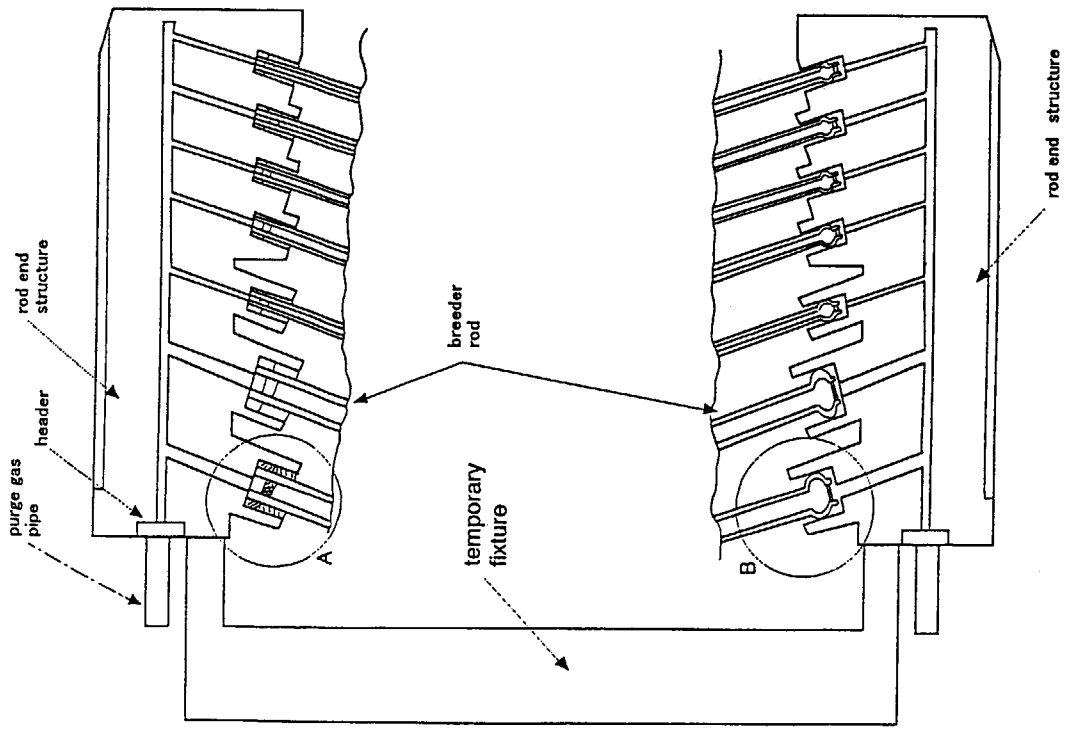

Fig. 5.15 Assembly of breeder rod and rod end structure

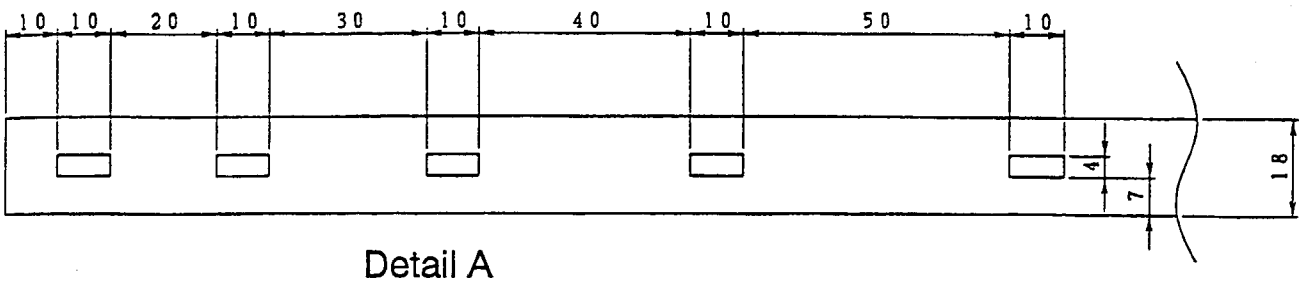

Detail A

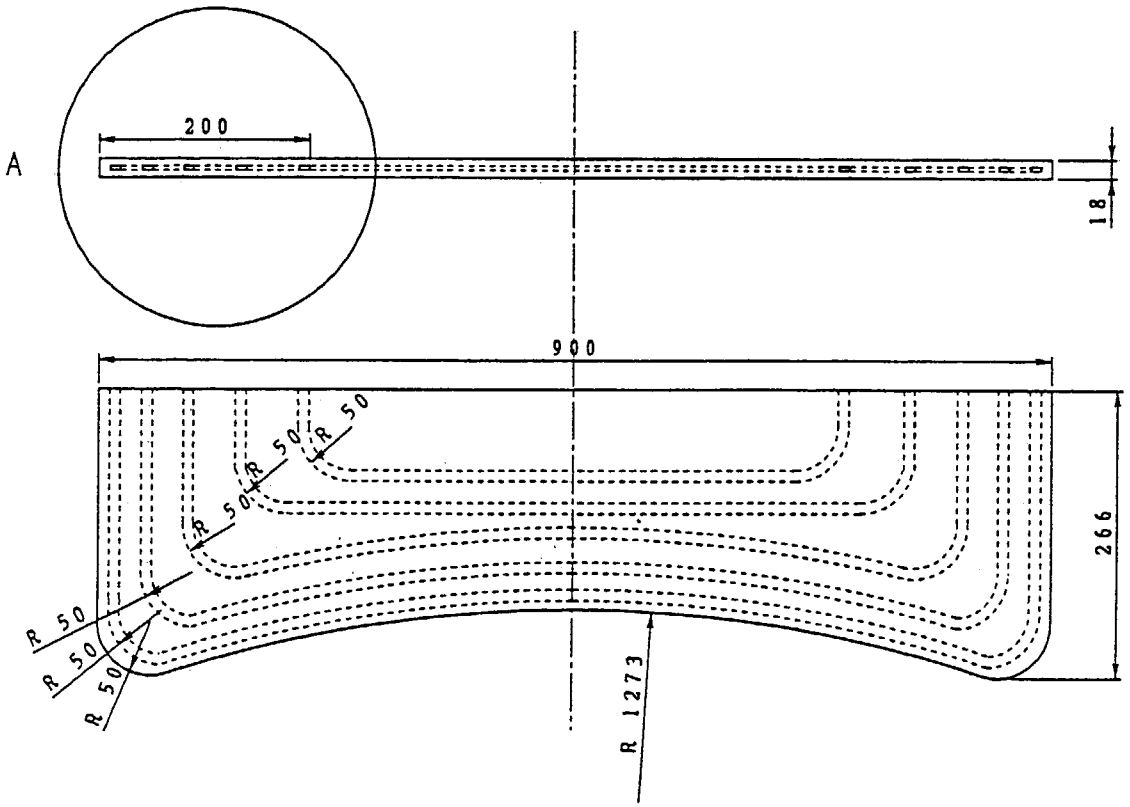

Fig. 5.16 Toroidal end wall

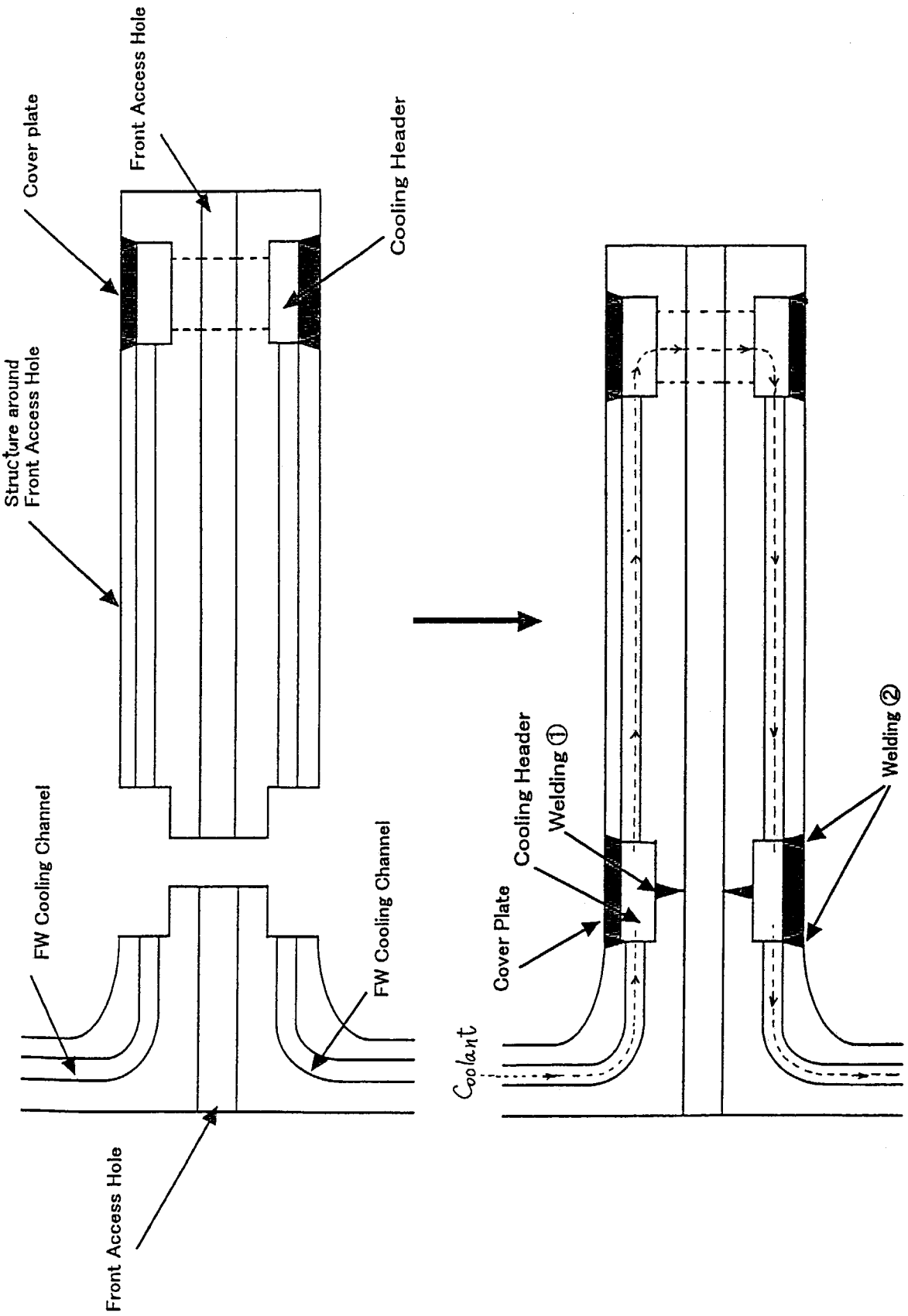

Fig. 5.17 Coolant connection and welding of front access hole structure

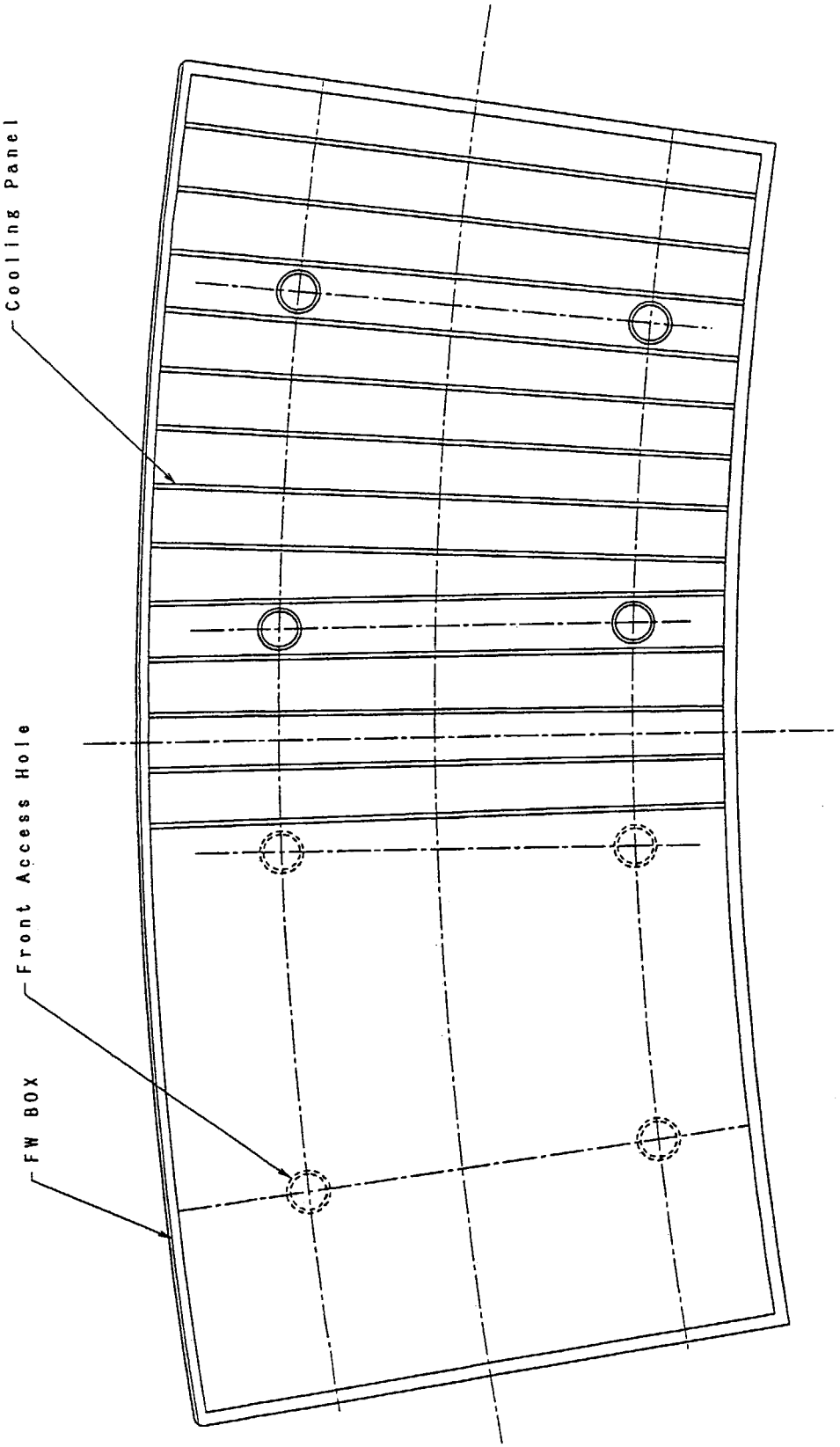

Fig. 5.18 Assembly of front access structure and cooling panel

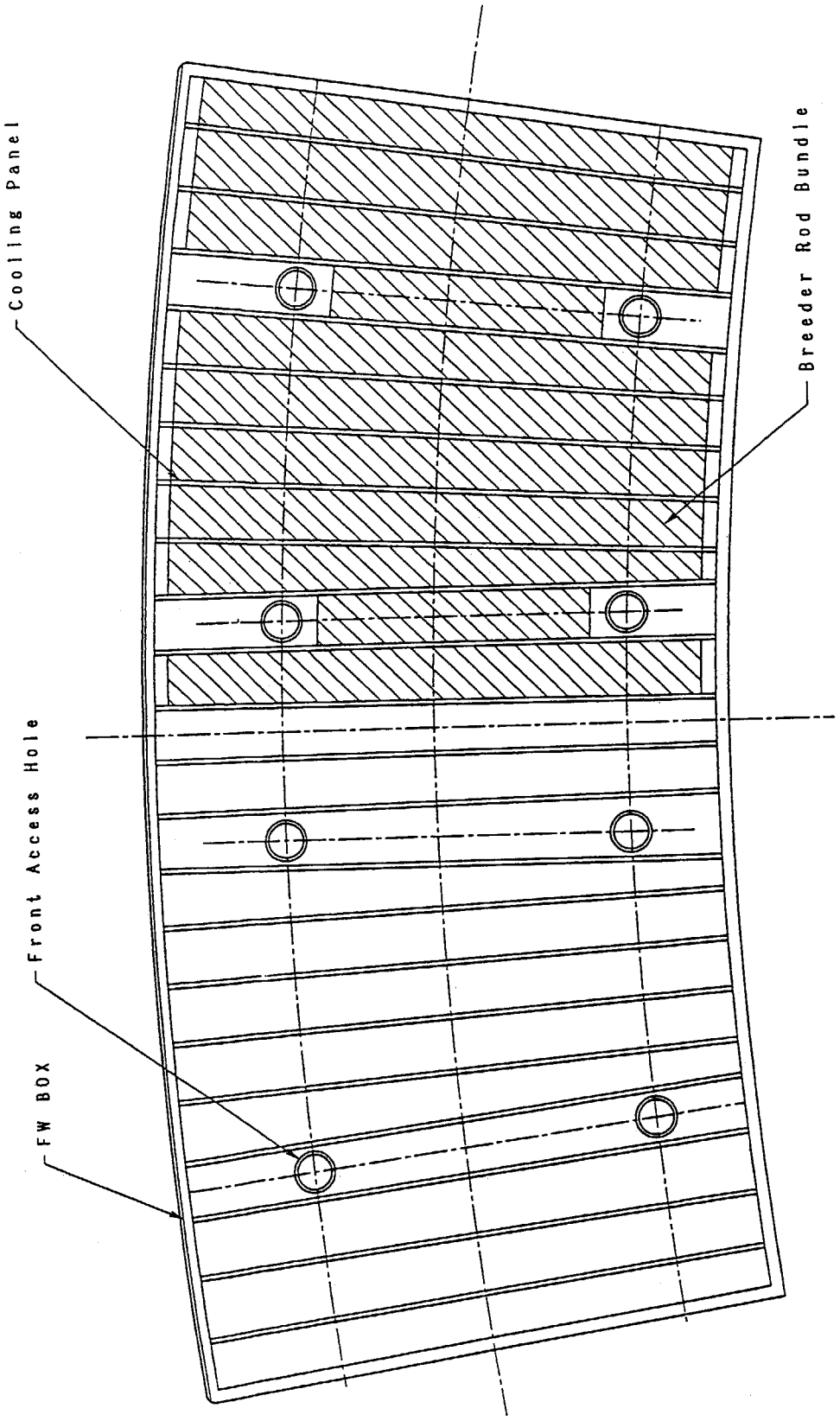

Fig. 5.19 Assembly of breeder rod bundle

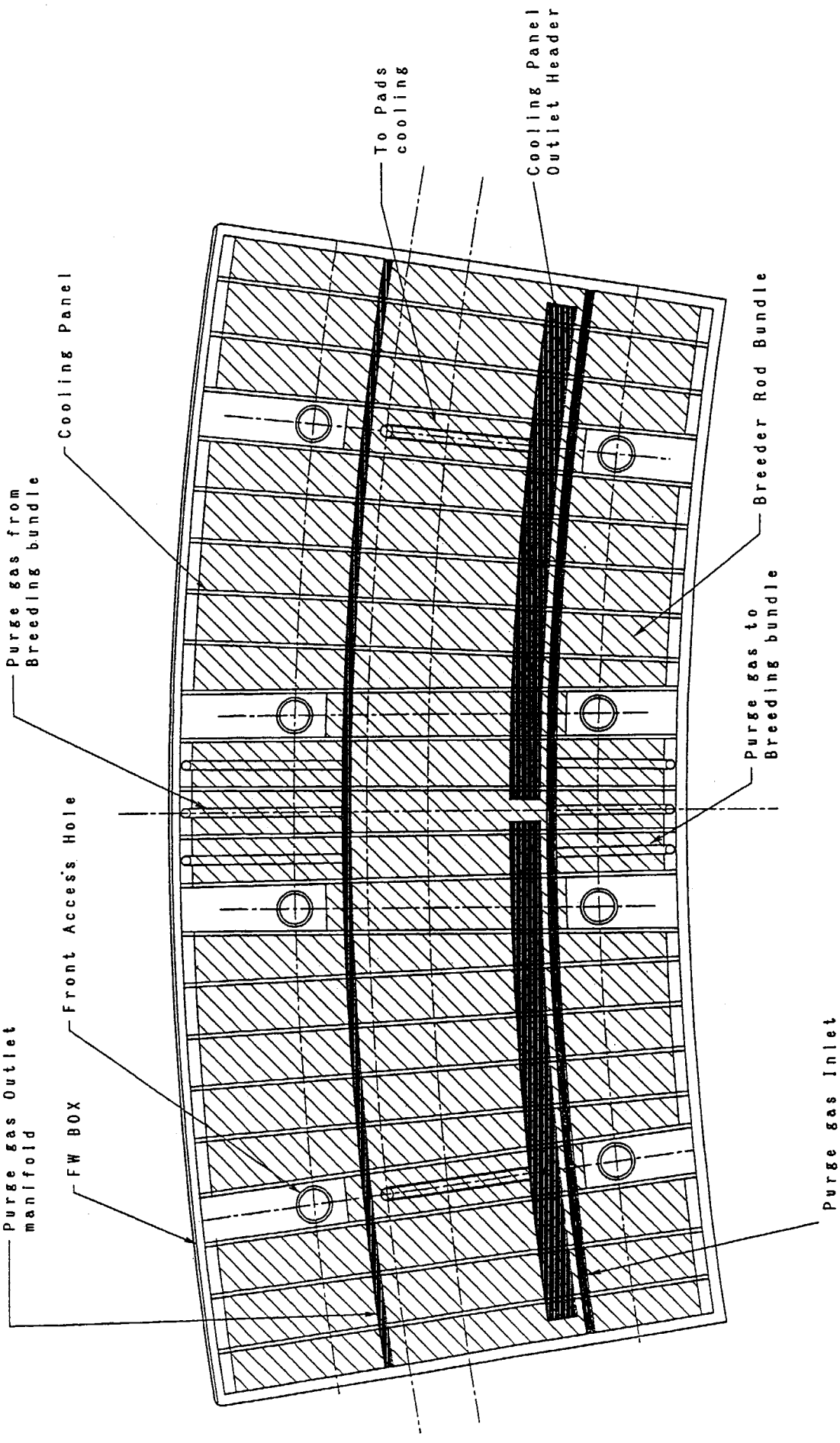

Fig. 5.20 Assembly of coolant and purge gas manifolds

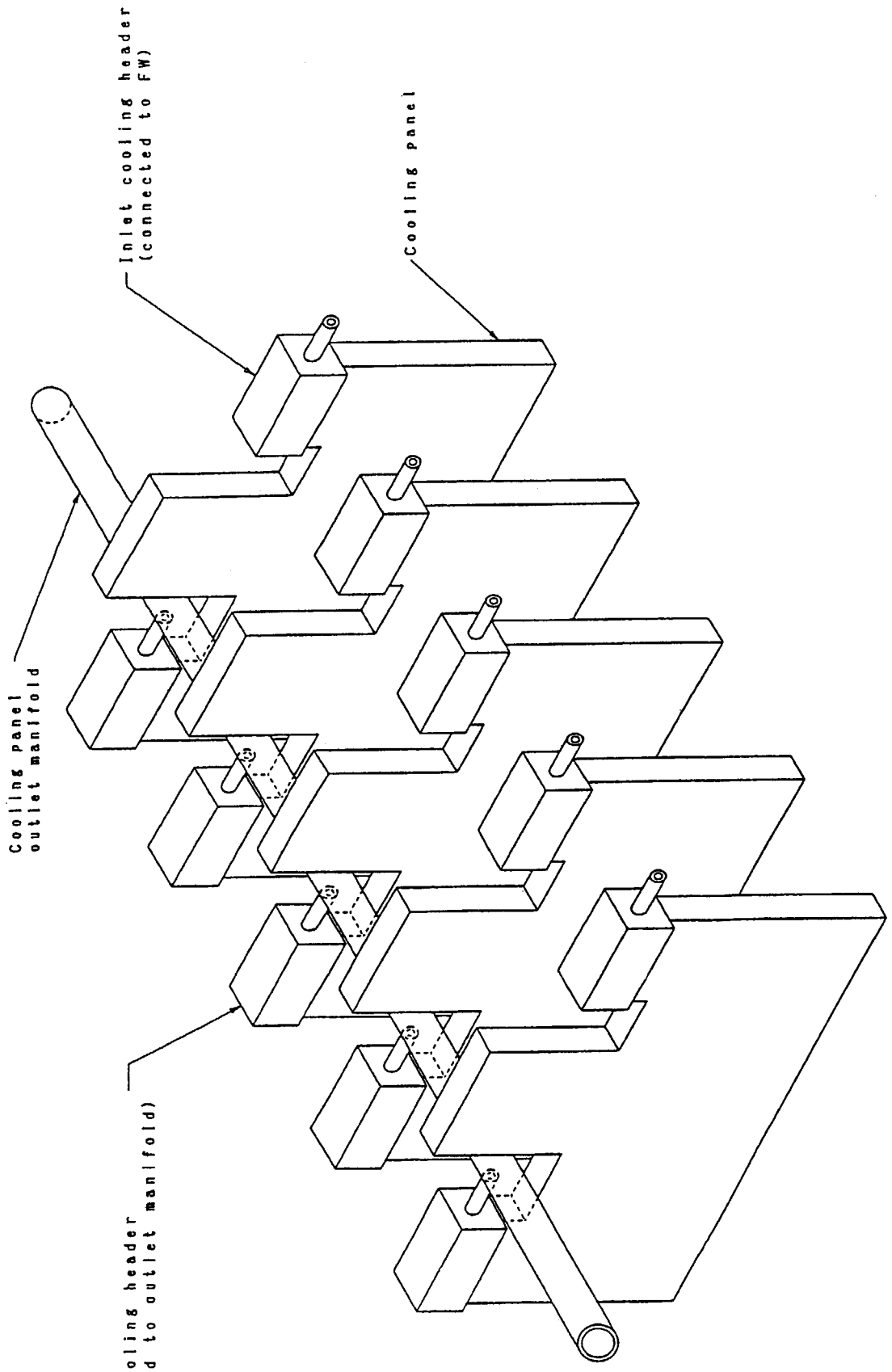

Fig. 5.21 Assembly of coolant manifold (1)

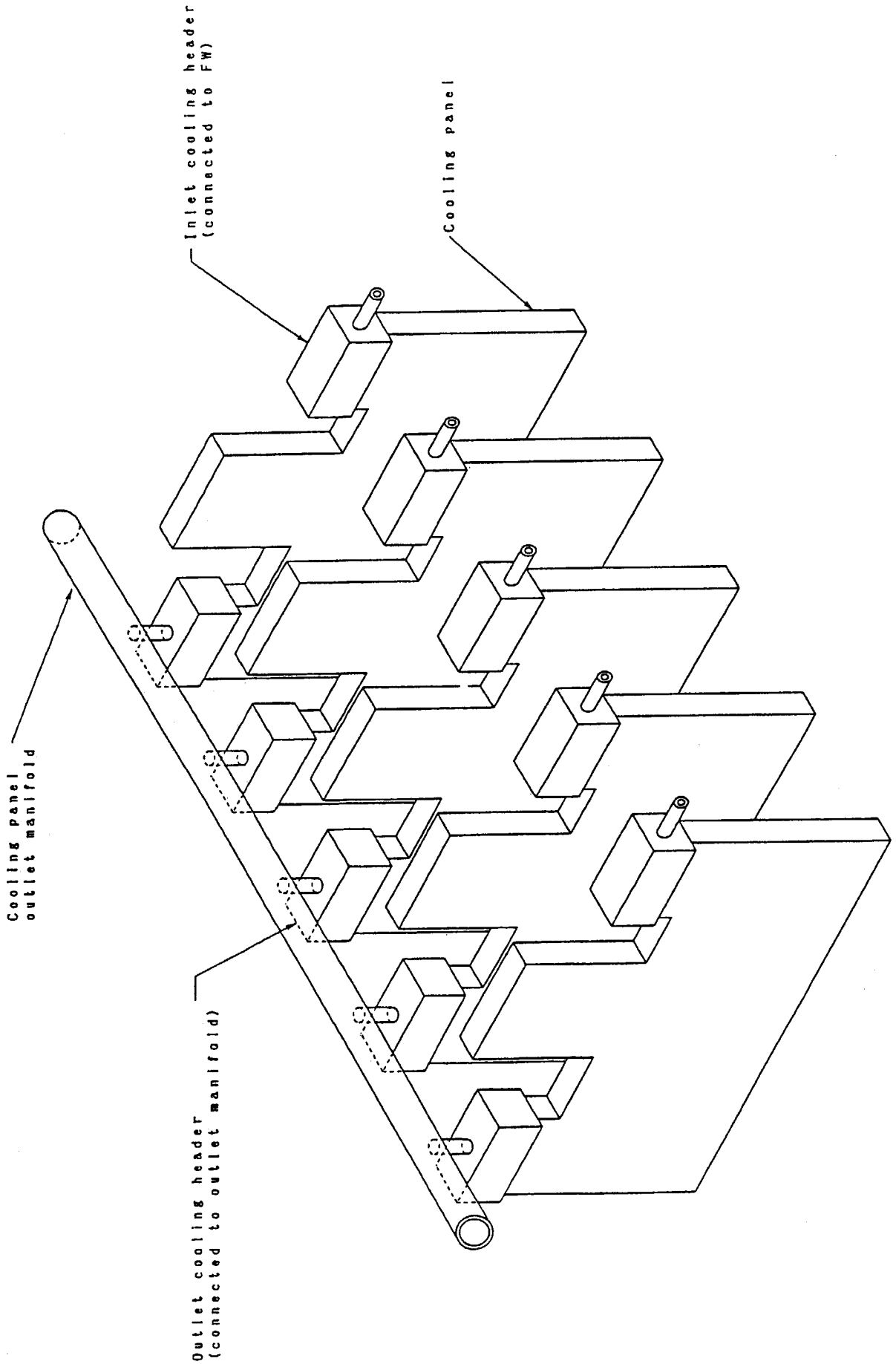

Fig. 5.22 Assembly of coolant manifold (2)

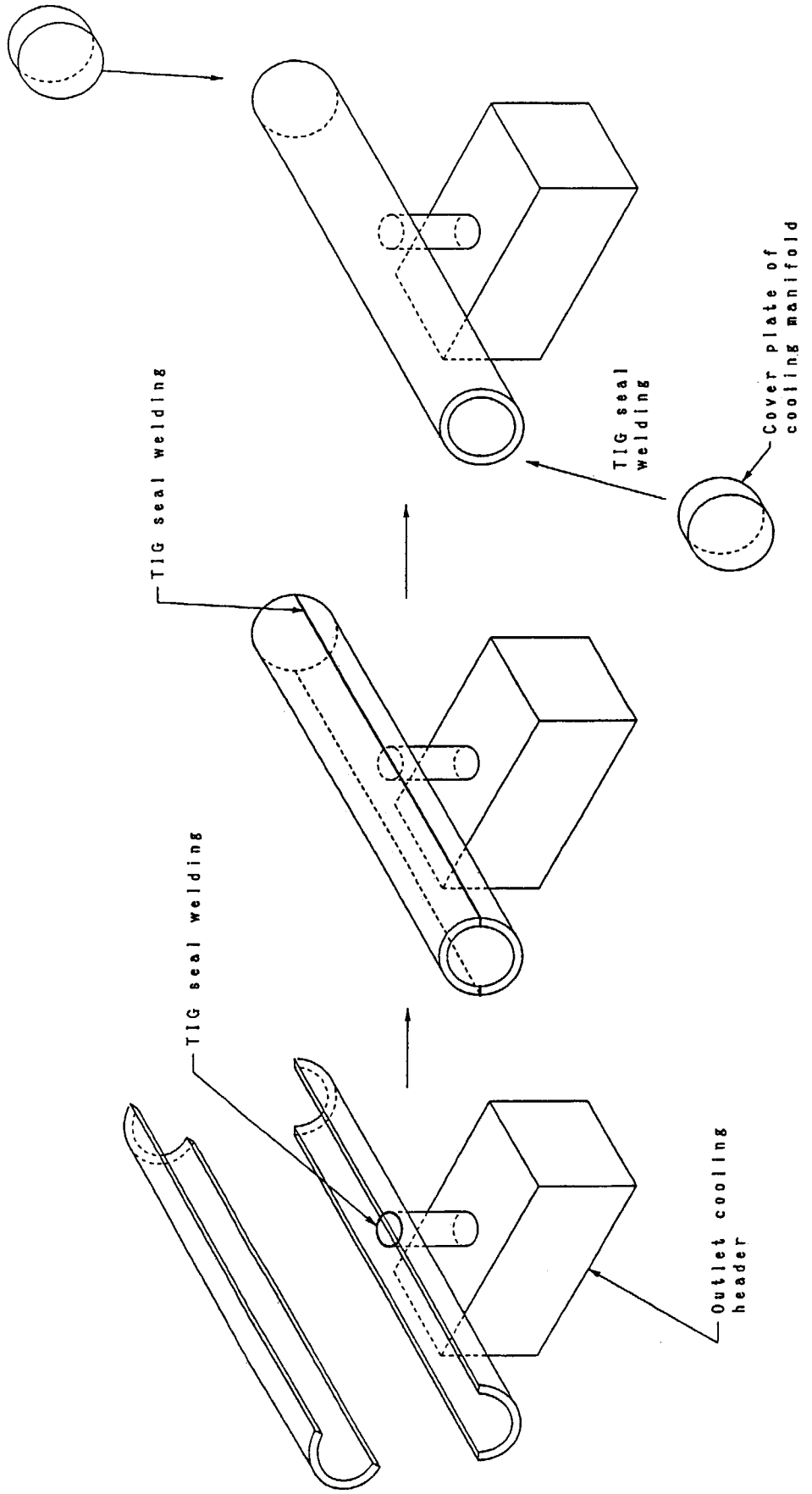

Fig. 5.23 Welding procedure of coolant manifold

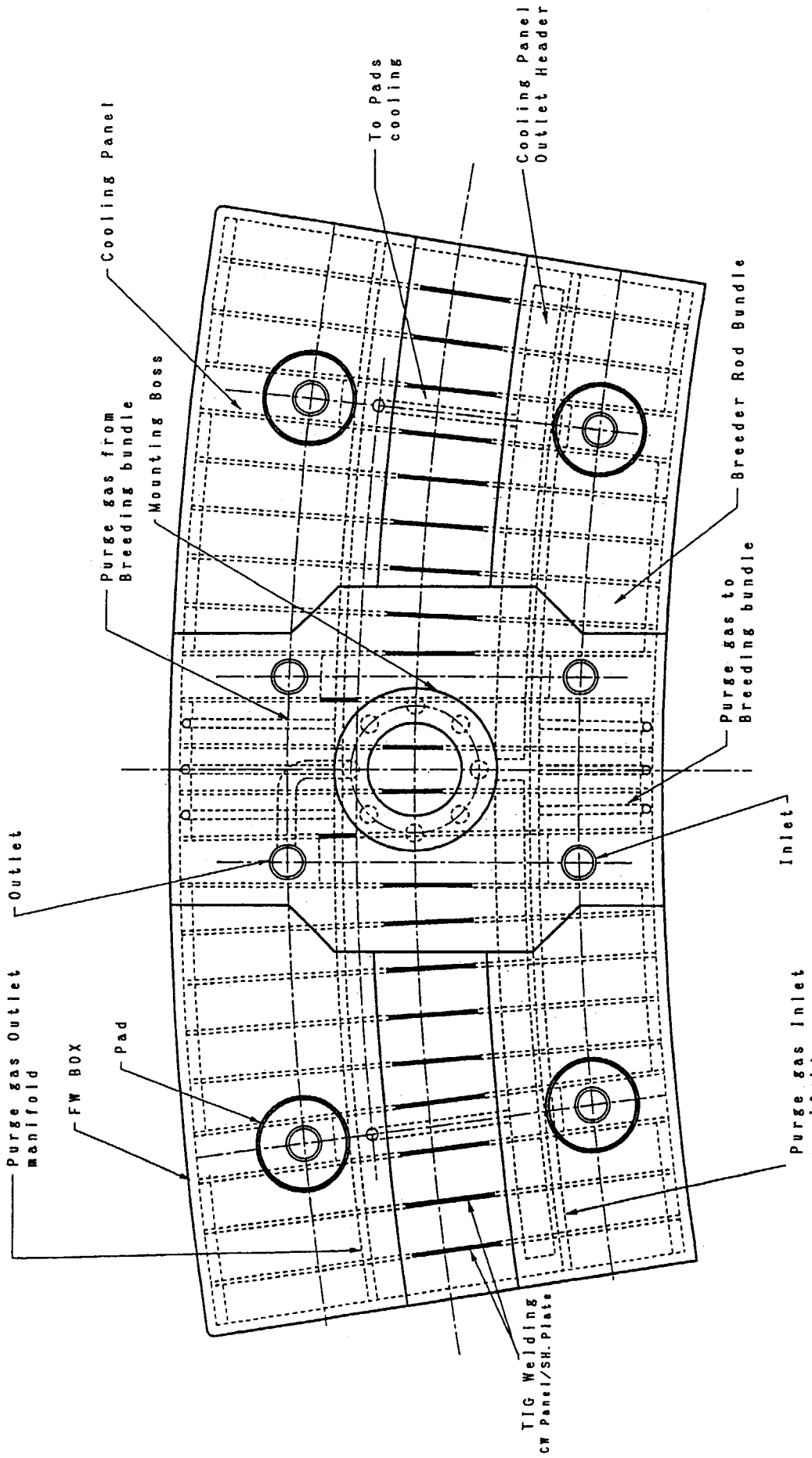

Fig. 5.24 Assembly of shield plate

6. Conclusions

The design of the ITER breeding blanket has incorporated pebble-beds of breeder and neutron multiplier materials and poloidal-radial cooling panels. The internal structure of the breeding blanket exhibits toroidally repeated basic cells, each of which consists of two adjacent cooling panels, a bundle of breeder rods placed between the adjacent cooling panels and beryllium (Be) pebbles filled in the space between the breeder rods and surrounding structures (cooling panels, the first wall and the back shield plate). Beryllium armor tiles are bonded on the stainless steel (SS) first wall structural material. For examining the performance and further development of this blanket, thermo-mechanical analyses on the pebble bed configuration in the blanket and Be/SS bonding at the first wall have been performed. The fabrication procedure of this blanket has also been investigated.

Thermo-mechanical analysis of the unit cell in the ITER blanket has been conducted taking into account the spatially varying effective thermal conductivity and heat transfer coefficient at the contacting wall of Be pebble bed depending on stresses due to the differential thermal expansion of the blanket. Special calculation option of ABAQUS code is used so as to deal with mechanical features of pebble bed such as shear failure flow and hydrostatic plastic compression. The coupled temperature-displacement procedure of ABAQUS code is also utilized so that the thermal conductivity of the pebble beds is automatically calculated according to the stress. The calculated results qualitatively agreed with the pebble bed behavior observed in experiments. As for quantitative improvement, further experimental measurements and accumulation of mechanical property data of pebble beds including Young's modulus, Poisson's ratio and the data with regard to shear failure are needed.

The structural response of the breeding blanket module under internal pressure of 4 MPa has also been calculated for the toroidal end wall. Since the calculated stress is rather high as 390 MPa in comparison with the specified limit of SS316L(N)-IG (206 MPa), a stiffening rib should be attached inside the toroidal end wall, or the thickness of the toroidal end wall, presently 18 mm, needs to be increased to 26 mm.

With regard to the Be/SS bonding at the first wall, two-dimensional thermal and stress analyses have been carried out in order to estimate stress and strain distribution at Be/SS bonded interface in the fabrication process and following thermal cycle process due to pulsed plasma operation. For the joining of Be/SS, HIP method is assumed to be applied. Elasto-plastic analyses have been applied to consider the plastic behavior of the materials. The stress analyses are focused on the stress distribution along the bonded interface, especially at the interface edge. The thermal cycle due to the pulsed plasma operation causes stress-strain hysteresis for the stresses at the bonded interface. The maximum tensile stress perpendicular to the bonded interface appears at the end of cooling process after the HIP bonding.

The fatigue lifetime for the Be/SS bonded interface would be related to the stress range or the strain range at the bonded interface. The presently evaluated maximum stress and strain ranges at the bonded interface are 241 MPa and 0.17 %, respectively for SS, and 87 MPa and 0.39 %, respectively for Be. These assessment parameters should be used properly according to the point of failure, i.e., at the bonded interface or in the base materials near the interface. A procedure to assess

and/or confirm the bonding integrity is finally proposed.

Fabrication procedure of the breeding blanket has been investigated. The breeding blanket is basically fabricated parts by parts, i.e., first wall, front access hole structures, cooling panels, breeder rod bundles, toroidal end walls and shield plate. Since the first wall, cooling panels and toroidal end walls are all with built-in rectangular coolant channels, they are fabricated by HIP with temperature at 1050 °C, pressure at 150 MPa and holding time of 2 hours. After the fabrication of the first wall, above parts are assembled one by one. The shield plate is finally welded to close the blanket box structure. However, small openings are left in the shield plate through which beryllium multiplier pebbles are filled into the blanket. After the filling of Be pebbles, the plugs of the opening are welded.

The Be armor would be bonded to the first wall SS by HIP. To prevent the bonded Be armor from being damaged and to reduce the handling of Be, the bonding of the Be armor would be desirable to be the final step, e.g., after the plug welding mentioned above. However, the HIP bonding of Be would affect the materials filled in the blanket, especially the breeder and the Be multiplier pebbles. More careful investigation is needed to decide the step of Be armor bonding. To reduce the fabrication cost of the breeding blanket, the design improvement to have flat first wall is most desired.

Acknowledgment

The authors wish to acknowledge Drs. S. Matsuda, Y. Seki, T. Nagashima, T. Tsunematsu and M. Seki for their support. Dr. Y. Ohara is gratefully acknowledged for his support and encouragement. This work has been performed in the framework of ITER Design Task. Then the authors are also grateful to Drs. Y. Gohar, K. Mohri and K. Ioki of the ITER Joint Central Team for valuable information on the breeding blanket configuration and constructive discussions.

References

[1] Y. Gohar (Breeding Blanket Group Leader of ITER Joint Central Team), private communication
[2] S. Kikuchi et al., Thermo-mechanical Analysis of ITER Pebble Bed Breeding Blanket, to be published in JAERI-Tech report (1998)
[3] K. Walton, The Effective Elastic Modulus of a Random Packing of Sphere, J. Mech. Phys. Solids, Vol. 35, No. 2(1987)213-226.
[4] A. Ying et al., Mechanical Behavior and Design Database of Packed Beds for Blanket Designs, 4th Int. Symp. Fusion Nucl. Technol., Apr., 1997, Tokyo, Japan, and to be published in Fusion Eng, Des.
[5] M. Dalle Donne et al., Measurement of the Thermal Conductivity and Heat Transfer Coefficient of a Binary Bed of Beryllium Pebbles, Proc. 3rd IEA Int. Work Shop on Beryllium Technol. for Fusion, Oct., 1997, Mito, Japan, JAERI-Conf 98-001 (1998)17-24.
[6] P. Smith et al., Summary of ITER Structural Design Criteria Appendix A, p. 32, Dec., 1997.
[7] M. Ferrari et al., ITER Reference Breeding Blanket Design, 20th Symp. Fusion Technol., Sept., 1998, Marseille, France.
[8] T. Kuroda et al., Development of Joining Technology for Be/Cu-alloy and Be/SS by HIP, 8th Int. Conf. Fusion React. Mater., Oct., 1997, Sendai, Japan, and to be published in J. Nucl. Mater. (1998).
[9] S. Hara et al., Packing Behavior Observed by CT Scan for Development of Pebble Bed Breeding Blanket, 20th Symp. Fusion Technol., Sept., 1998, Marseille, France.

This is a blank page.

国際単位系 (SI) と換算表

表1　SI基本単位および補助単位

量	名称	記号
長さ	メートル	m
質量	キログラム	kg
時間	秒	s
電流	アンペア	A
熱力学温度	ケルビン	K
物質量	モル	mol
光度	カンデラ	cd
平面角	ラジアン	rad
立体角	ステラジアン	sr

表2　SIと併用される単位

名称	記号
分，時，日	min，h，d
度，分，秒	°，′，″
リットル	l，L
トン	t
電子ボルト	eV
原子質量単位	u

1 eV = 1.60218 × 10^{-19} J

1 u = 1.66054 × 10^{-27} kg

表5　SI接頭語

倍数	接頭語	記号
10^{18}	エクサ	E
10^{15}	ペタ	P
10^{12}	テラ	T
10^{9}	ギガ	G
10^{6}	メガ	M
10^{3}	キロ	k
10^{2}	ヘクト	h
10^{1}	デカ	da
10^{-1}	デシ	d
10^{-2}	センチ	c
10^{-3}	ミリ	m
10^{-6}	マイクロ	μ
10^{-9}	ナノ	n
10^{-12}	ピコ	p
10^{-15}	フェムト	f
10^{-18}	アト	a

表3　固有の名称をもつSI組立単位

量	名称	記号	他のSI単位による表現
周波数	ヘルツ	Hz	s^{-1}
力	ニュートン	N	m·kg/s^2
圧力，応力	パスカル	Pa	N/m^2
エネルギー，仕事，熱量	ジュール	J	N·m
工率，放射束	ワット	W	J/s
電気量，電荷	クーロン	C	A·s
電位，電圧，起電力	ボルト	V	W/A
静電容量	ファラド	F	C/V
電気抵抗	オーム	Ω	V/A
コンダクタンス	ジーメンス	S	A/V
磁束	ウェーバ	Wb	V·s
磁束密度	テスラ	T	Wb/m^2
インダクタンス	ヘンリー	H	Wb/A
セルシウス温度	セルシウス度	℃	
光束	ルーメン	lm	cd·sr
照度	ルクス	lx	lm/m^2
放射能	ベクレル	Bq	s^{-1}
吸収線量	グレイ	Gy	J/kg
線量当量	シーベルト	Sv	J/kg

表4　SIと共に暫定的に維持される単位

名称	記号
オングストローム	Å
バーン	b
バール	bar
ガル	Gal
キュリー	Ci
レントゲン	R
ラド	rad
レム	rem

1 Å = 0.1 nm = 10^{-10} m

1 b = 100 fm^2 = 10^{-28} m^2

1 bar = 0.1 MPa = 10^5 Pa

1 Gal = 1 cm/s^2 = 10^{-2} m/s^2

1 Ci = 3.7 × 10^{10} Bq

1 R = 2.58 × 10^{-4} C/kg

1 rad = 1 cGy = 10^{-2} Gy

1 rem = 1 cSv = 10^{-2} Sv

（注）

1. 表1－5は「国際単位系」第5版，国際度量衡局 1985年刊行による。ただし，1 eVおよび1 uの値はCODATAの1986年推奨値によった。
2. 表4には海里，ノット，アール，ヘクタールも含まれているが日常の単位なのでここでは省略した。
3. barは，JISでは流体の圧力を表わす場合に限り表2のカテゴリーに分類されている。
4. EC閣僚理事会指令ではbar，barnおよび「血圧の単位」mmHgを表2のカテゴリーに入れている。

換算表

力	N(=10^5 dyn)	kgf	lbf
	1	0.101972	0.224809
	9.80665	1	2.20462
	4.44822	0.453592	1

粘度　1 Pa·s(N·s/m^2) = 10 P(ポアズ)(g/(cm·s))

動粘度　1 m^2/s = 10^4 St(ストークス)(cm^2/s)

圧力	MPa(=10 bar)	kgf/cm^2	atm	mmHg(Torr)	lbf/in^2(psi)
	1	10.1972	9.86923	7.50062 × 10^3	145.038
	0.0980665	1	0.967841	735.559	14.2233
	0.101325	1.03323	1	760	14.6959
	1.33322 × 10^{-4}	1.35951 × 10^{-3}	1.31579 × 10^{-3}	1	1.93368 × 10^{-2}
	6.89476 × 10^{-3}	7.03070 × 10^{-2}	6.80460 × 10^{-2}	51.7149	1

エネルギー・仕事・熱量	J(=10^7 erg)	kgf·m	kW·h	cal(計量法)	Btu	ft·lbf	eV
	1	0.101972	2.77778 × 10^{-7}	0.238889	9.47813 × 10^{-4}	0.737562	6.24150 × 10^{18}
	9.80665	1	2.72407 × 10^{-6}	2.34270	9.29487 × 10^{-3}	7.23301	6.12082 × 10^{19}
	3.6 × 10^6	3.67098 × 10^5	1	8.59999 × 10^5	3412.13	2.65522 × 10^6	2.24694 × 10^{25}
	4.18605	0.426858	1.16279 × 10^{-6}	1	3.96759 × 10^{-3}	3.08747	2.61272 × 10^{19}
	1055.06	107.586	2.93072 × 10^{-4}	252.042	1	778.172	6.58515 × 10^{21}
	1.35582	0.138255	3.76616 × 10^{-7}	0.323890	1.28506 × 10^{-3}	1	8.46233 × 10^{18}
	1.60218 × 10^{-19}	1.63377 × 10^{-20}	4.45050 × 10^{-26}	3.82743 × 10^{-20}	1.51857 × 10^{-22}	1.18171 × 10^{-19}	1

1 cal = 4.18605 J（計量法）

= 4.184 J （熱化学）

= 4.1855 J （15 °C）

= 4.1868 J（国際蒸気表）

仕事率　1 PS（仏馬力）

= 75 kgf·m/s

= 735.499 W

放射能	Bq	Ci
	1	2.70270 × 10^{-11}
	3.7 × 10^{10}	1

吸収線量	Gy	rad
	1	100
	0.01	1

照射線量	C/kg	R
	1	3876
	2.58 × 10^{-4}	1

線量当量	Sv	rem
	1	100
	0.01	1

（86年12月26日現在）